DELFT UNIVERSITY OF TECHNOLOGY

MASTER THESIS

Modeling Dual Fuel Internal Combustion Engine (ICE) Running on Methanol and Diesel

Author:
A.M. DE JONG

Supervisors:
Dr. ir. M. MIKULSKI
Ir. K. VISSER
Prof.dr. D.J.E.M ROEKAERTS
Dr. R. PECNIK

This thesis is confidential and cannot be made public until September 2023.

A thesis submitted in fulfillment of the requirements
for the degree of Master of Science
in the

Sustainable Energy Technology

TU Delft

TNO innovation for life

September 11, 2018

"Success is not final, failure is not fatal: it is the courage to continue that counts."

Winston Churchill

DELFT UNIVERSITY OF TECHNOLOGY

Abstract

by A.M. DE JONG

Waterborn transport currently runs on diesel driven Internal Combustion Engines (ICE). To reduce Green House Gas (GHG) emissions an option is to shift towards alternative fuels, like alcohols. This thesis focusses on methanol in ICEs. The combustion of methanol in ICEs can be done in numerous manners, where fuel altering, external ignition and dual fuel concepts are the most commonly known. Methanol is chosen as fuel due to its renewable character, which is a discussion point. Methanol is mostly produced in a gasification process of coal and Natural Gas (NG), whom are not renewable fuels, however methanol can be produced from the gasification of biomass or hydrogenation of CO_2. Producing methanol from hydrogenation of CO_2 is not economical beneficial at this stage, the knowledge and experience for this method is limited, meaning this will be gained in the next couple of years resulting in lower prices. A couple of vessels are already running on methanol, where dual fuel and fuel blending concepts are predominance. The conventional dual fuel is therefore modelled in thesis with a Vibe based model and a two zone model.

Currently marine engines are Compression Ignition (CI) engines running on diesel as fuel. Methanol has other properties compared to diesel. The biggest difference is the lower cetane number, which is an indication on the fuels self-ignition abilities. This defective self-ignition abilities of methanol results in the necessity of adjusting a marine engine when using methanol as fuel. The most redundant and known method is the conventional dual fuel engine. The diesel injectors might need adjustments due to the smaller diesel input and there is need for a methanol injector. Methanol can be injected in the input air duct. Two different models are available for moddeling dual fuel combustion, namely the Vibe based model and the two zone model. The two zone model is available for NG and needs to be adjusted for methanol applications and the Vibe based model is already available for a methanol applications. Experiments are done on a methanol diesel conventional dual fuel engine and the results are described in a paper [1].

The Vibe model is a model that, in the basics, is build on reaction kinetics and combustion duration resulting in 'shape parameters', whom shape the Combustion Reaction Rate (CRR). The model was constructed from the experimental pressure trace converted into CRR by the 'Heat Release Model', which was used in the 'in-cylinder model' to establish the shape parameters. When the shape parameters are known the in-cylinder model can run by itself (without the use of the heat release model) producing a pressure and temperature versus crank angle traces. The Start Of Combustion (SOC) and the End Of Combustion (EOC) are assumed. The shaping parameters are valid for specific cases and therefore the model is not predictive when changing the fuel composition or Start Of Injection (SOI).

The two zone model is a model based on two zones, the burnt zone and the unburnt zone. The burnt zone is created by fuel injection and diffusion caused by

flame speed. In the burnt zone combustion can take place where the CRR is dependent on a version of the Arrhenius equation. The SOC is calculated with another version of the Arrhenius equation. Predictive behaviour was expected for the two zone model, however the results contradict.

The two models generate a pressure trace. To compare the two models the so called 'post processing' model is introduced. This 'post processing model' is based on the 'Heat Release Model' from the Vibe based model, meaning that for the calibrated case the HHR of the 'Vibe based model' is correct. The pressure traces generated by the two models are inserted into the post processing model where the output is the Heat Release Rate (HRR), Indicated Thermal Efficiency (ITE), maximum mean in-cylinder temperature and Initial Mean Effective Pressure (IMEP). The post processing model is first validated to the experiments, which resulted in an acceptable match. The calculated mechanical efficiencies are between 80% and 90% which is conform reality.

The Vibe based model results in slightly higher values for IMEP and ITE compared to the post processing model. When changing the blend ratio to less methanol use the IMEP and ITE decreases and the mean max in-cylinder temperature increases similar to the experiments. The HRR does not show the premixed combustion, but it is in the same range as the experiments. The two zone model results in a better fit for the HRR when looking at the shape for the calibrated case. When changing the SOI or the blend ratio, the model generates can even negative efficiencies or no results at all.

Both models are suitable for a calibrated case, however when changing the input settings, both models do not work predictive as wanted.

Acknowledgements

First of all I want to thank my supervisor Ir. K. Visser, professor at TU Delft, who gave me the opportunity and the confidence to proceed on a subject I was really motivated by, but lacked the knowledge. Secondly, I want to thank Dr. Ir. M. Mikulski, supervisor at TNO, for giving me the guidance to master this subject and for giving me the best feedback I can imagine. I want to thank Prof. Dr. Roekaerts, professor at TU Delft, who helped me extensively with his different insights on combustion which gave me the opportunity to look from a different angle to the subject. I also want to thank my last committee member Dr. R. Pecknik, professor at TU Delft, for joining my thesis committee. Thanks to my colleagues at TNO for giving me an amazing time during my graduation project. In particular I want to thank my colleague P.R. Balakrishnan for helping me improving my report by giving me feedback.

I want to thank my parents for giving me the opportunity to go back to school to show the world what I can do. I also want to thank my two sisters for the support they gave me. I want to thank my boyfriend for supporting me through the whole thesis struggle and for giving me feedback on the report as well.

Contents

List of Figures

List of Tables

List of Abbreviations

AFR	**A**ir to **F**uel **R**atio
BMEP	**B**reak **M**ean **E**ffective **P**ressure
BTE	**B**reak **T**hermanl **E**fficiency
CA	**C**rank **A**ngle
CHR	**C**ummulative **H**eat **R**elease
CI	**C**ompression **I**gnition
CN	**C**etane **N**umber
CRR	**C**ombustion **R**eaction **R**ate
DMFC	**D**irect **M**ethanol **F**uel **C**ell
DME	**D**i**M**ethyl **E**ther
DI	**D**irect **I**njection
DICI	**D**irect **I**njection **C**ompression **I**gnition
DISI	**D**irect **I**njection **S**park **I**gnition
EGC	**E**xhaust **G**as **C**leaning
EGR	**E**xhaust **G**as **R**ecirculation
EOC	**E**nd **O**f **C**ombustion
EOI	**E**nd **O**f **I**njection
EVO	**E**xhaust**V**alve **O**pen
FAME	**F**atty **A**cidic **M**etal **E**sters
GAHRR	**G**ross **A**apparent **H**eat **R**elease **R**ate
GHG	**G**reen **H**ouse **G**asses
GHV	**G**ross **H**eating **V**alue
GI	**G**as **I**njection
HC	**H**ydro **C**arbon
HCCI	**H**omogeneous **C**harge **C**ompression **I**gnition
HCDI	**H**omogeneous **C**harge **D**irect **I**njection
HFO	**H**eavy **F**uel **O**il
HHV	**H**igher **H**eating **V**alue
HPDI	**H**igh **P**ressure **D**irect **I**njection
HR	**H**eat **R**elease
HRR	**H**eat **R**elease **R**ate
IC	**I**nternal **C**ombustion
ICE	**I**nternal **C**ombustion **E**ngine
ID	**I**gnition **D**elay
IMEP	**I**initial **M**ean **E**ffective **P**ressure
ITE	**I**ndicated **T**hermal **E**fficiency
IVC	**I**nlet**V**alve **C**losed
LGI	**L**iquid **G**as **I**njection
LHGI	**L**iquid **G**as **I**njection
LHV	**L**ower **H**eating **V**alue
LNG	**L**iquified **N**atural **G**as
LPG	**L**iquified **P**etroleum **G**as
ME-GI	**ME**thanol **G**as **I**njection

MEP	**M**ean **E**ffective **P**ressure
MGO	**M**arine **G**as **O**il
MPI	**M**ulty **P**oint **I**njection
NG	**N**atural **G**as
NAHRR	**N**et **A**apparent **H**eat **R**elease **R**ate
PEM	**P**olymer **E**lectrolyte **M**embrane
PPC	**P**artially **P**remixed **C**ombustion
PCCI	**P**remixed **C**harge **C**ompression **I**gnition
PM	**P**articulate **M**atter
RCCI	**R**eactivity **C**ontroled **C**ompression **I**gnition
RMD	**R**atio **M**ethanol **D**iesel
SI	**S**ark **I**gnition
SOI	**S**tart **O**f **I**njection
SOC	**S**tart **O**f **C**ombustion
SPI	**S**ingle **P**oint **I**njection
TDC	**T**op **D**eath **C**enter
THC	**T**otal **H**ydro **C**arbons
TWC	**T**hree **W**ay **C**atalyst
TNO	**T**oegepast **N**atuurwetenschappelijk **O**nderzoek
TU	**T**echnical **U**niversity
WFS	**W**ater**F**ront **S**hipping
WOT	**W**ide **O**pen **T**rottle

List of Symbols

A	Surface area	m^3
A	Tuning parameter Arrhenius equation	$-$
a	Constant in Vibe function	$-$
B	Bore diameter	m
C_d	Discharge coefficient	$-$
c_m	Mean piston velocity	$\mathrm{m\,s^{-1}}$
c_p	Specific heat constant pressure	$\mathrm{J\,kg^{-1}\,K^{-1}}$
c_v	Specific heat constant volume	$\mathrm{J\,kg^{-1}\,K^{-1}}$
c	Constant	$-$
$d_{h,0}$	Nozzle hole diameter	m
D	Diameter	m
e	Specific energy	$\mathrm{J\,kg^{-1}}$
E	Energy	J
h	Specific enthalpy	$\mathrm{J\,kg^{-1}}$
h_c	Heat transfer coefficient	$-$
H	Enthalpy	$\mathrm{J\,mol^{-1}}$
k	Constant in Vibe function	$-$
L	Length	m
LHV	Lower heating Value	$\mathrm{J\,m^{-3}}$
m	Shape parameter in Vibe function	$-$
m	Mass	kg
M	Molar mass	$\mathrm{kg\,mol^{-1}}$
n	Molecular quantity	mol
N	Rotational speed	$\mathrm{rad/s}$
n_{comp}	Polytropic compression constant	$-$
p	Pressure	Pa
Q	Heat	J
R	Universal gas constant	$\mathrm{J\,K^{-1}\,mol^{-1}}$
r_c	Compression ratio	$-$
S	Stroke length	m
S	Penetration length	m
s	Mass-based stoichiometric coefficient	$-$
t	Time	s
T	Temperature	K
v	Velocity	$\mathrm{m\,s^{-1}}$
V	Volume	m^3
V_s	Swept volume	m^3
W	Work	W
w_t	Swirl velocity	$\mathrm{m\,s^{-1}}$
x_b	Fraction of unburnt gas dillutant	$-$
X	Normalized combustion progress	$-$
y	Mass fraction	$-$

Z	Normalized combustion progress rate	–

Greek symbols

α	Crank angle	rad
γ	Specific heat ratio	$-$
ϵ	Geometric compression ratio	$-$
θ	Initial jet angle	rad
λ	Air excess ratio	$-$
λ_{CA}	Crank rod ratio	$-$
μ	Multiplication factor break-up in radicals	$-$
ξ	Combustion reaction rate	$\mathrm{kg\,s^{-1}}$
ρ	Density	$\mathrm{kg\,m^3}$
τ	Dimensionless time	$-$
τ	Time	s
ϕ	Crank angle	$^\circ$ CA
ϕ	Fuel-air equivalence ratio	$-$

Subscripts

b	Burnt
B	Bore
$comb$	Combustion
eng	Engine
EVC	Exhaust valve open
f	Fuel
$fuel$	Fuel
i	Indicated
i	Species 'i'
inj	Injection
IVC	Inlet valve close
l	Laminar
noz	Nozzle
p	Piston
s	Stroke
t	Turbulent
u	Unburnt

Chapter 1

Introduction

1.1 Thesis objective

Despite electrification and hybridization are rapidly progressing into all branches of transport, it is anticipated that internal combustion engines will remain prime movers for heavy duty road and waterborne transport. The goal is to reduce Green House Gas (GHG) emissions and conventional combustion engines, running on fossil fuels, do not meet that requirement. Alternative fuels could have the potential to reduce the GHG- emissions of internal combustion engines.

The objective of this research is the application of renewable methanol (synthetic or bio-methanol) in internal combustion engines for inland shipping. European policy goals would benefit significantly of a transition from fossil fuels to renewable fuels. However research questions remain as the combustion parameters of methanol differ from conventional fuels. Heat release, peak efficiency and fuel consumption have to be established, related to the broad operational profile of an inland vessel. After these questions are clarified, consequences must be established for ship design and if possible experimental validation will be part of the research.

The study will investigate the characteristics of the combustion of methanol in an internal combustion engine. A model will be made to predict performance parameters of the methanol engine in the inland shipping context. At the start of this project two models were proposed, one at TU Delft, which is called the Vibe based model, and one at TNO, called the two zone model. A comparison will be made between the two models to verify the accuracy of them.

1.2 Research questions

Methanol as second fuel for a duel fuel internal combustion engine is considered to be a good alternative for the inland shipping and heavy road transport. This research focuses on the marine application where the possibilities for refuelling are limited and therefore the storage of fuel becomes a more important issue.

Primary question: *How can we predict the behaviour of an internal combustion engine using methanol and diesel as fuels in a compression ignition engine?*

To answer this question two models are set up and validated. To set up the models more information need to be known:

1. Is it technically feasible to use methanol as second fuel in a duel fuel internal combustion engine?

2. What kind of internal combustion engines are currently available?

3. What are the properties of methanol?
4. How does the Vibe based model work?
5. How does the two zone model work?

1.3 Methodology

Literature research is done to understand methanol as fuel and the currently known methods for using methanol in Internal Combustion Engines (ICE).

The Vibe based model is expected to be used as validation model for the two zone model. The model RMD 1.54 is used as basic model, where the RMD will be changed in order to establish the predictable behaviour. The outcome is the pressure trace against crank angle which is evaluated by the post processing model.

The two zone model needs to be adjusted towards methanol used instead of Natural Gas (NG) use. After implementing the adjustments towards methanol use, the model is validated to the experimental values for the pressure trace, Heat Release Rate (HRR) and Cumulative Heat Release (CHR).

The two models will be validated with the results of the post processing model. The 'post processing model' is the 'Heat Release Model' used to set up the Vibe based model with extra calculations to calculate the Initial Mean Effective Pressure (IMEP), Indicated Thermal Efficiency (ITE), maximum mean in-cylinder temperature and indicated work. To validate the post processing model pressure traces from the experiments described in the paper [1] are inserted into the post processing model, whom converts the pressure trace into HHR, and validated with the HHR of the experiments [1]. When the post processing model is approved the 'Vibe based model' and the 'two zone model' are compared to the post processing model with the experimental pressure trace as input. Figure 1.1 shows the process where three pressure traces are inserted into the post processing model and compared to each other. The process lines from the 'data from the paper' to the two models, Vibe based and the two zone model, indicates that engine parameters from the paper are used as input parameters for the two models.

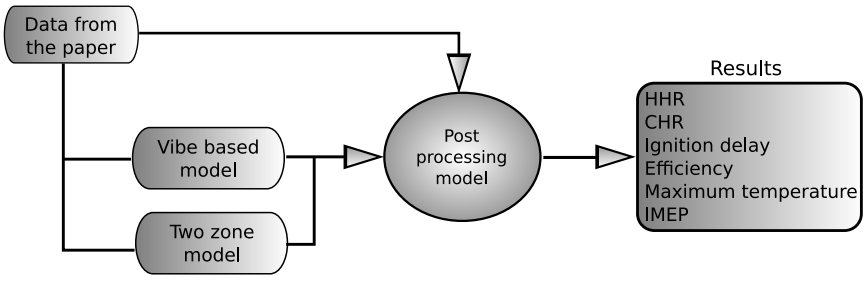

FIGURE 1.1: Validation process

1.4 Thesis outline

In chapter 2 the chemical properties of methanol are described. This chapter is divided in methanol as a fuel for ICEs and the production of methanol from biomass

and CO_2. Chapter 3 gives information on internal combustion engines. The first paragraph is about the state of the art of the use of methanol in marine engines. The second paragraph is about different approaches in using methanol in an internal combustion engine. Chapter 4 describes the two available models, the Vibe based and two zone model and the post processing model is introduced in this chapter to evaluate the two models. Chapter 5 shows the validation of the models and chapter 6 gives the conclusions and recommendation.

Chapter 2

Methanol

Global warming is an increasingly prominent international concern. One of the key challenges is to reduce the GHG emissions for environmental benefits. In marine power trains, mostly diesel fuelled Compression Ignition (CI) engines are used. To reduce the emissions of such a system without after treatment, another fuel can be used; like alcohols. In this report methanol is discussed as fuel for ICEs. In chapter 2.1 the general and combustion properties of methanol are discussed.

Methanol is mostly produced in a non-renewable production process, namely by synthesis from NG and/or coal. It can also be produced renewably, such as synthesis of biomass and from CO_2 hydrogenation. This will be discussed in chapter 2.2. [2]

2.1 Methanol as fuel for ICEs

Since 1965 methanol is used in the USAC Indy car competition, also drag racing and monster truck racing use methanol as fuel [3]. In this chapter an overview of the general and combustion properties of methanol is given.

2.1.1 General properties methanol

Methanol (or methyl alcohol) is a chemical compound with the structure: CH_3OH and can be classified as a low carbon fuel due to its low hydrogen to carbon ratio (H/C). CO_2 emissions can be reduced by 37% when combusting methanol instead of gasoline [4]. Table 2.1 describes properties of methanol, diesel, gasoline and Liquefied Natural Gas (LNG).

Methanol is harmful to human beings and can cause blindness and death when ingested. In the environment methanol can be decomposed easily. Possible fuel spills in the sea are less damaging for methanol than for diesel. Large methanol spills would contribute to an increase sea vegetation.[4]

At roomtemperture and pressure methanol is colorless. In water methanol is miscible, only 25% of methanol mixed in water leads to a flammable liquid. As shown in Table 1, the boiling point of methanol is 64.5^{o}C and its freezing point is -97^{o}C, which results in a liquid phase of methanol at room temperature. This gives the possibility to use similar storage methods as for gasoline. The molecular weight of methanol is greater than of air, this means that methanol will collect in low positioned areas, this should be considered when stored. Methanol is also known for its corrosive character, this can be a disaster for engines when the wrong material is

used. A detailed list of corrosion sensitive materials, can be found in [5].

2.1.2 Combustion properties

Combustion engine fuels are defined by their cetane and octane numbers. Whereby, the cetane number quantifies the ability to self-ignite, and the octane number quantifies the ability to resist knock. Methanol has a higher octane number than gasoline, therefore suitable for SI engines with a higher compression ratio without the occurrence of knock. This makes it possible to obtain higher efficiencies when methanol is used in Spark Ignition (SI) engines. The cetane number of methanol is low which indicates the unfavourable self-ignition properties (confirmed by high auto-ignition temperature) and, therefore, not suitable for direct implementation in CI engines and modifications to the fuel or engine are necessary.

The chemical structure of methanol contains no Sulpher (S), this results in the lack of SO_x emissions caused by the methanol. The stoichiometric Air to Fuel Ratio (AFR) indicates the amount of air needed to establish complete combustion. Due to the fact methanol already contains oxygen, it has a lower stoichiometric AFR compared to gasoline and diesel.

The viscosity of methanol (0.58 cSt at 40^oC) is lower than diesel (3.00 cSt at 40^oC), which has its advantages and disadvantages. A higher viscosity causes a decrease in injection spray angle and an increase of the penetration of the tip spray which results in a insufficient combustion where soot emissions increase. In addition higher viscosity fuels have the ability to lubricate injectors and injection pumps; which can be mitigated by injection sealing oil for pump lubrication. The pressure requirement for the injection pump will be higher for higher viscous fuels. [6]

Shown in the Table 2.1, the Lower Heating Value (LHV) of methanol is approximately half the value of the LHV of diesel, resulting in the necessity of using more methanol compared to diesel to reach equivalent power output. Heating values show how much heat will be released during combustion of the compound, where the LHV subtracts the energy needed for vaporization of water in the gas. Resulting, the lower the LHV the less energy is released during combustion. A lower heat release means a lower NO_x formation.[6]

The higher demand of methanol compared to diesel, to obtain similar energy outputs, results in bigger fuel storage facilities. The increased fuel flow can result in the need to install injectors that can cope with this bigger fuel demand. Due to the fact that the stoichiometric AFR of methanol is less than half of diesel, the doubled injection mass of methanol requires roughly the same amount of air to accomplish a complete combustion. Therefore with the same engine volume and volumetric efficiency, no power loss is expected when the engine is converted to methanol.

When liquid is injected in the cylinder heat will be extracted from the surroundings, to evaporate the fuel. In case of methanol more energy will be extracted due to higher heat of vaporization compared to diesel fuel. The more energy extracted the lower the in-cylinder temperature which causes longer Ignition Delays (ID) for Direct Injection Compression Ignition (DICI) concepts fuelled with methanol. NO_x formation is heavily dependent on high temperatures, therefore, lower in-cylinder

temperature means lower NO_x.

Methanol has a broader range of flammability limits compared to gasoline. Leaner mixtures can be used which provides higher thermal efficiencies. Methanol has a laminar flame propagation velocity which is higher than conventional fuels which results in a faster combustion and higher efficiency.

TABLE 2.1: Chemical properties of methanol, diesel and gasoline as fuel [4] [6] [7] [8] [9] [10]

Properties	**Gasoline**	**Diesel**	**Methanol**	**LNG**
Chemical structure	C4H10–C12H26	C12H26–C14H30	CH3OH	CH4
Molecular weight	95-120	190–220	32.042	16
Density ($kg\ m^{-3}$)	740	830	790	419
Viscosity at 298.15 K ($mPa\ s$)	0.29	3.35	0.59	0.146
Boiling point (^oC)	27-245	180-360	65	-161.4
Freezing point (^oC)	-57	-1 to -4	-98	-182.5
Auto-ignition temperature (^oC)	228-470	220-260	450	585
Lower heating value ($MJ\ kg^{-1}$)	44.5	42.60	19.9	51.85
Vaporization heat ($kJ\ kg^{-1}$)	310	260	1110	-
Octane number (-)	80-98	15-25	111	127
Cetane number (-)	0-10	45–50	3	
Stoichiometric air/fuel ratio	14.6	14.5	6.5	17.2
Flame speed ($cm\ s^{-1}$)	37-43		45–52.3	40
Flammability limits (in volume % of air)	1.47-7.6	1.85-8.2	6.7-36	5-15
Adiabatic flame temperature (^oC)	2030	2054	1870	2197
Flash point (^oC)	-45	78	11	-136

2.2 Methanol production

The production of methanol can be accomplished in different ways and from different fuels. The different production methods will be described in this sub chapter.

2.2.1 Methanol production from natural gas, coal and biomass

In this subsection the production of methanol from syngas is described. Syngas is a gas mixture comprises of hydrogen (H_2), carbon monoxide (CO) and CO_2. The conversion from NG, coal and biomass to syngas is done with a gasification reaction followed by a syngas cleaning step and a synthesis reaction (Figure 2.1).

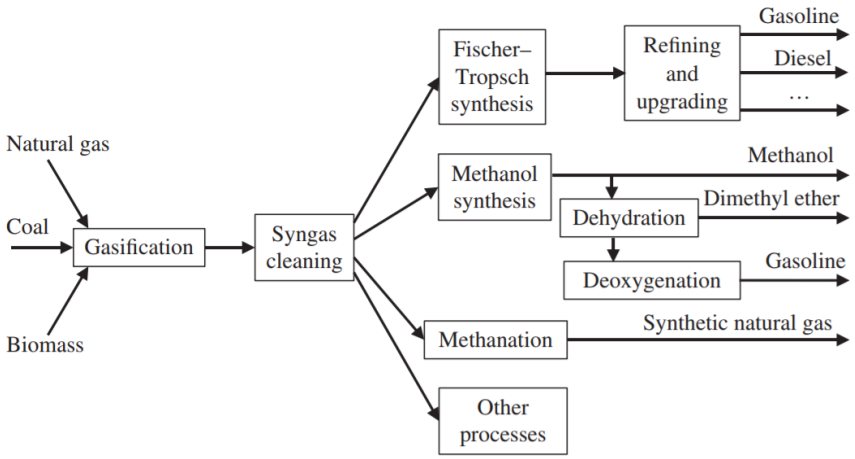

FIGURE 2.1: Schematic overview of the main routes from syngas to synthetic fuels [11]

The first step in the production of methanol is gasification. The basic fuels; coal and biomass both consist of HydroCarbons (HC), which are mulecules, containing carbon and hydrogen. NG is a gas, containing mostly methane (CH_4). NG is formed by decomposing plants and animals combined with heat and pressure over a lot of time. Coal is formed similarly as NG but the pressure is higher and the time needed for the formation is longer. Biomass is formed from the living kind of flora and fauna. [11]

Gasification is a process where a solid or a gas is converted into a combustible gas, containing H_2, CO, CO_2, CH_4 and other higher molecular weight HC, by heating and adding an oxidizing agent like steam into a fluidized bed reactor. The oxygen added is not enough to have a complete combustion, however it is higher than a pyrolysis reaction. Combustion is described by the stoichiometric oxygen ratio. Whereby $\lambda > 1$ refers to complete combustion, $\lambda = 0$ refers to pyrolysis and $0 < \lambda < 1$ to gasification. [11].

In figure 2.2 an example of output products of a biomass gasification for different λ's is shown. It is shown that the most favorable λ is equal to 0.35, based on the output products where there is a lot of CO and H_2. The unwanted side products are removed with syngas cleaning.

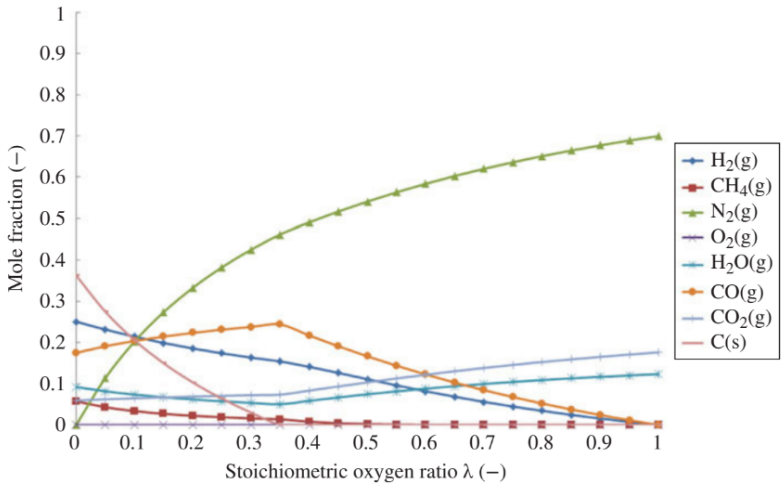

FIGURE 2.2: Output products gasification of wood with differenet λ's [11]

The last step before creating methanol is methanol synthesis. The formation reaction equation is shown in equation 2.1. This reaction is exothermic which means that thermal energy is released during this process from left to right, therefore, if the temperature increases, the reaction shifts to the left, however with an increased pressure the reaction shifts to the right. Preferable is that the reaction shifts to the right, so low temperature and high pressures are obtained. [11]

$$CO + 2H_2 \rightleftharpoons CH_3OH + Energy \tag{2.1}$$

The production cost of methanol from biomass compared to NG is more. The production costs of methanol from biomass with a $400MW_{th}$ production unit, is 9-12$/GJ when biomass costs are US$2/GJ. Hydrogen is also produced for the price of US$ 8-11/GJ in the same system. The disadvantage of this system for the Netherlands is that it requires a lot of biomass import and more transport costs. This makes this option less attractive to produce methanol from biomass in the Netherlands.

2.2.2 Production from CO2

Homogenous metal catalyzed hydrogenation of CO_2 towards MeOH was first performed in 1995 and in 2011 this research was picked up as a result of the increasingly prominent international concern of global warming [12]. The proces converts CO_2 into MeOH according the following reaction [13]:

$$CO_2 + 3H_2 \rightleftharpoons CH_3OH + H_2O \quad \text{where} \quad \Delta H_{25^oC} = -49.5kJ * mol^{-1} \tag{2.2}$$

The advantages of this type of production is that CO_2 is captured and recycled, which gives a CO_2 neutral process from producing methanol and combusting methanol to gain energy in an ICE. This is beneficial for the greenhouse effect. The stock of CO_2 is called unlimited for the reason that it will always be produced through combustion of, for example, methanol. In order to make the whole process CO_2 neutral, the hydrogen needs to be produced with renewable sources. This can

be done with the electrolysis of water with electricity coming from solar, wind or other renewables. A schematic overview of this process is shown in figure 2.3.

The H_2 used in this process has disadvantages too. Hydrogen is hard to store due to its low gas density at room temperature. Normal steel cannot be used due to embrittlement of the material caused by hydrogen. The production of hydrogen is not cost effective when produced in a renewable way. The production of H_2 can be by gasification of coal, steam methane reforming and electrolysis of water. The electrolysis is considered renewable when the electricity comes from a renewable energy source such as solar and wind. The costs of producing electricity from renewable energy sources are high compared to the production of electricity from fossil fuels (gasification of coal and steam methane reforming). [13]

CO_2 can be easily stored in liquid form under mild pressure, while it is not toxic, corrosive nor flammable.

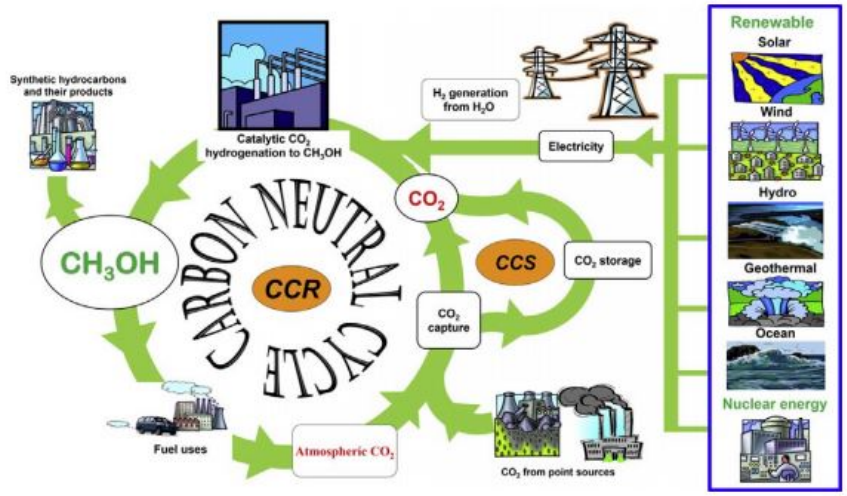

FIGURE 2.3: Carbon Neutral Cycle [12]

Production of methanol by this renewable cylde can be profitible economically if methanol is sold for more than 600 $€ton^{-1}$) [14]. The current price for methanol is 330 $€Mt^{-1}$ [15]. The big difference in renewable production price and selling price comes from the high investment costs of the Polymer Electrolyte Membrane (PEM) electrolyser used. It is expected that these costs will lower through the years due to development. [14]

2.3 Conclusion on production of methanol

Currently the costs of producing methanol through hydrogenation of CO_2 is economical not feasible. Depending on future developments on technology and increasing of political motive this cost analysis can be reconsidered. The storage of Hydrogen is also not fully developed which makes storage costly.

Methanol from fossil fuels currently has a price of 330 $€Mt^{-1}$ [15]. This makes it the most dominant and economically attractive production process. However the production of CO_2 is still existing where the goal was to reduce it or at least neutralized the process. In the future there might be CO_2 tax that makes this option less attractive.

Methanol from biomass is slightly more pricey than the production costs of methanol from NG. However in case of the Netherlands the production costs are higher than the 9-12 $\$ GJ^{-1}$ stated in [16] due to the high transportation costs of biomass due to the lack of inland biomass stock.

The conclusion is that renewable methanol is not yet profitable, however future perspective is that we will run out of fossil fuels, which makes the production of methanol through NG or coal impossible and the renewables will take over. In future prospective, methanol as fuel is most likely a renewable.

Chapter 3

Internal combustion engines

Methanol is currently of interest due to its renewable character, as discussed in chapter 2.2. However, this is not always valid due to the dominant production from NG and coal. In the future methanol can probably be produced beneficially from renewable feedstock. Without the renewable character methanol is still a more sustainable fuel than current used diesel fuel for marine CI engines, due to the lower emissions exhaust (explained later in this chapter). This chapter will give an overview of current projects on methanol use in ICEs in marine applications and currently known combustion concepts for using methanol as fuel.

3.1 State of the art of methanol use in marine engines

In this chapter, several projects on running marine engines with methanol are discussed.

MAN Diesel & Turbo

MAN Diesel & Turbo developed in late 2012 an dual fuel engine on methanol, the ME-GI (methanol gas injection) engine based on the High Pressure Direct Injection (HPDI) combustion concept (explained in Chapter 3.2. In 2015 the MAN B&W ME-LGI (Liquid Gas Injection) series was introduced. The ME-LGI can run on low flash-point alternative fuels. [17]

A MAN B&W 6G60ME-C9.5 engine is available for standard marine diesel use and as dual-fuel engine running on LNG (ME-GI) or methanol (ME-LGI). The engine is capable to produce 15 knots at 90% engine load. The propulsion power is calculated to be 5.3 MW to reach 12.5 knots. The efficiency calculations based on LNG/ Liquified Petroleum Gas (LPG) / Methanol compared to HFO / MGO (conventional fuels: Heavy Fuel Oil / Marine Gas Oil) are shown in figure 3.1. The graph shows a small efficiency improvement of around 1% on average. [18]

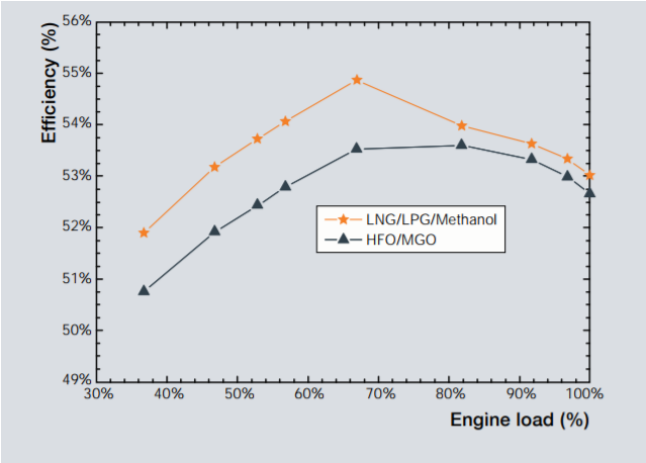

FIGURE 3.1: Calculated efficiencies of the MAN B&W 6G60ME-C9.5 engine at different engine loads and fuels [18].

Wärtsilä

Wartsila is a company working in the marine and energy industry. Wärtsilä developed an ICE for a major ship owner, with strict sulphur content, running on methanol. In 2015 the first retrofitted engine was born. [19]. Figure 3.2 shows the advantages of methanol compared to HFO+EGC (Exhaust Gas Cleaning), MGO, LNG used in a retrofitted dual fuel engine. It shows that methanol is a suitable current and futuristic solution for marine engines, while the compliance for now in the futer are good, the availability is medior, the capex costs are also medior and the opex costs are considred good. [20]

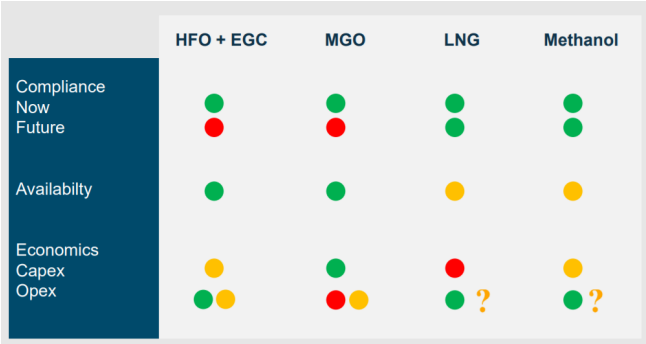

FIGURE 3.2: Retrofitted wartsila engines [20]

MethaShip

MethaShip is a 'methanol as fuel' project, started in 2014 and funded by the German government for passenger vessels with medium speed, where the goal is to examine the potential of using methanol as fuel. The motivation is due to the thightened regulations of emissions, the grow of environmental awareness for example the Paris agreement. The project contains the combustion of methanol in ICEs in two ships, a ro-pax ferry and a cruise ship. The biggest partners involved were, Meyer Werft,

Lloyd's Register and FlensburgerFlensburger SchiffbauGesellschaft [21]. Figure 3.3 shows an overview on the size of the ferry and the amount of passengers able to travel with the ferry.

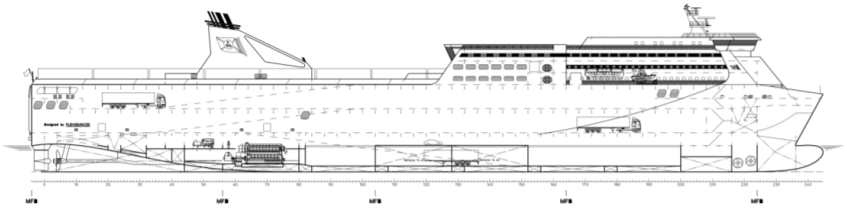

Main data	
Length	199.8 m
Width	28.6 m
Draught	6,5 m
Passengers	600 + 50 Crew
Engines	Dual Fuel 2 x 9 MW medium speed
Main fuel	Methanol

FIGURE 3.3: RoPax ferry MethaShip [21]

Lean Ships

Lean Ships is a project which "aims to demonstrate the effectiveness and reliability of energy saving and emission reduction technologies at real scale" [22]. It focuses on ships of mid and small size meant for European transport, offshore vessels and the cruise market. The aim is to reduce CO_2 emissions with 25%, to save fuel up to 25% and to completely loose the SO_x, NO_x and Particulate Matter (PM) pollutants. For the offshore sevice vessels the demonstrator case will be a marine engine operating on a dual fuel combustion mode where methanol will be the main fuel. The project is broad and also LNG modes are investigated. [22]

Stena Line

Stena Line is a ferry that travels between Goteborg (Sweden) and Kiel (Germany). It is the first ferry that runs on methanol with 4 dual fuel engines from Wärtsilä since March 2015. The system is redundant for the reason that the engines can still run on only marine diesel and on the combination of methanol and marine diesel as a dual fuel combustion engine. The fuel system for methanol is a common rail system that uses a high pressure pump and double-walled pipe lines and fuel tank. [23]

FIGURE 3.4: Stena Line [23]

Waterfront Shipping

WaterFront Shipping (WFS) introduced 7 vessels running on methanol in May 2016. The vessles contain two stroke dual- fuel engines and have been running reliable and safely for the last couple of years. [24]

FIGURE 3.5: Celebration of one year running on methanol, efficient, safe and reliable [24]

Effship

Effship project is a project to create a more sustainable marine industry, where emissions are reduced and energy is used more efficiently. The project started in December 2009 and aims to reach solutions for 20% energy efficiency improvement, 40% GHG reduction and the use of 10% renewable energy in 2020 [25] [26]. The project contains more aspects, from using wind, solar and wave, heat recovering systems, exhaust gas cleaning and different engine fuels. The use of methanol came out as best solution for marine application, therefore a spin-off project known as SPIRETH is managing the engine testing and the regulatory side. The currently used engines will be provided with a glow plug to [25]

FIGURE 3.6: EffShip project [25]

SUMMETH

SUMMETH project concentrates on the overall development of technology of using methanol as fuel for marine applications, such as inland waterway and coastal vessels. The SUMMETH project focuses on engines from 250 kW to 1200 kW. Tests will be done to evaluate a variety of methanol combustion concepts to suggest the best solution for implementation where the whole fueling system is considred. [27]

GreenPilot Project

GreenPilot Project has the objective to introduce the use of methanol in marine on board of small ships. The currently lack of rules of low flaspoint fuels will be included in the project with the outcome of a proposal of relevant rules. The project contains research on the best combustion engine for the combustion of methanol and the best applicable solution will be further investigated for implementation. The test results of the SUMMETH project are utilized for adaption and evaluation of the ICE.[28]

FIGURE 3.7: GreenPilot pilot boat running on methanol[28]

SPIRETH project

The SPIRETH project is a spin-off of the Effship project where the main goal is to test alternative fuels for marine engines to reduce emissions. One concept is focused on running on DiMethylEther (DME) where on board conversion from methanol to DME is established. The other concept is running mainly on methanol with a diesel like pilot ignition fuel. [29]

FIGURE 3.8: Ferry running on DME [29]

3.2 Methanol in conventional ICEs

There are multiple ways to make use of duel fuel systems in marine ICEs. An overview is given in figure 3.9. The two main ICEs known are the so-called SI or gasoline engines and the CI or diesel engines. The fuels usually used in these type of engines are gasoline and diesel, respectively.

3.2.1 Working principle of most common engines types- not specified on methanol

In **Spark Ignition (SI)** engines, air and fuel are premixed and inserted into the cylinders during the suction stroke. This gives a homogeneous distribution of the air fuel

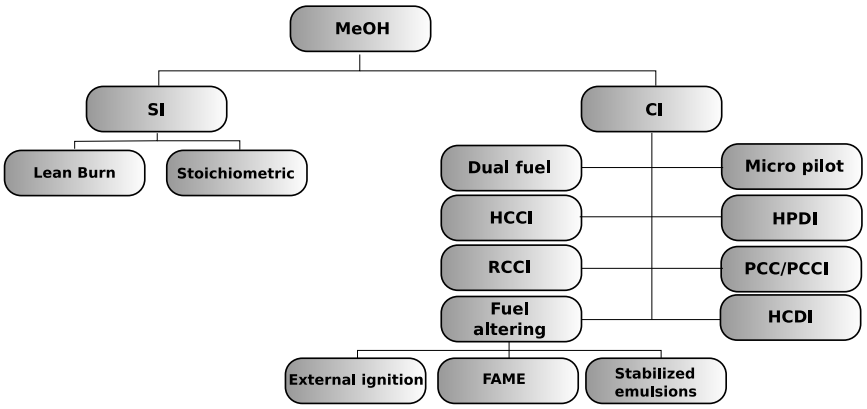

FIGURE 3.9: Conversion paths for the use of methanol in CI engines

mixture. The piston raises and compression will occur, resulting in high temperature and pressure. Close to Top Dead Center (TDC) the spark plug ignites the mixture and explosion takes place. The explosion ensures the piston to go down with a certain power, which is mechanical power used for driving forces. The amount of fuel injected in the cylinder is controlled with a throttle in the induction channel. The device squeezes the inlet pipe which makes the suction stroke less effective due to the higher forces, also called pumping losses. In CI engines pumping losses are not present, as a result of direct injection of the fuel where the amount of fuel is controlled directly. Another drawback of a SI engine is the limited compression ratio. If the compression ratio is too high the fuel will self ignite which creates a less optimal combustion. In CI engines the fuel used can deal with higher compression ratios due to the higher cetane number, which makes the engine more efficient. The last major drawback is the the large part of unburnt fuel leaving the cylinder, where CI engines have an injection point centering all the fuel, SI engines have a homogeneous fuel distribution which causes spots where fuel remains unburnt, crevices. The main advantage of SI engines is the controllability of the ignition. Another advantage is that the engine can be really clean in combination with a Three-Way Catalytic (TWC) converter aftertreatment system and stoichiometric combustion. Figure 3.10 shows how SI engines work.

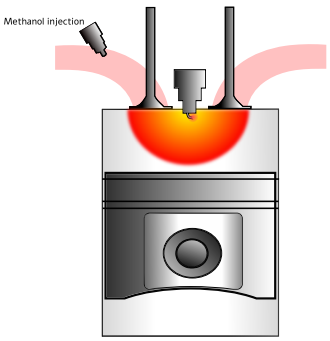

FIGURE 3.10: Conventional SI engine.

To reduce the negative concequences of the homogeneous distribution of fully premixing, for example the unburnt fuel resulting in high CO and HC emissions,

can be tackled by using a **Direct Injection Spark Ignition** (DISI). The fuel is directly injected in the cylinder where the fuel has to evaporate resulting in a temperature reduction in the cylinder. This reduces the risk of pre-ignition and knock. On the other hand, for similar knock and pre-ignition risks, the compression ratio can be increased, which makes the combustion more efficient. At environmental perspective NO_x emission and HC and CO emissions are lowered if the temperature in the cylinder is lowerd, however with increased compression ratio the temperature will not dercrease significantly. The disadvantage of DISI is the higher soot emissions compared to the SI engine caused by the direct injection in the cylinder. However the soot emissions compared to the currently used diesel engines are significantly lower due to methanol use [30]

Direct Injection Compression Ignition (DICI) engines are commonly used in the marine and commercial vehicles. The working principle is different than SI engines. Air is inserted into the cylinder during the suction stroke, due the rising piston the air is compressed resulting in a pressure and temperature increase in the cylinder. Close before TDC the fuel with a high cetane number is injected into the cylinder where the combustion starts by self-ignition. CI engines do not have pumping losses, because the load is controlled by the amount of fuel injected into the cylinder. The combustion efficiency for CI engines is higher compared to SI engines due to higher compression ratios and lesser fuel cooling by cylinder walls. The fuel will not reach the crevice volumes so less unburnt fuel remains compared to SI engines, which results in lower emissions of CH and CO. On the other hand due to the more concentrated fuel in the middle of the cylinder, there are hot spots in the cylinder. The temperature in these spots is higher than in the rest of the cylinder. This results in a higher NO_x and soot emissions. The injection of the fuel needs a high pressure fuel injection system which is complex and expensive compared SI engines.[30]

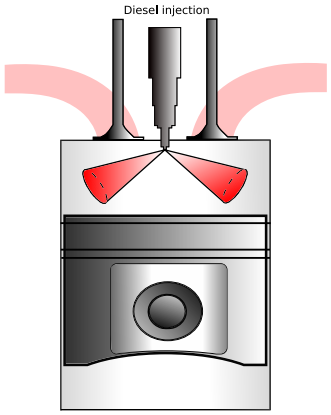

FIGURE 3.11: Conventional CI engine.

NO_x and **PM** emissions can be formed in cylinders in specific conditions. NO_x in CI engines are mainly formed from the N_2 and O_2 from air combined with high temperatures. This is shown in the following chemical equations [31]:

$$N_2 + O \leftrightarrow NO + N \tag{3.1}$$

$$N + O_2 \leftrightarrow NO + O \tag{3.2}$$

$$N + OH \leftrightarrow NO + H \tag{3.3}$$

These chemical reactions need activation energy to shift to the right (318 kJ mol^{-1}). This means, that when high temperatures are reached (> 1800K) these reactions occur. [31]

PM emissions are formed with a combustion reaction with not enough air to fully combust the fuel. The decomposition of fuel is started and precursors for soot are created. If fuel is injected in the cylinder quite concentrated, it means that when the combustion starts, air cannot reach the core of the concentrated fuel, which results in an air absent region resulting in PM emissions. This occurs mainly in direct injection engines based on the concentrated fuel distribution. [31]

3.2.2 Methanol in SI engines

Spark ignited (SI) engines are engines with fuel that vaporizes rapidly in air. The fuel is pre-mixed with air and inserted in the cylinder, where a spark ignites the fuel mix. This gives a even distribution of the fuel in the cylinder and therefore an even divided combustion [32]. In Table 2.1 an overview is given of some important properties for combustion of methanol in a gasoline ICE.

Methanol evaporates quickly in air, therefore it is feasible to use methanol in a gasoline engine. Densities of gasoline and methanol are similar, however the octane number and the auto-ignition temperature of methanol are higher. Nevertheless methanol has a lower volumetric energy density (LHV times the density) than gasoline which makes it seem that the energy produced in a cylinder is less for methanol than for gasoline. Methanol, on the contrary, has a higher octane number which results in the possibility to have a higher compression ratio before detonating leading to higher efficiencies. The flame temperature of methanol is also lower, which means that there is less heat loss in the cylinder. In Figure 3.12 a graph shows the increased Break Thermal Efficiency (BTE) of using methanol in a SI engine compared to using gasoline in a SI engine. However compared to the currently, in marine applications used CI engines running on diesel this is an efficiency decrease. [32]

Methanol has a high 'latent heat of vaporization', which is the ability to absorp heat during the phase change. This results in lower in-cylinder temperatures and therefore less NO_x will be formated. This is shown in Figure 3.13 [32].

SI lean burn

Lean burn is a concept similar to SI stoichiometric where more oxygen than needed is inserted into the cylinder to limit the pumping losses and therefore higher efficiencies are established. Lean burn operations have similar efficiencies as CI engines, however the ignition is problematic. To mitigate this ignition issue, lean burn operation makes use of a pre-chamber to create locally rich fuel areas where ignition possibilities are enlarged.

Figure 3.14 shows the improved efficiency of using methanol in lean burn operation versus stoichiometric operation. The efficiencies are up to 42% which is comparable with CI engines. In Figure 3.15 the NO_x formation at different rotational speeds

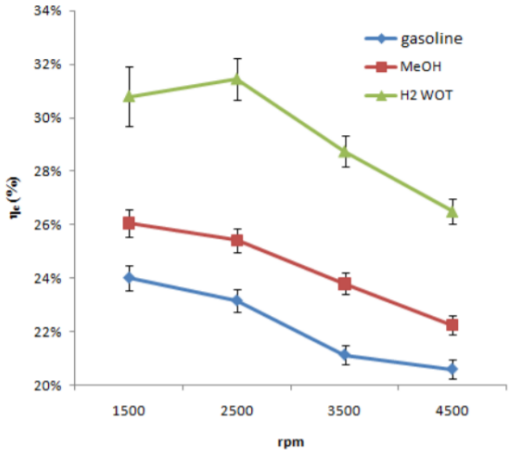

FIGURE 3.12: BTE at 40 Nm tests done with a 1.8 l Volvo 4-cylinder gasoline production engine modified for tri-fuel operation. [32]

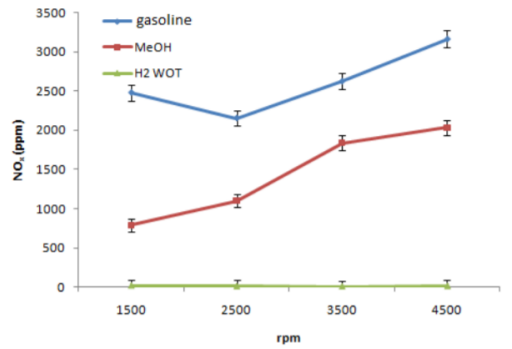

FIGURE 3.13: NOx emissions tests done with a 1.8 l Volvo 4-cylinder gasoline production engine modified for tri-fuel operation.[32]

is given at 30 Nm. Here is shown that the lean burn operation creates less NO_x than stoichiometric operation which indicates lower temperatures in the cylinder.

Conclusion

Using methanol in gasoline engines is possible, the efficiency will increase and the NO_x emissions will decrease. For lean burn operation the NO_x emissions will decrease even more and efficiencies are higher compared to stoichiometric methanol operation. The fuel methanol has similar properties as gasoline, that means that the transition towards methanol does not need many adjustments. However, retrofitting a CI engine towards SI engine, the engine needs implementation of spark plugs in every cylinder.

3.2.3 Methanol in CI engines

A CI engine works with self ignition, however methanol does not self-ignite easily. Therefore, an ignition mechanism is needed or an adjustment of the fuel to be able to self ignite. As shown in Figure 3.9 there are multiple concepts running as CI engines which will be discussed in this chapter.

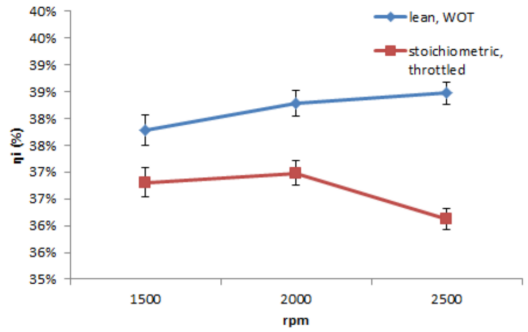

FIGURE 3.14: Efficiency of lean burn, Wide Open Trottle (WOT) operation versus stoichiometric operation [32].

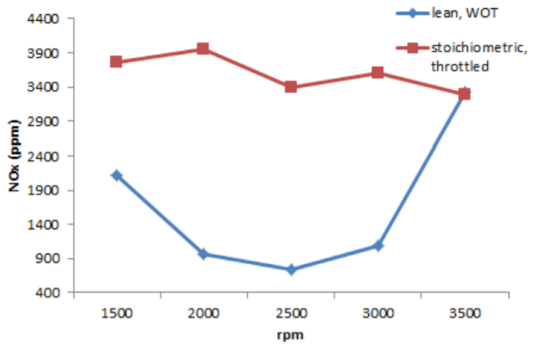

FIGURE 3.15: NOx production of lean burn, Wide Open Trottle (WOT) operation versus stoichiometric operation [32].

External ignition

External ignition is divided into two priniciples, namely the **SI** and the **glow plug** principle. The SI principle is where fuel and air are pre mixed and ignited with a spark plug. An electric spark will ignite the fuel and combustion will occur. The second principle for external ignition is called **glow plug**, where the plug becomes as hot that the plug starts glowing and causes the ignition to start. The glow and spark plugs are, during operation, susceptible for erosion. Advantages and disadvantages are similar to the advantages and disadvantages of the gasoline engine. Also the efficiency will be similar. [30]

FAME

FAME stands for Fatty Acid Methyl Ester and is more familiar under the name biodiesel, which is a fuel produced from animal fats and/or vegetable oils. Based on methanol and the fats (molar ratio of 6 to 1), a transesterification proces creates FAME. The oils itself can be directly used, however, there are some problems associated with coke polymerization and formation, which makes the disadvantages overrule. Therefore, the use of FAME is more popular. FAME has a viscosity higher than or equal to diesel fuel, which creates the possibility to use the fuel in a DICI engine without modifications. The energy content of FAME, which can be described

with the LHV, is around 10% less than for diesel which results in a higher fuel consumption [33]. The cost of regular diesel is lower than FAME, that means that regular diesel is cheaper to use. The use of FAME results in more NO_x emissions, it is about 25% on average compared to engines running on diesel. However, the big advantage of using FAME is the reduction of CO_2 emissions due to CO_2 neutral situation and Total Hydro Carbons (THC) due to its higher oxygen content [34].

CN improvers

An ignition improvement additive can be added to methanol to improve its cetane number to improve the self ignition properties of methanol. This can be done with blending methanol with a substance called 'Avocate'. There are no technical issues why ICEs cannot run on a combination of 'Avocate' and methanol, however the costs are currently not competable with diesel. [35] [36].

Stabilized emulsions

The main problem of methanol-diesel fuel blending is that the mix-ability is poor. Homogeneous distribution of methanol-diesel can be created by adding stabilisers, to stabilize the emulsion to prevent re-stratification from happening. Research shows that up to 20% methanol, combustion in common CI engines can take place without any modifications [37]. The methanol content and NO_x formation decrease simultaneously. The stabilized emulsion results in higher HC due to fumigation of methanol, but a decrease in NO_x and PM [4]. A disadvantage of this concept, when keeping the ignition timing similar, is the increase of the ID and losses of power caused by the lower LHV of methanol. The ignition timing can be adjusted to establish the most optimal combustion timing where power losses are minimal. Isopropyl alcohol (30%) was used in [38] for the improvement of mixing methanol (30%) - diesel (40%). It reports that the BTE was increased by 5% compared to only diesel operation.

Conventional dual fuel IC engine

The conventional duel fuel contains 50% to 80% of methanol. The methanol air mixture is inserted in the inlet stroke while the diesel for ignition is inserted close to TDC. Often the combustion is lean-burn which is the name for using excess air during the combustion to reduce CO and THC emissions, while the conventional dual fuel engine has high THC and CO emissions due to the port fuel injection of methanol. The NO_x and PM emissions are lower than for conventional dual fuel concepts [39]. The efficiency, when using methanol combined with diesel, can be higher than for a normal ICE because methanol combustion is faster than normal diesel and higher compression ratios can be accomplished. This gives a higher thermodynamic efficiency (up to 70%) for similar size conventional ICEs running on diesel. Similar to SI engines, air and fuel are premixed and inserted into the cylinder. Close to TDC the high-cetane fuel is injected directly into the cylinder. The high pressure and temperature will ignite the diesel fuel which will ignite the air-methanol mixture and combustion occurs [30].

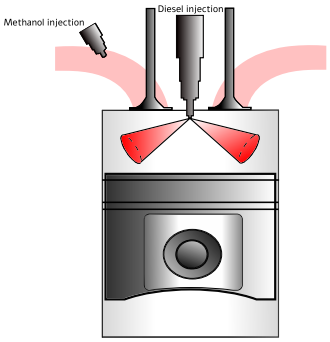

FIGURE 3.16: Dual fuel engine.

Micro pilot

Micro pilot engines are similar to duel fuel engines. However, the amount of diesel injection is lower with a shorter time span. Test were done with ethanol and diesel [40]. The ethanol/diesel ratio is usually arround 95% but the ratio can also be increased to lower NO_x and soot emissions. The disadvantage is the narrow injection timing to establish combustion. This is narrow enough to suggest to add a substance that improves the reactivity of the ethanol to air mixture to make sure the combustion occurs and misfiring is prevented. [40]

HCCI

Homogeneous Charge Compression Ignition (HCCI) is comparatively new and therefore commercially underdeveloped. Similar to the SI engine, air and fuel are premixed before entering the cylinder, however HCCI does not need a spark plug while CI is used to enhance the ignition. Due to this CI the combustion is simultaneously divided through the whole cylinder, which results in an even divided temperature throughout the cylinder. The intake charge needs to be diluded in regular operation, to limit the rate the pressure and temperature rises during combustion. The result is low temperatures in the cylinder, which consequences in low NOx emissions. On the contrary this low temperature leads to high emissions of HC and Carbon mono-Oxide (CO) which is a effect of an incomplete combustion. To optimize the HCCI the temperature, pressure and fuel intake needs to be controlled and that comes with a challenge [30]. Methanol needs an ignition improver to be able to self ignite, DME is suggested for the job [41].

HPDI

High pressure direct injection (HPDI) is another form of direct injection based on pressure ignition. The injection takes place late in the compression cycle with high pressure. First a pilot diesel injection to indicate the combustion followed by the injection of premixed air with NG. This process has similarities to the compression ignition engine, however the injection pressure is higher and NG is the main fuel which is predominantly combusted in a non-premixed manner, where gas and air is premixed in the cylinder itself. Due to the non premixed character the engine is resistant to knock and the compression ratio is still high enough to create a good efficiency. The higher injection pressure increases the atomisation speed which creates

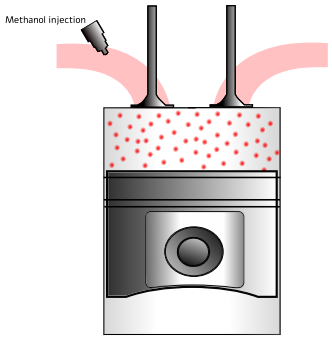

FIGURE 3.17: HCCI engine.

better combustion efficiencies. Figure 3.16 is a good indication on how a HPDI engine works, however the injection of the gas and air mixture is inserted with higher pressure. [42]

RCCI

Reactivity Controlled Compression Ignition (RCCI) proceeds with two fuels with different cetane and octane numbers. One fuel similar to diesel (high cetane number) and one to NG (high octane number). Air and NG are premixed and injected into the cylinder. A high cetane number fuel is injected just before TDC where auto-ignition starts. RCCI and a duel fuel concepts are similar to each other. However the temperature is lower compared to the dual fuel concept, hench the lower NO_x emissions, and RCCI uses diluted fuels similar to HCCI. An overview on the different concepts is shown in figure 3.18. The advantages of RCCI in comparison with HCCI is the controlebility. However soot emissions and NO_x emissions will increase slightly compared to the HCCI concept but less unburnt fuel and CO exhaust. Also, the controlebillity of RCCI is a big advantage compared to HCCI.[43] [30].

PPC or PCCI

Partially Premixed Combustion (PPC) or Premixed Charge Compression Ignition (PCCI) is a combination of HCCI and DICI. Fuel combined with air is injected into the port, and combustion is initiated by the fuel injection before TDC. The use of gasoline has the advantage that the fuel is less reactive and therefore longer premixing can occur which reduces the NO_x emissions compared with SI and CI concepts. However this concept has like HCCI the disadvantage of unburnt fuel in the exhaust with CO emissions. On the conterary research has shown that with boosted PCCI concepts, the combustion efficiency can be close to 100%. The improvement of the pistons is the main reason that crevice volumes are reduced and the use of high pressure intake is an advantage. [43]

HCDI

Homogeneous Charge Direct Injection (HCDI) is an alternative for PCCI where higher loads can be achieved. The working principle is shown in Figure 3.19. First a gas air mixture is inserted into the cylinder in the suction stroke. With the compression stroke diesel is injected close to TDC to ignite the gas to air mixture. To obtain the

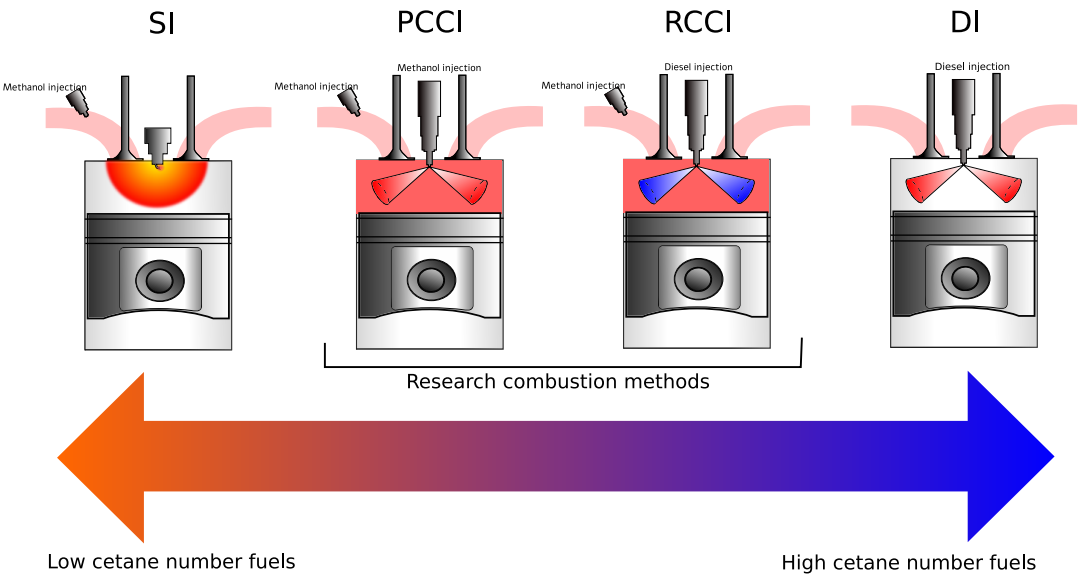

FIGURE 3.18: Comparisson of SI, PPC, RCCI and DICI engines.

higher load extra gas to air mixture is injected to create more energy during combustion. [42]

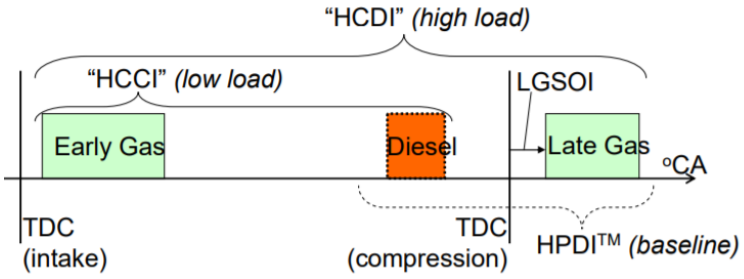

FIGURE 3.19: Comparisson of HCDI HPDI HCCI engines. [42]

3.2.4 Summary of combustion concepts

Figure B.1 is an overview of the benchmark. The combustion concepts are compared with a DICI engine. This results in when using a SI engine, the PM exhaust is already lower due to the premixed injection. The efficiency of a SI engine is lower than a CI engine, due to lower compression ratios to avoid knock, however when using methanol, in lean burn operations it reaches similar efficiencies as a CI engine. This is caused by the higher octane number of methanol and in lean burn operations excess air is supplied resulting in lower temperatures, giving the opportunity to operate at higher compression ratios. SI engines have crevices resulting in spots where fuel remains unburnt resulting in more HC and CO exhaust.

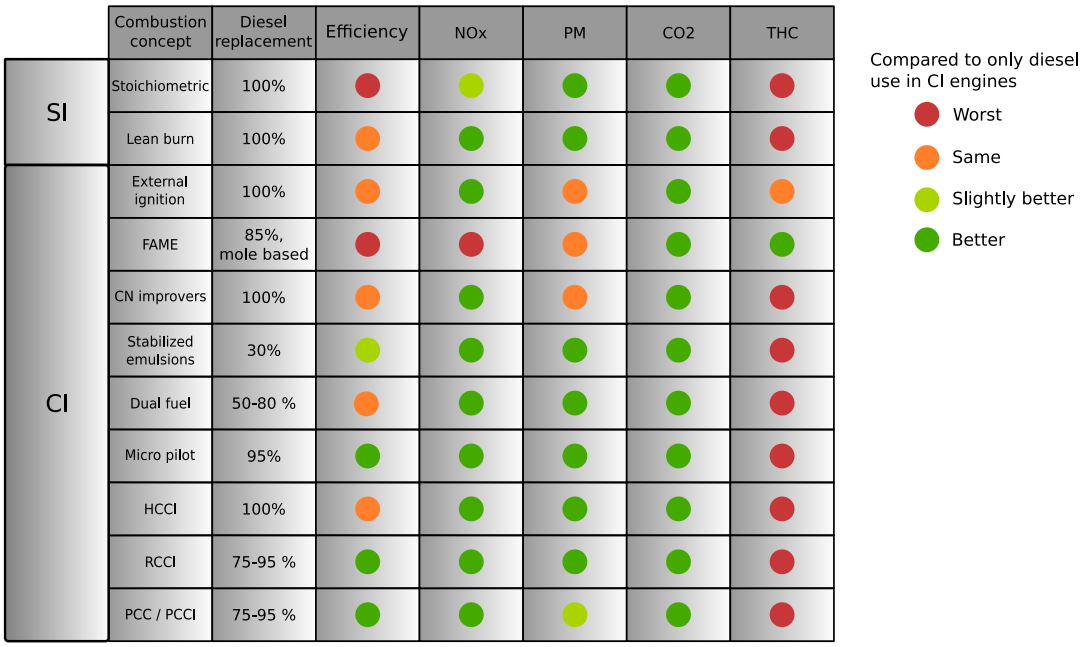

FIGURE 3.20: Benchmark methanol in IC engines

3.2.5 Conclusion why dual fuel ICE is researched in this thesis

Duel fuel compression ignition engines are already researched for combinations with alternative fuels. The advantage is the redundancy, caused by the ability to also run on only diesel operation. Therefore, it can be used in dual fuel operation when the methanol is available for a lower price for example. As shown in the benchmark overview (Figure B.1) it has the least disadvantageous exhaust emissions. RCCI and PCCI are concepts have less NO_x emissions compared to dual fuel combustion and efficiencies are higher, but the robustness and the power of using the conventional fuel in the engine makes it reliable and a first step up in the growth into the future. It has already big advantages compared to the current situation where all marine engines run on DICI diesel based engines. Therefore the research is done on dual fuel combustion engines with as first fuel Methanol and ignition fuel diesel. This can also be bio-diesel to make it more sustainable.

Chapter 4

Modeling of a conventional dual fuel CI combustion engine

Chapter 3 shows the currently known methods to combust methanol in marine engines. The methods differ from altering the fuel, adding new hardware and running on more than one fuel. The different combustion methods ask for a different modeling approach. In this chapter, the modeling methodology for conventional dual fuel combustion, the post processing model and the results are described. Two models are tested, a two zone model and a Vibe based model. The Vibe based model, created by Buyongjoo Lee [44], is already running on methanol-diesel configuration and therefore possibly suitable for the verification of the second model, the two zone created by TNO, which is currently specified for dual fuel combustion with NG and needs adjustments towards methanol combustion.

4.1 Vibe based conventional dual fuel combustion model

Byungjoo Lee [2016] [44] created a dual fuel combustion model with methanol and diesel as fuels. The model is calibrated for a RMD (Ratio Methanol Diesel) of 0, 0.55 and 1.54, where RMD = 0 shows that only diesel was used. In this thesis the calibrated model for RMD = 1.54 is used. Verification of the model was done by Byungjoo Lee (2016) [44] based on the experimental data of Lijiang Wei et al., (2015) [1].

4.1.1 Set up Vibe based model

The model approach is based on the 'in-cylinder pressure model' and the 'heat release rate model'. The 'Heat Release (HR) model' is part of the 'in-cylinder model', this is shown in Figure 4.1. 'HR' is the 'heat release model' and is shown in Figure 4.2.

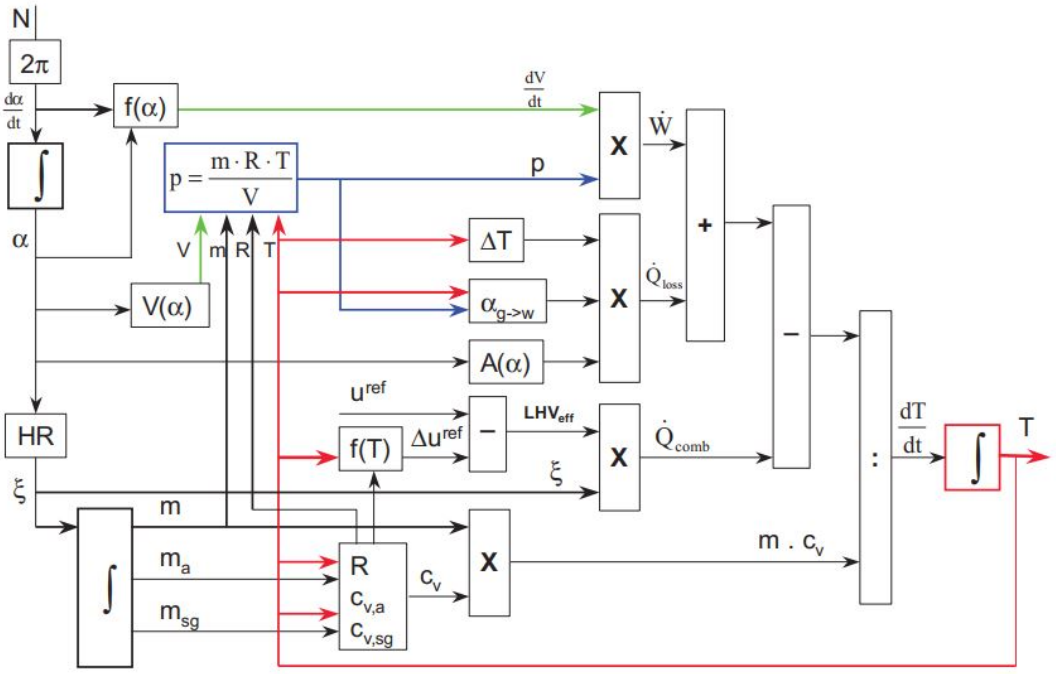

FIGURE 4.1: In-cylinder process modeling [45]

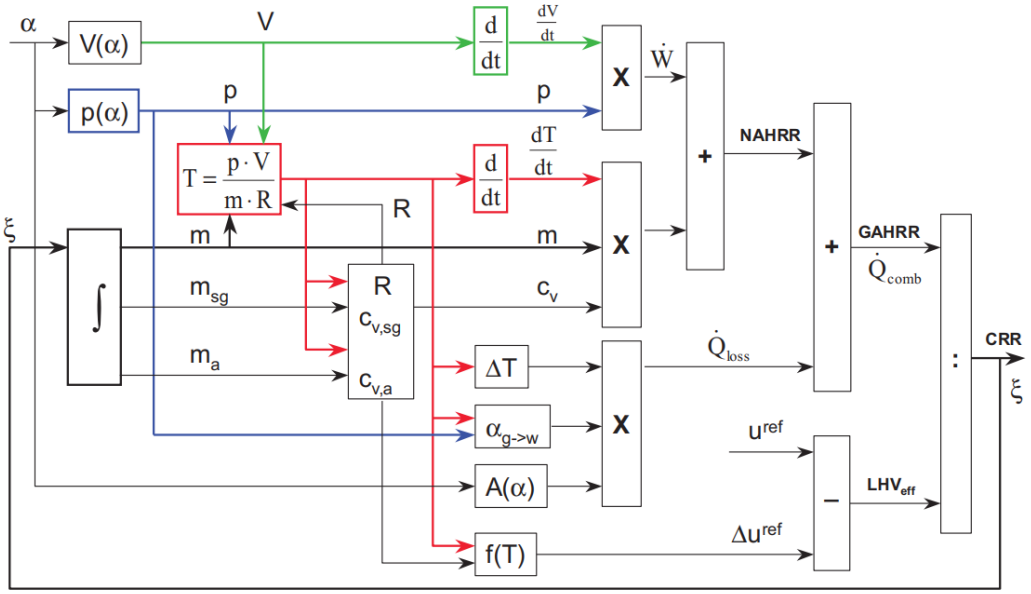

FIGURE 4.2: Heat release rate from pressure trace [45]

The Combustion Reaction Rate (CRR) is calculated in the Heat Release (HR) model. The HR model uses, among others, volume and pressure as function of the crank angle as inputs. Whereby, volume versus crank angle is calculated in Chapter 4.1.5 and pressure versus crank angle is obtained from the paper [1].

CRR can be calculated with Vibe functions (Chapter 4.1.6). Vibe functions have shape parameters, which are constants influencing the CRR gradient. The shape parameters are calibrated to match the CRR obtained from the HR model.

The in-cylinder model uses the CRR obtained from the Vibe functions, which replaces the HR model in Figure 4.1. The in-cylinder temperature is calculated with the in-cylinder model, which is used to calculate the pressure as function of the crank angle. The pressure trace is used, among others, as input for the post processing model.

The in-cylinder model using Vibe functions is considered the Vibe based model and the heat release model is considered the post processing model, which will be explained in Chapter 4.4.

4.1.2 Conservation of energy

The following equation is the first law of thermodynamics which describes the conservation of energy. This equation shows the origin of the heat release rates equations GAHRR and NAHRR. [45]

$$m * c_v \frac{dT}{dt} = \dot{Q}_{comb} - \dot{Q}_{loss} - p\frac{dV}{dt} \tag{4.1}$$

$p\frac{dV}{dt}$ is the work done by the system, $\dot{Q}_{comb}$ is the combustion heat release rate, $\dot{Q}_{loss}$ heat loss rate and $m * c_v \frac{dT}{dt}$ is the energy change in the system.
The NAHRR is calculated with the following formula (formula 4.2): [45]

$$NAHRR = \dot{Q}_{comb} - \dot{Q}_{loss} = m * c_v \frac{dT}{dt} + p\frac{dV}{dt} \tag{4.2}$$

The GAHRR is calculated with (Equation 4.3) [45]:

$$GAHRR = \dot{Q}_{comb} = NAHRR + Q_{loss} \tag{4.3}$$

p is the pressure in the cylinder and V is the volume of the cylinder, T the average temperature and c_v the specific heat at constant volume.

4.1.3 Heat loss model

The heat loss through the wall is calculated with a convection heat transfer formula specified on cylinder applications shown in Equation 4.4.

$$Q_{loss} = \sum_{i=1}^{3} A_{th_i} h_c (T - T_{w_i}) \tag{4.4}$$

Where h_c is the heat transfer coefficient estimated by the Woschni model, A_{th_i} is the surface area and T_{w_i} is the temperature of that area. The cylinder walls (i=1), head (i=2) and piston crown (i=3) are all considered in this equation.

Woschni assumes dealing with an ideal gas and therefore the equation used to calculate the heat transfer coefficient is the following:

$$h_c = 130 \frac{1}{D_B^{0.214}} \frac{p^{0.786}}{T^{0.525}} \left(C_3 * c_m + C_4 \frac{p - p_0}{p_1} \frac{V_S}{V_1} T_1 \right)^{0.786} \tag{4.5}$$

D_B is the bore diameter, c_m is the piston (stroke) velocity, T is the temperature in the cylinder. C_3 and C_4 are coefficients changing with the process. C_3 has a different value for 'during gas exchange' phase and 'during compression and expansion' state. In the models for the combustion phase the 'during compression and expansion' value is picked. The formula to calculate this parameter is the following:

$$C_3 = 2.28 + 0.308 \frac{w_t}{c_m} \tag{4.6}$$

Here is assumed that the tangential swirl velocity (w_t) is equal to 0 conform the original model [46]. Therefore the value of 2.28 is assumed for C_3. C_4 has the 'direct injection' and 'pre-chamber' options. In this case it will be the direct injection, resulting in the value of 0.00324 $\frac{m}{sK}$.

4.1.4 Heat Release model

The Heat release model calculates the CRR. CRR is the reaction rate at which fuel combust and can be calculated with the following formula:

$$CRR = \xi = \frac{GAHRR}{LHV_{eff}} \tag{4.7}$$

Where:

$$LHV_{eff} = u_{comb}^{ref} - \Delta u_{comb}^{ref} \tag{4.8}$$

u_{comb}^{ref} is the reference internal energy, that is inserted into the cylinder. The second term shows the change in internal energy compared to the reference term due to temperature changes in the cylinder.

4.1.5 Volume calculation

The volume of the cylinder is

$$V(\alpha) = A_b + L_s * \left[\frac{1}{\epsilon - 1} + \frac{1}{2} * \left\{ \left(1 + cos(\alpha) + \frac{1}{\lambda_{CR}} * \left(1 - \sqrt{1 - \lambda_{CR}^2 * sin^2(\alpha)} \right) \right) \right\} \right] \tag{4.9}$$

Where L_s is the stroke length, λ_{CR} the crank/rod ratio and ϵ is the geometric compression ratio.

4.1.6 Vibe function

The in-cylinder model makes use of the so called Vibe function, which is based on chain reactions occurring in the cylinder, resulting in a prediction of the fuel burn rate.

The approach assumes that oxygen attacks cause fuel molecules to split in active radicals. This can be translated in the following formula:

$$\frac{dn_f^+}{dt} = k * n_f \tag{4.10}$$

When the active radicals increase there is a proportional decrease in fuel molecules:

$$dn_f^+ = -\mu * dn_f \tag{4.11}$$

Combining the two equations gives the following formula for the combustion reaction rate (ξ) also shown in Figure 4.1:

$$\frac{dn_f}{dt} = -\frac{k}{\mu} n_f = \xi \tag{4.12}$$

Where k and μ are reaction constants. In case of a non-Linear Vibe model the two reaction constants are estimated to be as follows:

$$k = f(t) = c_1(t - t_0)^m \tag{4.13}$$

$$\mu = constant = c_2 \tag{4.14}$$

Inserting the above equations in Equation 4.12 gives:

$$\frac{dn_f}{dt} = -\frac{c_1}{c_2} * (t - t_0)^m * n_f = -c_3(t - t_0)^m * n_f \tag{4.15}$$

Further integration over time yields in:

$$\frac{n_f}{n_{f,0}} = e^{-\frac{c_3}{m+1} * (t - t_0)^{(m+1)}} \tag{4.16}$$

The Vibe function is described by X and Z which are the normalized combustion progress and the normalized combustion progress rate respectively:

$$X = 1 - \frac{n_f}{n_{f,0}} = \frac{m_f}{m_{f,0}} \tag{4.17}$$

The m_f is the burnt fuel mass, $m_{f,0}$ denotes the initial mass of the fuel. Introducing Equation 4.16 into Equation 4.17 gives:

$$X = 1 - e^{-\frac{c_3}{m+1} * (t - t_0)^{(m+1)}} \tag{4.18}$$

To simplify this equation parameter 'a' and τ are introduced:

$$a = \frac{c_3}{m+1} * (\Delta t_{comb})^{(m+1)} \tag{4.19}$$

$$\tau = \frac{t - t_0}{\Delta t_{comb}} \tag{4.20}$$

This gives a simplified equation for X: This gives:

$$X = 1 - e^{-a\tau^{m+1}} \tag{4.21}$$

The normalized combustion progress rate can be calculated with integrating Equation 4.21 over τ, resulting in:

$$Z = a * (m+1) * \tau * e^{-a\tau^{m+1}} \tag{4.22}$$

Where 'a' is dependent on the combustion efficiency (η_{comb}), and can be calculated with the following formula:

$$a = -ln(1 - \eta_{comb}) \tag{4.23}$$

The shape parameter 'm' will be changed to gain the best suited pressure trace. Based on an assumed combustion time (Δt_{comb}).

The dual fuel combustion contains the combustion of multiple fuels resulting in a double Vibe function. A Vibe function for diesel (X_{diesel}) and for methanol ($X_{methanol}$).

$$X_{diesel} = b_1 * (1 - e^{-a\tau_{diesel}^{m_1+1}}) + b_2 * (1 - e^{-a\tau_{diesel}^{m_2+1}}) \tag{4.24}$$

$$X_{methanol} = b_3 * (1 - e^{-a\tau_{methanol}^{m_3+1}}) \tag{4.25}$$

The parameters b_1, b_2 and b_3 are tuned to a specific case. Meaning that the model is only specified per RMD and SOI.

When knowing the formulas for X it can be differentiated over τ to obtain Z, which is used to calculate the CRR:

$$\xi = CRR = Z * \frac{m_f^{comb}}{\Delta t_{comb}} \tag{4.26}$$

This means that the combustion time Δt_{comb} needs to be known and earlier assumed to be equal for methanol and diesel. This is estimated to be the time between Start Of Combustion (SOC) and End Of Combustion (EOC), whom are also assumed.

4.1.7 Assumptions

Byungjoo Lee used the in-cylinder pressure, gained from graphs out of Lijiang Wei et al., (2015) [1], read by the naked eye, as input to create the model, to set the Vibe parameters for the in-cylinder model. Important assumptions made in the Vibe based model are summarized below:

1. The initial conditions are not known, therefore p_1 is calculated, based on its polytropic character, with the following equation:

$$p_1 = \frac{p_2}{r_c^{n_{comp}}} \tag{4.27}$$

   Where p_2 is the pressure at point TDC, right before the iso-volumetric combustion. n_{comp} the polytropic compression constant and r_c describes the effective compression ratio and can be calculated with:

$$r_c = \frac{V_1}{V_2} \tag{4.28}$$

2. The gasses are considered ideal, which means that the internal enthalpy and energy of the gasses in the cylinder are functions of the temperature.

3. Methanol is assumed to be completely evaporated in the intake port before the inlet valve closes. The model is set up to calculate from the assumed SOC, meaning ID estimation is included.
4. Methanol is homogeneous pre-mixed before entering the cylinder.
5. The fuel is combusted completely when opening the exhaust valve.
6. Both fuels have the same combustion duration.

4.2 Two zone conventional dual fuel combustion model

The two zone model, created by TNO, is a model for dual fuel internal combustion engines using NG and diesel. This model has to be adjusted for the purpose of combusting methanol instead of NG.

The two zone model is divided into two zones, namely the burnt (b) and unburnt (u) zone. A schematic is shown in Figure 4.3.

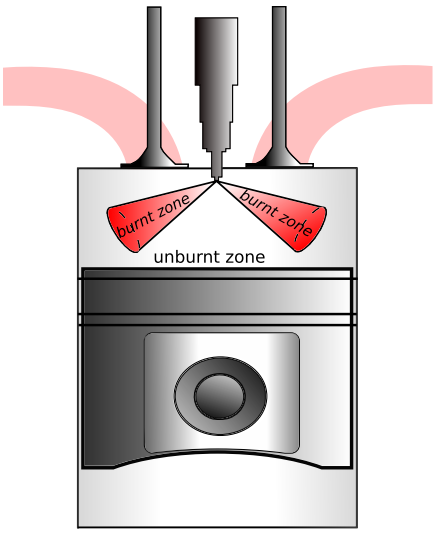

FIGURE 4.3: Schematic burnt and unburnt zone.

At t = 0 the cylinder contains only one zone, the unburnt zone. This is the mixture of methanol and air. The burnt zone is formed when the injection of diesel is introduced. The fuel injection causes the burnt zone to increase. The second factor that causes the burnt zone to increase is the entrainment of the unburnt zone into the burnt zone, resulting in a decrease of the unburnt zone. In the burnt zone, combustion can take place, meaning the burnt zone is the reaction zone. Caused by fuel combustion, only the composition of molecules changes in the burnt zone. In the unburnt zone no reactions take place and therefore the composition remains the same.

The two zones have their own properties like volume, temperature, mass and amount of molecules. The pressure is assumed to be equalized in both zones (p_u=p_b) at all times.

4.2.1 Thermodynamic equations

The model describes the combustion with, energy conservation equations, equations of state and mass conservation equations. The ODE 15s solver in Matlab is used to solve these differential equations.

The **energy conservation equation** for the burnt zone is derived:

$$\Delta E = \sum E_{in} - \sum E_{out} + \Delta Q + \Delta W \tag{4.29}$$

$$= [e\Delta m]_{in} - [e\Delta m + p\Delta V]_{out} + [h\Delta m]_{reaction} + \Delta Q + \Delta W \tag{4.30}$$

$$= [h\Delta m]_{in} - [h\Delta m]_{out} + [h\Delta m]_{reaction} + \Delta Q + \Delta W \tag{4.31}$$

E is the energy going into the system and out of the system, ΔQ is the change of heat in the system and ΔW is the work done by the system. p is the pressure inside the system, V is the volume of the system, e is the specific energy and h the specific enthalpy. When deriving the differential equation of the energy conservation equation the following formula is the result:

$$\frac{\delta E}{\delta t} = \sum \left[h\frac{dm}{dt}\right]_{exchange} + \left[h\frac{dm}{dt}\right]_{reaction} + \frac{dQ}{dt} - p\frac{dV}{dt} \tag{4.32}$$

$$\frac{\delta E}{\delta t} = m\frac{de}{dt} + e\frac{dm}{dt} \tag{4.33}$$

$$\frac{de}{dt} = c_v\frac{dT}{dt} + T\frac{dc_v}{dt} \tag{4.34}$$

$$\frac{dc_v}{dt} = \frac{d}{dt}\left[\sum y_i c_{v_i}\right] = \sum \left[c_{v_i}\frac{dy_i}{dt} + y_i\frac{dc_{v_i}}{dt}\right] \tag{4.35}$$

$$y_i\frac{dcv_i}{dt} = 0 \tag{4.36}$$

m is the mass, c_v specific heat with constant volume, T is the temperature in the system and y the mass fraction of species i. The species considered in this model are: diesel, O_2, N_2, CO_2, H_2O and methanol. Combining these equations gives the following usable equation for the burnt zone:

$$mc_v\frac{dT}{dt} + mT\sum c_{v_i}\frac{dy_i}{dt} + e\frac{dm}{dt} = \sum \left[h\frac{dm}{dt}\right]_{exchange} + \left[h\frac{dm}{dt}\right]_{reaction} + \frac{dQ}{dt} - p\frac{dV}{dt} \tag{4.37}$$

Reactions do not occur in the unburnt zone resulting in:

$$\frac{dy_i}{dt} = 0 \tag{4.38}$$

$$\left[h\frac{dm}{dt}\right]_{reaction} = 0 \tag{4.39}$$

That gives the following energy conservation equation for the unburnt zone:

$$mc_v\frac{dT}{dt}+e\frac{dm}{dt}=\sum\left[h\frac{dm}{dt}\right]_{exchange}+\frac{dQ}{dt}-p\frac{dV}{dt} \tag{4.40}$$

The **state equation** is used and is based on the assumption of having an ideal gas, which gives the ideal gas law:

$$pV=nR_1T=m\frac{R}{M}T \tag{4.41}$$

R_1 is the specific gas constant and R is the universal gas constant, n is the amount of mole, and M the molar mass. The differential equation of the state equation is:

$$\frac{d}{dt}(pV)=\frac{d}{dt}(nRT)=\frac{d}{dt}\left(m\frac{R}{M}T\right) \tag{4.42}$$

The chain rule is used to differentiate this equation, resulting in the following equation:

$$p\frac{dV}{dt}+V\frac{dp}{dt}=m\frac{R}{M}\frac{dT}{dt}+mT\frac{1}{M}\cancelto{0}{\frac{dR}{dt}}_{R=const}+mTR\frac{d}{dt}\left(\frac{1}{M}\right)+\frac{R}{m}T\frac{dm}{dt} \tag{4.43}$$

$$\frac{d}{dt}\left(\frac{1}{M}\right)=\frac{d}{dt}\left(\sum\frac{y_i}{M_i}\right)=\left(\sum\frac{1}{M_i}\frac{dy_i}{dt}\right) \tag{4.44}$$

Implementing Equation 4.44 into Equation 4.43 it results in the final equation for the burnt zone:

$$p\frac{dV}{dt}+V\frac{dp}{dt}=m\frac{R}{M}\frac{dT}{dt}+mTR\sum\left(\frac{1}{M_i}\frac{dy_i}{dt}\right)+\frac{R}{M}T\frac{dm}{dt} \tag{4.45}$$

For the unburned zone the same assumption as for the energy equation is made (Equation: 4.38). This assumption assumes that the fractions of the species in the unburnt zone do not change, meaning no reaction in the unburnt zone. This gives the following equation:

$$p\frac{dV}{dt}+V\frac{dp}{dt}=m\frac{R}{M}\frac{dT}{dt}+\frac{R}{m}T\frac{dm}{dt} \tag{4.46}$$

As described before the burnt and unburned zones have their own properties. So when using the equations the zone specific values are used. For example for the volume (V) in the unburnt case V_u is used and for the burnt case V_b is used.

The **mass conservation** equation is stated below. y_i is the mass fraction of species i. m the total mass and m_i the mass accessory to the species i.

$$m_i=y_im \tag{4.47}$$

The differential equation of this formula is:

$$\frac{dm_i}{dt}=y_i\frac{dm}{dt}+m\frac{dy_i}{dt} \tag{4.48}$$

These thermodynamic equations are valuable for all sorts of fuels, only the fuel parameters will change to methanol instead of NG.

4.2.2 The sub models

Making use of the thermodynamic equations the mass exchanges are essential. These exchanges are dependent on several processes. These processes are described in the sub models. The used sub models in the two zone model are listed as below:

- Fuel injection model
- Spray entrainment model
- Ignition model
- Methanol combustion model
- Diesel combustion model
- Heat transfer model based on Woschni

Fuel injection model

The fuel injection model describes the fuel entering the cylinder caused by fuel injection. In case of dual fuel combustion with methanol and diesel, the injected fuel is diesel.

The amount of fuel injected over time ($\frac{dm_{b,fuel}}{dt}$) is calculated by calculating the injection velocity based on its injection pressure (dP_{inj}), discharge coefficient (C_d) and the diesel fuel density (ρ_f) by:

$$v_{inj} = C_d \sqrt{\frac{2 * dP_{inj}}{\rho_f}} \tag{4.49}$$

The previous correlation is used to calculate the mass flow rate for a single nozzle hole by:

$$\left(\frac{dm_f}{dt}\right)_{max} = \rho_f * v_{Inj} * 0.25 * \pi * D_{noz}^2 \tag{4.50}$$

The injection time is dependent on the total amount of injected fuel (m_{inj}), the number of nozzles (N_{noz}) and the mass flow rate calculated in the previous formula. The equation below is used to calculate the time needed to inject all fuel:

$$dt_{inj} = \frac{m_{inj}}{N_{noz} * \left(\frac{dm_f}{dt}\right)_{max}} \tag{4.51}$$

In Figure 4.4 is shown how the massflow of diesel enters the cylinder. It is assumed that during the first 5% of the injection time the flow is linear increasing. The

last part of the injection is linear decreasing resulting in Figure 4.4. The injection mass flow is indicated with $\frac{dm_{b,Fuel}}{dt}$.

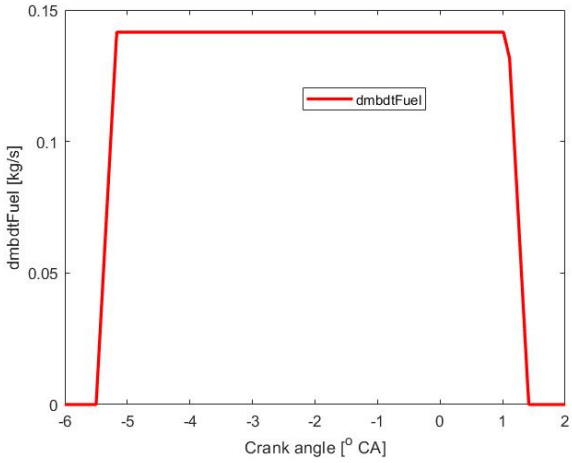

FIGURE 4.4: dmbdtFuel: The attribution of the injection of diesel in the burnt zone formation

Spray entrainment model

At the surface of the injection spray there will be mass entrainment of unburnt zone into the burnt zone. This mass entrainment is essential for combustion due to the entrainment of O_2 into the burnt zone. The **spray entrainment model** calculates this mass entrainment.

The total change in spray volume, including the influence of diesel injection and mass entrainment from the unburnt zone into the burnt zone, can be calculated with the spray formation based on the model of Hiroyasu.

The total mass change of the burnt zone ($\frac{dm_b}{dt}$) depends on the density of the unburnt zone (ρ_u) and the change in burnt zone volume over the time ($\frac{dV_b}{dt}$). The total mass change of the burnt zone can be calculated with the following formula: [47]

$$\frac{dm_b}{dt} = \rho_u * \frac{dV_b}{dt} \tag{4.52}$$

The burnt zone volume change ($\frac{dV_b}{dt}$) is calculated with Equation 4.53 out of paper [47].

$$\frac{dV_b}{dt} = \frac{\pi}{3} tan^2(\theta) \frac{dS}{dt} \tag{4.53}$$

θ is the spray angle and the $\frac{dS}{dt}$ is the change in penetration length and can be calculated by differentiating the penetration length (S).

The penetration length (S) changes over time and is dependent on the pressure difference of the injection pressure and the in-cylinder pressure (ΔP), ρ_u and the nozzle hole diameter ($d_{h,o}$) as shown in the equation below [47]:

$$S = 2.95 \left(\frac{\Delta P}{\rho_u} \right)^{0.25} * \sqrt{d_{h,0} * t} \tag{4.54}$$

The formula for the change in penetration length ($\frac{dS}{dt}$) is [47]:

$$\frac{dS}{dt} = 2.95 * \left(\frac{\Delta P}{\rho_u} \right)^{0.25} * \sqrt{d_{h,0}} * \frac{1}{2} \frac{1}{\sqrt{t}} \tag{4.55}$$

The spray angle (θ) can be calculated with the following formula, which is called Siber's vaporising equation [48]:

$$\theta = 2 * tan^{-1} \left(0.26 * \left(\frac{\rho_u}{\rho_f} \right)^{0.19} - 0.0043 * \sqrt{\frac{\rho_f}{\rho_u}} \right) \tag{4.56}$$

The diesel fuel density (ρ_f) is constant (830 kg/m^3).

The two zone model calculates the total volume change of the burnt zone with Equation 4.53. Tuning parameter, tweakSpray, is introduced to compensate the gap between reality and the calculated value.

The effect of entrainment of the unburnt zone into the burnt zone can be calculated when assuming only two effects causes the burnt zone to increase, namely entrainment and fuel injection. The effect of entrainment of unburnt zone into burnt zone ($\frac{dm_{b,Spray}}{dt}$) can be calculate by subtraction of the fuel injection from the total mass change of the burnt zone caused by the spray ($tweakSpray * \rho_u * \frac{dV_b}{dt}$). This correlation is shown in Equation 4.57. Figure 4.5 shows the relation between the fuel injection and the entrainment of unburnt zone into the burnt zone.

$$tweakSpray * \rho_u * \frac{dV_b}{dt} = \frac{dm_{b,Spray}}{dt} + \frac{dm_{b,fuel}}{dt} \tag{4.57}$$

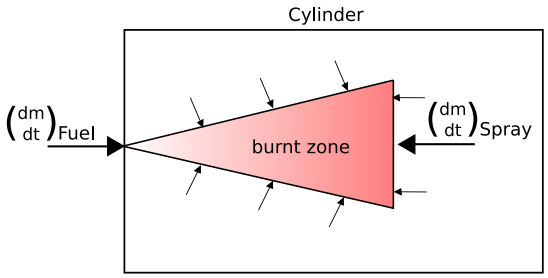

FIGURE 4.5: Schematic burnt zone mass change caused by the spray.

Equation 4.57 contains a tuning parameter, 'tweakSpray'. The smaller the tweakSpray the smaller the influence of the conversion of the unburnt zone by entrainment. Figure 4.4 and 4.6 are the mass of fuel injection and the total mass change

of the burnt zone, respectively. Figure 4.6 used tweakSpray = 1 and therefore the calculated total mass change of the burnt zone is as shown. Figures 4.4 and 4.6 show a big difference in the range, whereby the fuel injection influence ($\frac{dm_{b,fuel}}{dt}$) could be neglected. In reality, the injection of fuel also causes the burnt zone to increase. The small contribution of the spray injection is corrected by the tweakSpray. Based on the assumption that the injection of fuel has a considerable contribution in the conversion of unburnt zone into burnt zone, the tweakSpray has a value below 1, and above 0.

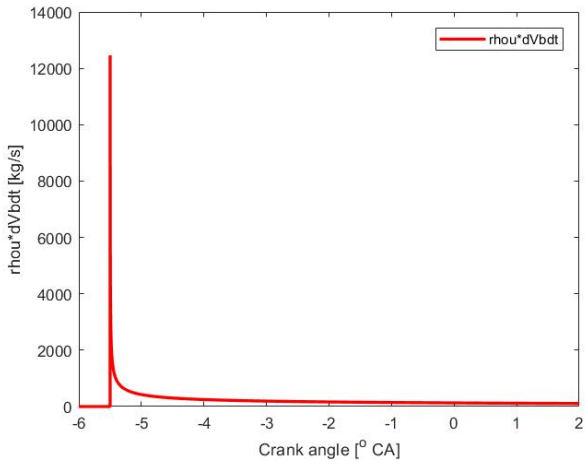

FIGURE 4.6: rhou x dVbdt: The total mass change of the burnt zone, when the tweakSpray=1.

Ignition model

The previous sub models describe the change of the burnt zone mass during injection. Now the start of ignition needs to be calculated which is done with the **Ignition model**.

The Ignition Delay (ID) is calculated with an Arrhenius equation [49]:

$$\tau = aIgn * p^{-n} * \phi^{-m} * e^{\frac{B}{T_b}} \tag{4.58}$$

In the model, the variables B, m, n are hard coded in the model with the values 5000, 1.04, 2.5 respectively. aIgn is also a tuning parameter whom describes the frequency of correct oriented collisions between molecules, which has a different value for each different reaction. The ID is caused by the ability of diesel to ignite under certain circumstances. The provided model was assigned to be used with NG and diesel as fuels, where diesel is the pilot fuel as well. Therefore the values for B, m and n are adopted from the provided model. The Equation 4.58 is dependent on ϕ therefore can be assumed that the ID has a predictive character when changing the fuel composition while this changes ϕ.

ϕ is the global fuel-air equivalence ratio calculated with the following formula:

$$\phi = \frac{1}{\lambda} \tag{4.59}$$

λ is the air excess ratio and can be calculated when knowing the mass fraction of oxygen in air (mf_{O_2}), the mass of air inserted into the cylinder divided by the stoichiometric air:

$$\lambda = \frac{m_{air} * mf_{O_2}}{(m_{methanol} + m_{diesel})s_{Fuel}} \tag{4.60}$$

s_{Fuel} is the mass based stoichiometric coefficient for heptane which is a simplification for the calculation of the stoichiometric air. The mass based coefficient for methanol is now considered similar to heptane (diesel), however, methanol needs less air.

In table 4.1, the variables B, m, n and aIgn are defined based on [50]. These values are specified for n-heptane and are different compared to the values used in the provided two zone model. A following research might be able to optimize the values of the variables B, m, n.

TABLE 4.1: Constants used for ID τ

Fuel	aIgn	B	m	n
n-heptane	10.2e9	3700	0.7	1.12

Methanol combustion model

At this point the formation of the burnt zone, also known as the reaction zone, is known and the Start Of Combustion (SOC) can be calculated. The ignition starts an a flame will propagate. The methanol combustion model describes the flame propagation which takes place at the boundaries of the burnt zone and results in an added factor for the conversion of unburnt zone into burnt zone.

The **methanol combustion** model calculates the turbulent flame propagation velocity (u_t) from the laminar flame propagation velocity (u_1) with Equation 4.61. This equation contains tuning parameter, CTFlame. CTFlame is a conversion factor used to estimate the turbulent flame propagation speed based on the laminar flame propagation speed. With experiments it is possible to measure the value of CTFlame. An other possibility to obtain a value for CTFlame is making use of Equation 4.66 and 4.67.

$$u_t = CTFlame * u_l \tag{4.61}$$

The laminar flame propagation velocity for methanol can be calculated with the correlation below [51]:

$$u_l = u_{l,0} * \left[\frac{T_u}{T_0}\right]^{a_T} * \left[\frac{P}{P_0}\right]^{b_T} (1 - 2.06 x_b^{0.77}) \tag{4.62}$$

P is the pressure in the cylinder, T_u is the temperature of the unburnt mixture. x_b is the fraction of unburnt gas dilutend, which is assumed to be zero caused by the

absence of an Exhaust Gas Recirculation (EGR). T_0 and P_0 are the initial temperature and pressure. The reference laminar flame velocity ($u_{l,0}$) is based on the fuel-air equivalence ratio (ϕ). a_T, b_T and $u_{l,0}$ can be calculated with the following formulas[51]:

$$a_T = 2.18 - 0.8(\phi - 1) \tag{4.63}$$

$$b_T = -0.16 + 0.22(\phi - 1) \tag{4.64}$$

$$u_{l,0} = B_m + B_\phi * (\phi - \phi_m)^2 \tag{4.65}$$

ϕ_m, B_m and B_ϕ are 1.11, 0.369 m/s and -1.405 m/s respectively [51]. ϕ is the global fuel-air equivalence ratio described in Equation 4.59.

The laminar flame speed (u_l) has a value around 1.7 m/s, which is shown when CTFlame is equal to 1. In reality the turbulent velocity is higher than the laminar flame velocity. The method of "Damkohler and derivatives" has a correlation to calculate the turbulent flame speed [51] :

$$u_t = u^* + u_l \tag{4.66}$$

This results in a possible correlation for CTFlame (Equation 4.67). This correlation resulted in a value of CTFlame of 4.7. In a future research the "Damkohler and derivatives" correlation can be used in the model as a possible improvement.

$$CTFlame = \frac{u^* + u_l}{u_l} \tag{4.67}$$

$$u^* = u_{TDC} * \left(1 - 0.5 * \frac{CA}{45}\right) \tag{4.68}$$

$$u_{TDC} = c_m * 0.75; \tag{4.69}$$

CA is the crank angle, u_{TDC} is the c_m is the mean engine speed which is calculated by the rotational speed (N_{eng}) and the engine stroke (S) by:

$$c_m = S * \frac{N_{eng}}{60} \tag{4.70}$$

The range of CTFlame is expected to be between 1 and 4.7.

Diesel combustion model

The remaining combustion is the combustion of diesel in the burnt zone. Similar to the ignition model an Arrhenius equation is used. The burning rate of diesel (dmbdtIcinicine) in the burnt zone is calculated with:

$$dmbdtIcinicine = \left(\frac{1}{Yib(1)}\right) * min\left(mbFuel, \frac{mbO2}{sFuel}\right) * kIcinicine * p^{2.5} * \phi^{1.04} * e^{(-\frac{5000}{Tb})} \tag{4.71}$$

Where $Yib(1)$ is the fraction of diesel in the burnt zone. The term $min\left(mbFuel, \frac{mbO2}{sFuel}\right)$ calculates the limiting factor for combustion. This is either $mbFuel$, which is the mass of diesel inside the burnt zone and $\frac{mbO2}{sFuel}$ mass of oxygen in the burnt zone divided by the mass based stoichiometric ratio, which is the amount of diesel that can react with the oxygen in the burnt zone. The burning rate is established by the mass of diesel divided by the time it is needed for the diesel to react (τ) and is calculated with an Arrhenius equation. Similar to equation 4.58.

$$\frac{1}{\tau} = kIcinicine * p^{2.5} * \phi^{1.04} * e^{(-\frac{5000}{Tb})} \tag{4.72}$$

kIcinicine has a similar meaning as aIgn and describes the number of well oriented collisions between molecules. The same range as aIgn can be used due to the similar calculation method. Take in mind that :

$$kIcinicine^{-1} = aIgn \tag{4.73}$$

In the internship raport of A.A. Nair [52] the value for kIcinicine used was 1e-13 and therefore included in the range, giving a range of 1e-13 until 15e-10.

In Table 4.2 expected ranges for the tuning parameters are given. These tuning parameters influence the two zone model. In the validation chapter of the two zone model, the sensitivity of these tuning parameters will be verified. When the tuning parameters have limited influence on the model it means that the calculations made in the model are independent on tuning parameters, which makes it possible to use an unadjustable constant instead of a variable.

TABLE 4.2: Model tuning parameters

Parameter	**Range**	**Description**
TweakSpray	0 - 1	Coefficient that determines the effect of the burnt volume change to the burnt mass change rate when assuming a perfect cone spray.
aIgn	10.2e9 - 15e10.	Coefficient that influences the ID
CTFlame	1-4.7	This coefficient introduces the relationship between laminar burning and turbulent burning.
kIcinicine	1e(-13) - 15e(-10)	Determines the rate at which diesel burns

Heat transfer model

The last sub model is the **Heat transfer model**. This model is used to calculate the heat loss in the cylinder. Similar to the Vibe based model this is based on Woshni.

The swept volume (V_s) is used to calculate the heat transfer coefficient h_c and is calculated by the following formula:

$$V_s = (1/4) * \pi * B^2 * S \tag{4.74}$$

B is the bore diameter and S the stroke length.

p_m is the polytropic compression pressure. This is the pressure caused by the piston movements only, meaning pressure change caused by combustion is not taken into account. In Equation 4.5 this is referred to as p_0 and is calculated with the same formula as below:

$$p_m = p_0 = p_1 * \frac{V_1}{V}^k; \tag{4.75}$$

V_1 is in cylinder volume after the inlet valves are closed. p_1 is the initial pressure at V_1 and k is the polytropic compression constant and has a value of 1.37 in the two zone model. In the Vibe based model n_{comp} is used for the poyltropic compression constant and has the value of 1.365.

$$w = C_1 * c_m + C_2 * \frac{p - p_m}{p_1} \frac{V_s}{V_1} * T_1 \tag{4.76}$$

Coefficients C_1 and C_2 are 2.28 and 3.24e-3, respectively. Similar to the C_3 and C_4 values in the Vibe based model described in Equation **??** in Chapter 4.1.

Piston stroke velocity c_m is calculated with the engine velocity (N_{eng}) and the stroke length (S) using the following formula:

$$c_m = 2 * S * \frac{N_{eng}}{60} \tag{4.77}$$

The heat transfer coefficient (h_c) is than calculated with:

$$h_c = 130 * B^{-0.2} * p^{0.8} * T^{-0.55} * w^{0.8} \tag{4.78}$$

Inserting Equation 4.76 into 4.79 results in the following equation:

$$h_c = 130 * \frac{1}{B^{0.2}} * (p)^{0.8} * \frac{1}{T^{-0.55}} * \left(C_1 * c_m + C_2 * \frac{p - p_m}{p_1} \frac{V_s}{V_1} * T_1 \right)^{0.8} \tag{4.79}$$

The differences in the calculation between the two zone and the Vibe based model are the used exponents. This causes different outcomes for the heat transfer coefficient in the two models. The loss of heat is calculated according to Equation 4.4. In the Vibe based model this is split into the wall, head and piston crown. The two zone model only makes use of the wall temperature.

4.3 Experimental data evaluation

This chapter gives an overview on differences and similarities of the two models and the input parameters of the model.

The basic input parameters are the engine specifications and the fuel specifications, whom are similar for both models. These parameters are also used in the experiments in the paper [1]. Table 4.3 indicates the engine parameters of the engine used and Table 4.4 gives an overview of the fuel properties.

TABLE 4.3: Engine specifications [1]

Description	**Specification**
Engine type	6-cylinder DI engine
Bore x stroke [mm]	126 x 130
Connecting rod lengt [mm]	219
Crank radius [mm]	65
Displacement [L]	9.726
Compression ratio	17
Max. torque/speed [N m] / [rpm]	1500/ 1200-1500
Rated power/ speed [kW]/[rpm]	247/1900
Fuel injection system	Common rail
Combustion chamber	ω bowl in pistion
Intake valve open	-36^{o}CA ATDC
Intake valve close	246^{o}CA ATDC
Exhaust valve open	-258^{o}CA ATDC
Exhaust valve close	30^{o}CA ATDC

TABLE 4.4: Properties of methanol and diesel used during the experiments [1]

Properties	**Diesel**	**Methanol**
Molecular formula	C_{10} C_{15}	CH_3OH
Molecular weight	190-220	32
Cetane number	51	<5
Lower heating value [MJ/kg]	42.5	19.7
Density at 20^{o}C [kg/m^3]	840	790
Viscosity at 20^{o}C	2.8	0.59
Heat of evaporation [kJ/kg]	260	1179
Stoichimetric air to fuel ratio	14.7	6.45
Autoignition temperature [^{o}C]	316	464
Carbon content [%wt]	86	37.5
Hydrogen content [% wt]	14	12.5
Oxygen content [% wt]	0	50
Sulfur content [ppm wt]	<50	0
Flame temperature [^{o}C]	2054	1890

The specifications of methanol and diesel can differ in different papers. Diesel has the biggest fluctuations due to its variety in molar formulas. Therefore the specifications described in Table 4.4 are used for both models. This table was provided in the paper of [1], however the paper gives a reference on this table which suggest the fuels have not been tested before using them in the experiments. This gives the first assumption in the models, namely these properties are the exact properties of the fuels tested.

TABLE 4.5: RMD values

RMD	Diesel [kg/h]	Methanol [kg/h]	Energy fraction
0	46.62	0	0 %
0.55	37.29	20.46	20 %
1.54	27.98	43.01	40 %

To understand the RMD better, the corresponding energy fractions are specified in Table 4.5.

An extended overview of input parameters is shown in Table A.1 in Appendix A.

The differences and similarities of the models are addressed in order to compare the two models and verify them.

Both model use the basic principles of a thermodynamic system such as the **energy conservation** equations, **mass conservation** equations and **state** equations.
The initial pressure is not known and is calculated with the polytropic character as in Equation 4.27. The polytropic exponential (n_{comp}) is for both cases 1.365. P2 = 12.15 MPa is used in the two zone model, which was read out the experimental pressure trace [1] and in the Vibe based model P_2 is calculated as the pressure at SOC which is an input parameter in the model, which is in case of RMD = 1.54, SOI=-5.5 10.2MPa. SOC can only be known when experiments are done and therefore contains errors when applying this calculation. The effective compression ratio (r_c) can be calculated with Equation 4.28. The inconsistent value in this equation is V_1, which is calculated based on the Inlet Valve Closed (IVC) given in the paper [1]. The definition of IVC can be explained in more ways than one. One definition of IVC is when the valve is in its stamp. An other definition of IVC is when the air-fuel supply stops entering the cylinder. This makes the value of r_c unreliable and therefore in the two zone model this effective compression ratio is tuned to the best fit of the polytropic compression pressure trace. The Vibe based model uses the value of IVC given in the paper to calculate V_1 and therefore V_2 and r_c. This results in two different values for r_c, namely 12 and 13.2427 for the two zone and Vibe based models respectively.

The main difference is the way of moddeling the combustion reaction rate. In the Vibe based model this is described with a double Vibe function based on chain reactions occuring in the cylinder during combustion. This double Vibe function has multiple shape and tuning parameters described in Equations 4.24 and 4.25. b_1, b_2, b_3, m_1, m_2 and m_3 are tuned for each specific case, which means that the expectation is that the model is not accurate when changing the engine, RMD or SOI for example. The two zone model describes this combustion reaction rate with several sub models where the change of fuel mass is key. There are two mass flows described, namely the mass change of the burnt zone caused by injection of diesel, entrainment of unburnt zone into the burnt zone and after the ignition the flame propagation velocity. In the burnt zone only a combustion reaction can take place. The second flow is the combustion of fuel in the burnt zone resulting in a conversion of fuel into combustion products. The two zone model is

Heat loss in the cylinder is both calculated with Woshni, only the parameters have small differences in values.

An overview on the above described differences and similarities is given in Table 4.6

TABLE 4.6: An overview of differences and similarities in the two models

	Vibe based model	**Two zone model**
Energy conservation	Used	Used
Mass conservation	Used	Used
State equation	Used	Used
Initial pressure	Polytropic compression with P2 = 11.711MPa and V_1 based on the given IVC	Polytropic compression with P2 = 12.15MPa and r_c = 12
Combustion velocity	Vibe functions, assumption of SOC	Fuel injection, spray entrainment, ignition, methanol combustion (Flame propagation) and the diesel combustion model
Heat loss model	Woschni (Equation 4.5) T_{wall}, T_{piston} and T_{crown} are taken into account	Woschni (Equation 4.79) only T_{wall} is taken into account.
Model useage	Between SOC and EOC	4 strokes (intake, compression, power, and exhaust)

4.4 Post processing model

In this chapter the post processing model will be described. This model is the tool to validate the two zone and the Vibe based models. This post processing model needs a pressure trace as most important input. The output is: the HRR, CHR, ID, efficiency, maximum mean in-cylinder temperature and the IMEP. Figure 1.1 in Chapter 1.3 shows a graphical overview on how the post processing model is used.

The heat release model used in the set up of the Vibe based model (Figure 4.2 in Chapter 4.1) is used for the post processing model. Small adjustments are made to run the heat release model independently. Equations for calculating: CHR, indicated work, IMEP, the efficiency and the ID are added to the model and is called the **'post processing model'**.

The GAHRR was an output of the heat release model of Buyongjoo Lee and is used to calculate the cumulative heat release by integrating over Inlet Valve Close (IVC) and Exhaust Valve Open (EVO):

$$CHR = \int_{IVC}^{EVO} GAHRR \quad d\alpha \tag{4.80}$$

The total energy content inserted into the cylinder is the energy content of both fuels (E_{fuel}) and is calculated with Equation 4.81. In case there are no losses (total efficiency of 100%), E_{fuel} is the amount of energy released in the cylinder.

$$E_{fuel} = m_{methanol} * LHV_{methanol} + m_{diesel} * LHV_{diesel} \tag{4.81}$$

The indicated work (W_i) is the reversible work and can be calculated with Equation 4.82. The indicated work is bigger than the actual work delivered by the engine while not all engine losses are included.

$$W_i = \int_{V_{IVC}}^{V_{EVO}} P \quad dV \tag{4.82}$$

The pressure (p) is known from the input and the volume is calculated with Equation 4.84. The distance between the cylinder head and the piston (L_p) is calculated with Equation 4.83, which is used in the calculation of the cylinder volume togther with the piston cross-sectional area (A_b).

$$L_p = L_s * \left[\frac{1}{\epsilon - 1} + \frac{1}{2} \left\{ (1 - cos\alpha) + \frac{1}{\lambda_{CR}} \left(1 - \sqrt{1 - \lambda_{CR}^2 * sin^2(\alpha)} \right) \right\} \right] \tag{4.83}$$

$$V = L_p * A_b \tag{4.84}$$

IMEP is the indicated mean effective pressure and is calculated with:

$$IMEP = \frac{W_i}{V_s} \tag{4.85}$$

The indicated efficiency is calculated with the following formula:

$$\eta_i = \frac{W_i}{E_{fuel}} \tag{4.86}$$

The maximum in-cylinder temperature is the maximum value of the in-cylinder temperature trace. This in-cylinder temperature trace is calculated using the state equation. The ID is established to be the CA05 minus the Start Of Injection (SOI). CA05 is gained from the CHR where 5% of the total heat was already released. This gives the following formula for the ID:

$$ID = CA05 - SOI \tag{4.87}$$

Chapter 5

Model validation results

In this chapter the results of the two models, the two zone and Vibe based model, are described and validated. To validate these models, the post processing model described in chapter 4.4 needs to be validated with the experimental results [1]. When having validated post processing results, the two zone and Vibe based models are compared to the experimental data which is also inserted into the post processing model.

5.1 Post processing model

The post processing model needs a pressure trace as input. The measured pressure trace from the experiments [1] is used as input in the post processing model to calculated the GAHRR and is compared with the GAHRR from the experiments [1].

In Table 5.1 results from the reference paper [1] are shown. These results are used to verify the accuracy of the post processing model. This means that the input of engine parameters are equal to the engine parameters used in the paper[1]. The pressure traces of four cases are used for the validation, namely RMD = 1.54 with three different diesel injection timings -5.5, 0 and 3 aTDC and RMD = 0 with SOI = -5.5 ^{o}CA.

TABLE 5.1: Results from the experiments [1]

RMD	Injection timing [^{o}CA aTDC]	Break thermal efficiency [%]	BMEP [MPa]	T max [K]	ID [^{o}CA]
0	-5.5	40.9	1.46	1865	5.4
1.54	-5.5	39.8	1.46	1872	7.2
1.54	0	35.3	1.30	1730	8.7
1.54	3	33.7	1.23	1735	9.5

In the paper [1] the BTE is used instead of the Indicated Thermal Efficiency (ITE), which cannot be calculated from the data provided. The difference between BTE and ITE is the mechanical efficiency which should be between 70% and 92% [53]. Therefore the difference between BTE and ITE are the mechanical losses. The mechanical efficiency will differ when for example the engine load or the engine speed differs. The BMEP and IMEP have the same differences as the BTE and ITE due to including mechanical losses in the BTE.

In Figure 5.1 and 5.2, the differences of the heat release from the post processing model (heat release post processing) and the experimental data (Reference) are shown. Figure 5.1 is based on a RMD = 0 case, meaning only diesel operation, and in Figure 5.2 the fuel contains 40% methanol (energy based), indicating RMD = 1.54.

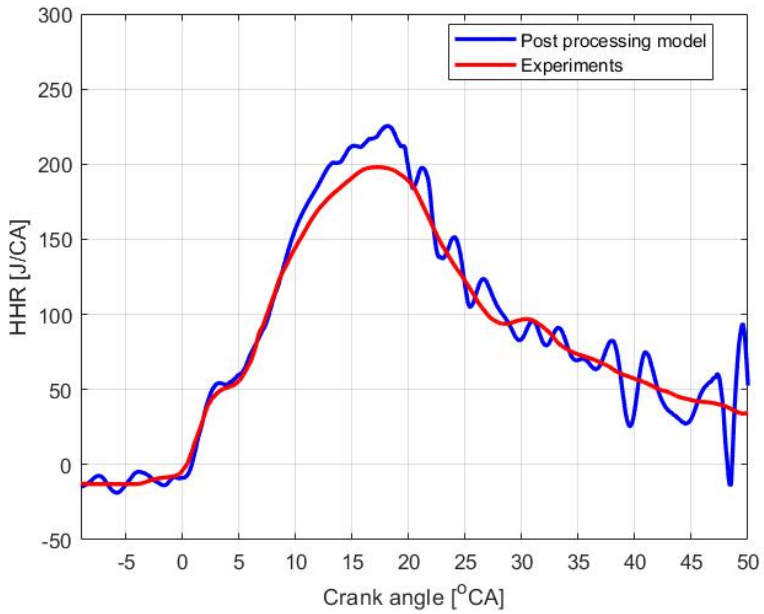

FIGURE 5.1: HRR from pressure trace and data with RMD=0

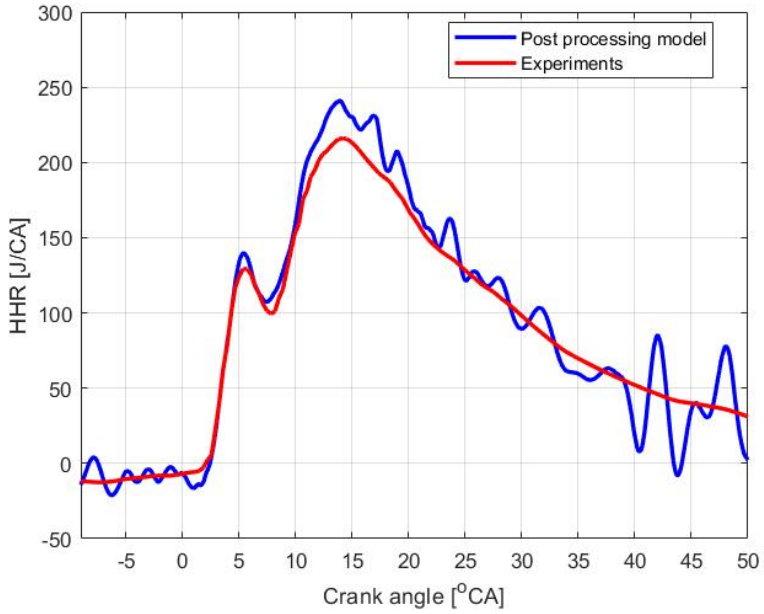

FIGURE 5.2: HRR from pressure trace and data with RMD=1.55

The graphs (Figure 5.1 and 5.2) give a good indication of the accuracy of the post processing model. The model corresponds closely with the experimental curve

(Figure 5.1 and 5.2), but slightly over estimates the HRR for both the RMD cases, however the peak heat release of the post processing model is slightly higher than the one from the experimental data. The spiky behaviour of the post processing model is due to use of a different filter compared to the paper. To establish the over-estimation the CHR is plotted against the crank angle in Figure 5.3. Higher CHR results in higher calculated indicated efficiencies, IMEP and indicated work (Table 5.2).

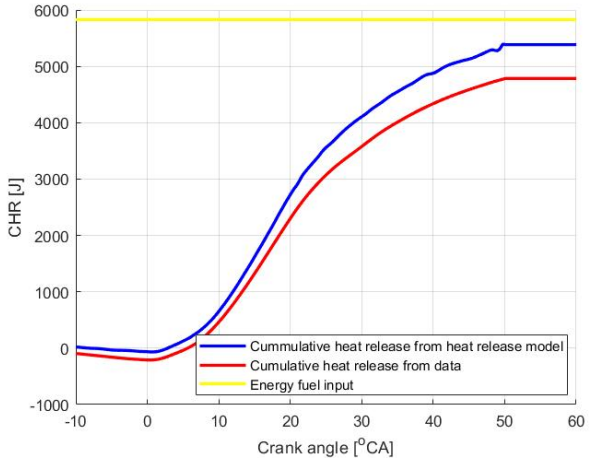

FIGURE 5.3: CHR from pressure trace and data at RMD = 0, SOI of 3^oCA aTDC

The GAHRR of the post processing model and the GAHRR of the experimental data [1] are plotted in Figure 5.3. The results for RMD = 0 are shown in Figure 5.3, where the yellow line is the energy content of the fuel inserted into the cylinder, the blue line denotes CHR of the post processing model and the red line is the CHR of the experimental data. As expected, the CHR of the post processing model is higher than the experimental CHR. Note that CHR should be below the fuel energy in order to meet the energy conservation law. Despite the deviation in the CHR results between the two approaches the post processing results meet the above criteria.

As evident from Figures 5.1 and 5.2, the post processing model gives higher HRRs compared to the experimental results [1]. This can indicate that the heat loss is calculated differently in the two approaches. In the post processing model the wall, piston crown and cylinder head temperature are assumed to be 400K, 580K and 600K respectively, where from the experiments [1] the temperatures are not known. In an attempt to study the models response to changes in initial temperatures, CHR values are plotted in Figure 5.4 for RMD 1.54 with with 80% and 120% of the initial temperatures (instead of 400K, 400*0.8K and 400*1.2 were used). CHR serves as a good indicator to analyse the sensitivity to initial temperature inputs. The diesel injection timing in the graph is 3^oCA.

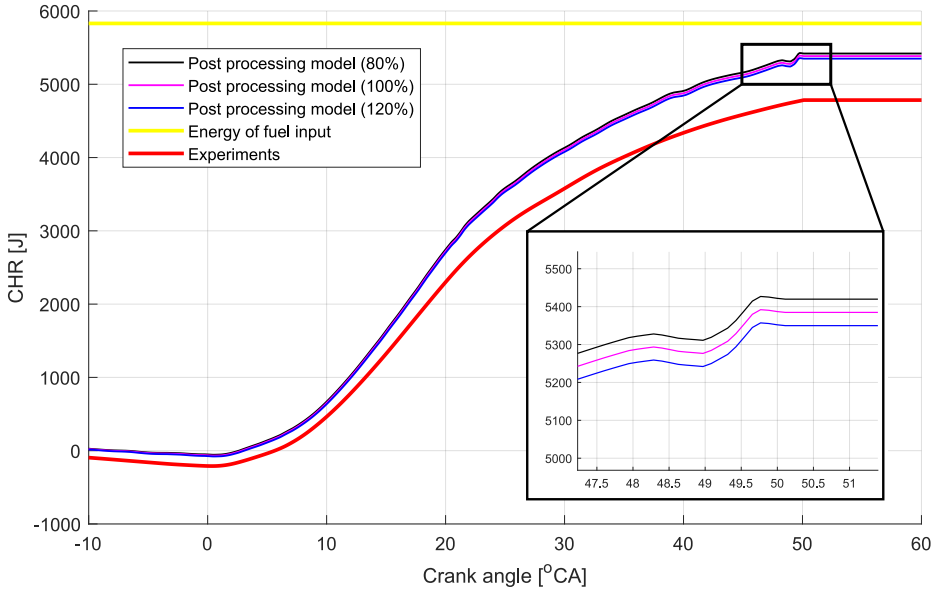

FIGURE 5.4: CHR of RMD=1.54 with an injection timing of 3°CA, change in cylinder temperatures. [1]

Figure 5.4 shows that the wall temperature differences do not explain the big differences in CHR. Other differences can be, different IVC conditions, reproduction of the pressure trace from the paper and differences in the heat loss model. The pressure trace was reproduced through manual digitization of the plots [1], resulting in reading errors. The paper [1] does not describe whether there are filters involved when creating the pressure trace. Differences in the actual pressure trace results and the shown results can cause differences in CHR. The inlet valve conditions of the post processing model are assumed by a polytropic expansion, where the polytropic exponential (n_c) is assumed to be 1.365, the effective compression ratio of around 13.24 which gives a initial pressure 3.6 bar. This assumption was done due to lack of data on initial conditions in the paper [1]. The last possible difference can be using a different heat loss model. The paper describes the use of Woschni as heat loss model, this is also used in the post processing model. However, different exponents in Woshni's formula can be used resulting in different CHR. Due to the fact that the CHR from the post process model is higher compared to the experiments, the efficiency and IMEP values are also overestimated (Table 5.1 and 5.2).

TABLE 5.2: Values from post processing model

RMD	Injection timing [°CA]	Energy of fuel [kJ]	Work indicated [kJ]	Indicated efficiency [%]	IMEP [MPa]	T max [K]	ID [°CA]
0	-5.5	5.8303	2.712	45.76	1.6732	1744.6	12.632
1.54	-5.5	5.9269	2.893	48.82	1.785	1752.4	12.06
1.54	0	5.9269	2.4924	42.05	1.5376	1677.7	19.02
1.54	3	5.9269	2.299	38.79	1.418	1684.6	24.71

The HRR obtained from the post processing model is higher than the one from the paper. Resulting in higher ITE and IMEP in table 5.2 compared to table 5.1. The paper uses BTE instead of ITE, and BMEP instead of IMEP. The BTE and BMEP are always lower compared to the indicated equivalents, caused by mechanical losses, however similar trends should be seen. As mentioned earlier in this chapter, the ITE and IMEP values are not presented in [1] and so the accuracy of the absolute values is not clear.

The results, when changing SOI, are shown in Figure 5.5 and 5.7 and 5.8 and 5.6 where only RMD 1.54 is shown due to the availability of multiple injection timings.

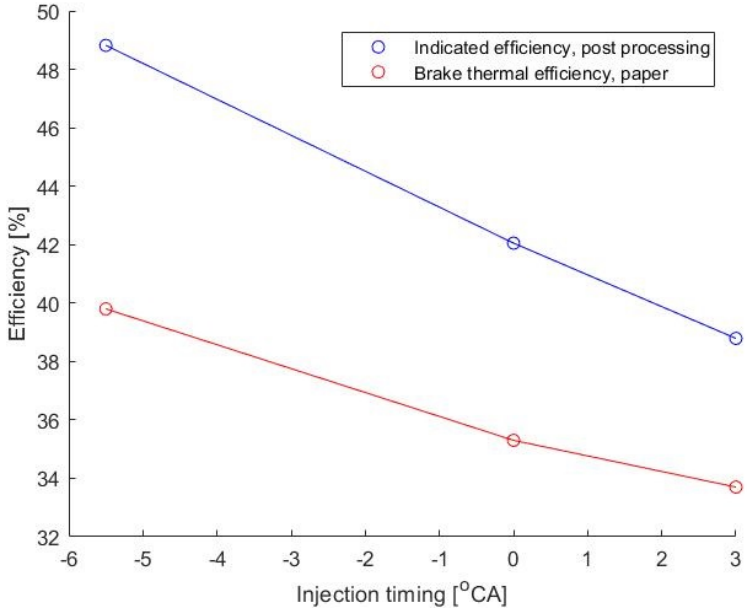

FIGURE 5.5: Efficiency comparison of the experimental values [1] versus the post processing model

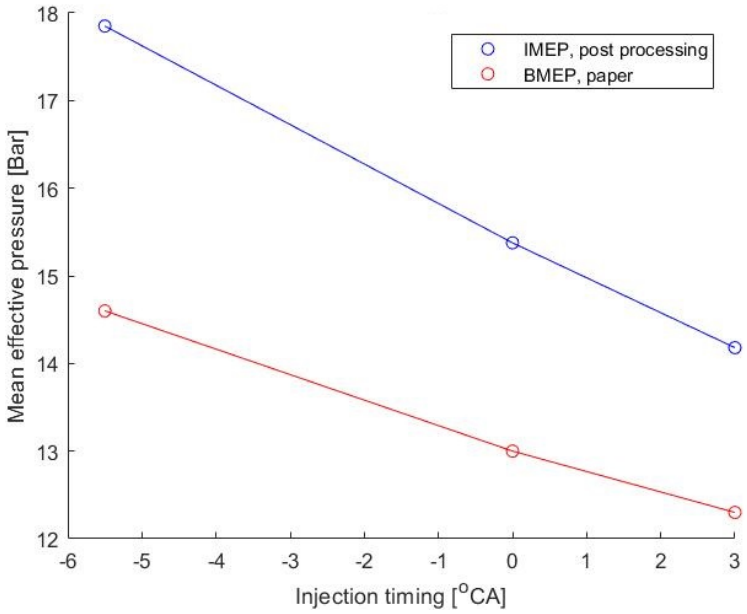

FIGURE 5.6: Mean effective pressure comparison of the experimental values [1] versus the post processing model

The post processing model calculates ITE instead of BTE, while mechanical losses are not known. To calculate BTE from ITE, ITE is multiplied by the mechanical efficiency. Therefore when BTE is divided by ITE it results in the mechanical efficiency. For the case RMD = 0 and SOI = -5.5 the mechanical efficiency is calculated to be 89.4% and for RMD = 1.54 the calculated mechanical efficiencies are 81.5%, 83.9% and 86.9% for SOI = -5.5, 0 and 3 respectively. The calculated mechanical efficiencies meet the requirement to be between 70% and 92% [53]. Figure 5.5 shows the trends in efficiency when changing the SOI. The same trend as the efficiency is expected for the Mean Effective Pressure (MEP), while these are also calculated using the indicated work (W_i). The MEP is shown in Figure 5.6 and shows the expected trend.

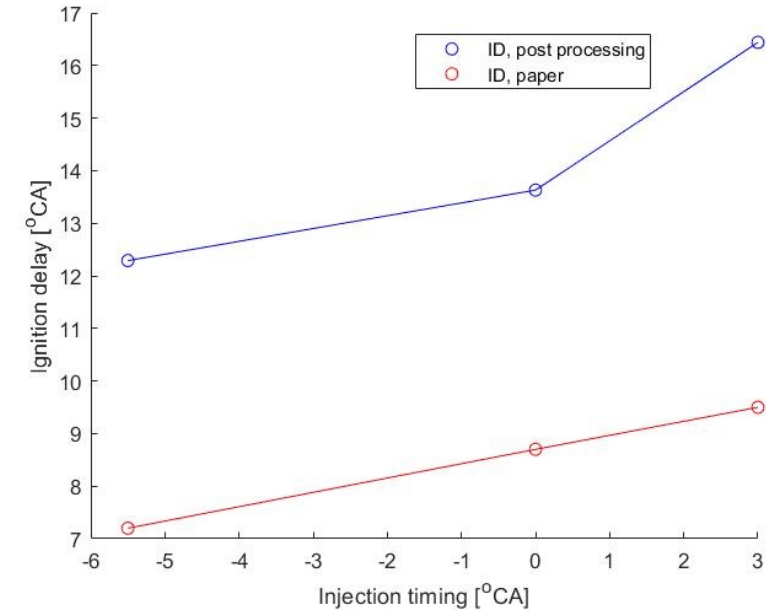

FIGURE 5.7: ID comparison between the experimental values [1] and the post processing model

The defenition adopted in the model relies on taking the CA05 value as ignition indicator. CA05 means that 5% of the heat was released. Note that no information is available on how ID is established in the paper [1]. The ID resulting from the experiments [1] and the calculated ID in the post processing model differ around 7°CA. The difference can be a result of a different methods on establishing ID.

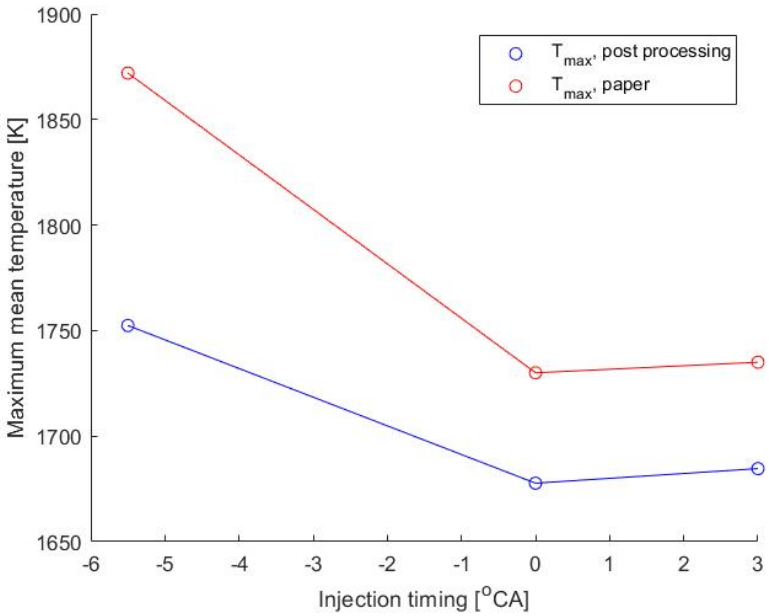

FIGURE 5.8: Mean maximal in-cylinder temperature comparison bewtween the experiments [1] and the post processing model

In Figure 5.8 is shown that the experimental results [1] for the mean maximum in cylinder temperature is 50-100^{o}C higher than the temperatures obtained from the post processing model based on the pressure trace out of the paper. The initial mass influences the maximum mean temperature in the cylinder calculated with the equation of state (ideal gas law). Increasing initial mass it decreases the temperature and visa versa. Errors can occur in the establishment of the initial mass by not taking into account a blow down effect. Exhaust and intake valves can be open simultaneously during the exhaust stroke to enable all exhaust gasses to leave the cylinder. The blow down effect refers to mass being lost from the intake manifold into the exhaust manifold through the cylinder when the valves overlap during the intake stroke.

Despite some variation in absolute values, the post processing model predicts the trends as expected and if more information is available in terms of the inputs and other modelling approaches, these corrections can easily be incorporated to calibrate the model for better accuracy. The results from the post processed experimental pressure trace [1] is from now on considered the experimental data which will be used to compare the Vibe based model and the two zone model.

5.2 Vibe based model

This section discusses the results of the Vibe based model. The in-cylinder pressure trace provided by the Vibe based model is compared to the pressure trace provided by the literature [1]. The HRR, CHR, IMEP, mean max in-cylinder temperature, ITE, ID and indicated work of the Vibe based model are also validated against the experiments.

The Vibe based model is a model where shape parameters are used to estimate the Combustion Reaction Rate (CRR) (Chapter 4.1). The RMD = 1.54 model (shape parameters are calibrated for RMD = 1.54), create by Byungjoo Lee [44], is used and the fuel composition are changed to the RMD = 0 configuration. The experimental results are available in the paper [1]. The Vibe based model relies on an assumption of Start of Combustion (SOC) and End of Combustion (EOC) as input parameters. The SOI timing can not be calculated in the Vibe based model [44], while the model runs from SOC until EOC. SOI can therefore not be verified.

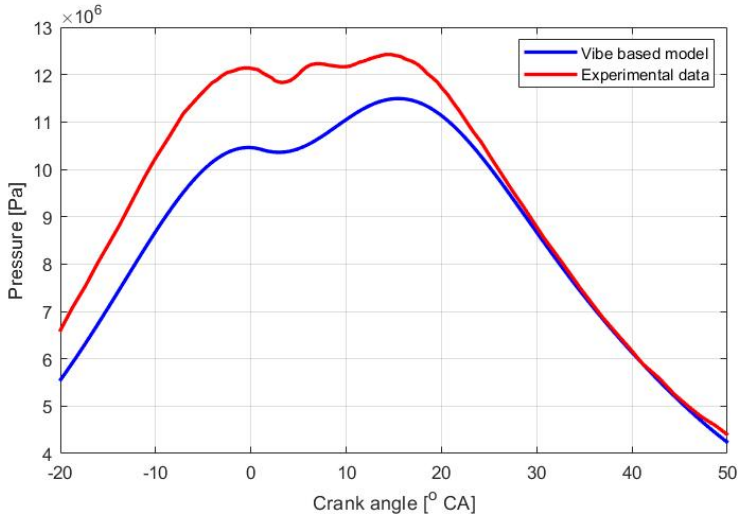

FIGURE 5.9: Pressure trace of Vibe based model and the experimental pressure trace for the case RMD = 1.54

The pressure trace simulated with the Vibe based model is shown in Figure 5.9 together with the experimental pressure trace. The case RMD = 1.54 SOI = -5.5 is shown. The experimental pressure trace contains more peaks compared to the Vibe based model. This difference can be caused by the use of two Vibe functions, one for methanol (single Vibe function) and one for Diesel (double Vibe function). Instead of two double Vibe functions, or even multiple Vibe functions. Also is assumed that methanol and diesel have the same combustion duration. This assumption is done due to lack of experimental data and does not necessarily has to be true.

The polytropic expansion is calculated with Equation 4.28, where in the Vibe based model, p_2 at the SOC is used, which is equal to a pressure of 10.47 MPa consistent with the peak value in the premixed combustion (first peak just before TDC (0^oCA)). r_c is calculated with V_1/V_2 which results in a value of 13.2427. V_2 depends on the IVC, which is an inconsistent definition as explained in Chapter 4.3. This can explain the inaccurate polytropic compression and can be adjusted to establish a better fit.

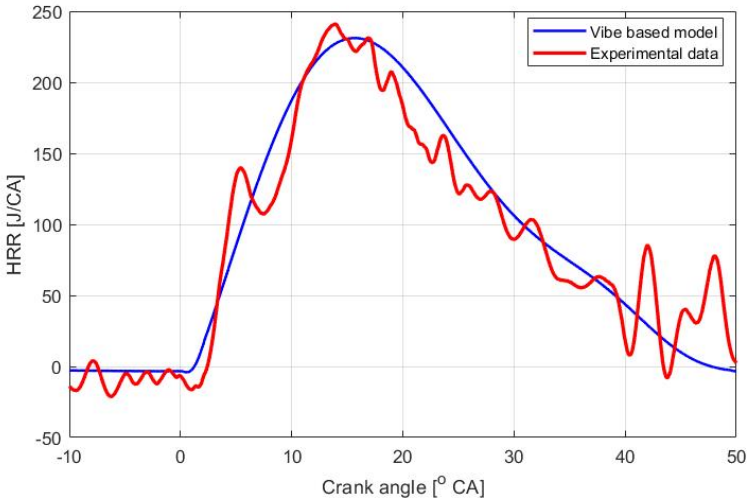

FIGURE 5.10: Heat release Vibe based model RMD 1.54

Figure 5.10 shows the HRR calculated with the post processing model. There are two HRR traces shown, namely the HRR from the Vibe based model and the experiments [1]. The HRR computed from the Vibe based model does not show the first peak in the HHR. This first peak (around 5^oCA) is the premixed combustion, meaning diesel is mixed with the methanol-air mixture and combusts rapidly, resulting in a heat release peak. The second peak (from around 15^oCA) is the combustion of the rest of the fuel where both diesel and methanol undergo combustion. The HRR of the Vibe based model does not distinguish the difference between these two peaks. As explained above, methanol combustion is calculated with a single Vibe function and diesel combustion with the double Vibe function. The methanol CRR is more effective during the first part of the combustion and the diesel in the second part. This is indicated by the higher bump (around 35^o) and the lower peak HRR (around 15^o) when increasing the diesel content and a decrease the methanol content (RMD = 0 is deacrease in methanol content and increase of RMD = 1.54). This difference probably is a result of the pressure trace which only contains two pressure peaks where, one is the result of polytropic compression and the other peak of combustion. The shape parameters might have a better tuning and methanol might be described better with a double Vibe function.

In the paper [1], the premixed combustion gives higher heat release rates when using more methanol, this is due to the longer ID where diesel can premix with the methanol-air mixture. More diesel is combusted in the premixed phase because of this. As concluded above, the premixed combustion phase is not shown in the Vibe based model caused by the choice of Vibe function used. However in the future the model needs to be adjusted in order to show the change in HRR in the premixed phase. The Vibe based model now assumes a SOC, meaning no distinction in the ID, and therefore not in the premixed HRR.

The simulated heat release rate of a diesel only case (RMD = 0) is shown in Figure 5.11. The Vibe based model calibrated for RMD = 1.54 is used, however the fuel composition is adjusted to RMD = 0.

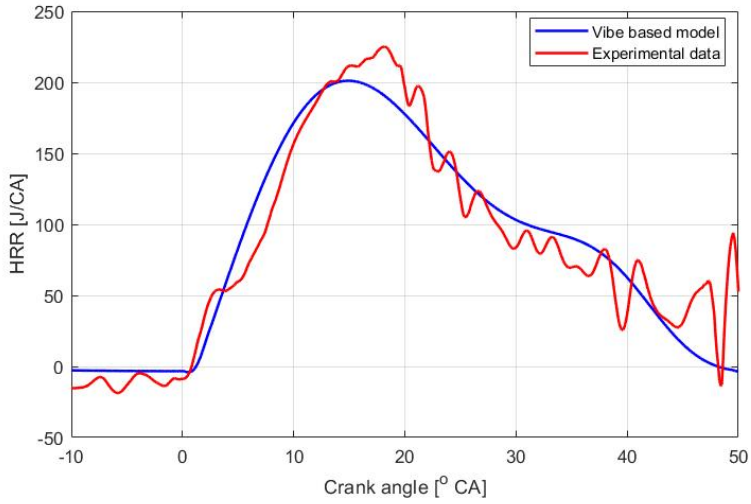

FIGURE 5.11: Heat release Vibe based model RMD 0

Figure 5.11 shows that the Vibe based model has a different shape of HRR. The peak HRR is located closer to TDC in the Vibe based model compared to the experiments. The premixed combustion peak is not showing, similar to the RMD = 1.54 case. Further correction of these differences is out of the scope of this research.

Table 5.3 shows the results for the calculated indicated work, ITE, IMEP, maximum temperature and the ID. The post processed Vibe based model results are compared to the post processed results of the literature pressure trace.

TABLE 5.3: Results Vibe based model v.s. literature

	RMD	Injection timing [^oCA aTDC]	Work indicated [kJ]	Indicated efficiency [%]	IMEP [bar]	T max [K]	ID [^oCA]
Vibe based model	1.54	-5.5	2.9725	50.15	18.34	1729.5	12.062
Experiments	1.54	-5.5	2.893	48.82	17.85	1752.4	12.06
Vibe based model	0	-5.5	2.756	46.50	17.00	1638.5	11.95
Experiments	0	-5.5	2.712	45.73	16.73	1744.6	12.63
Vibe based model	0.55	-5.5	2.8319	47.78	17.47	1669.4	11.95
Vibe based model	1	-5.5	2.8841	48.66	17.79	1692.8	12.06

Remarkable in this table (Table 5.3) is that the indicated work and ITE for the RMD = 0 situation lay more closely to the experimental results than the RMD = 1.54 case does. Due to the calculation of the work, which is the surface area under the P-V graph, it does not mean that RMD = 0 has the better result. The visual conclusion on how the heat release rate is shaped is more important, because it gives a better picture of the differences in fuel combustion. When the visual validation concludes

in an accurate model, the rest of the calculations can be made.

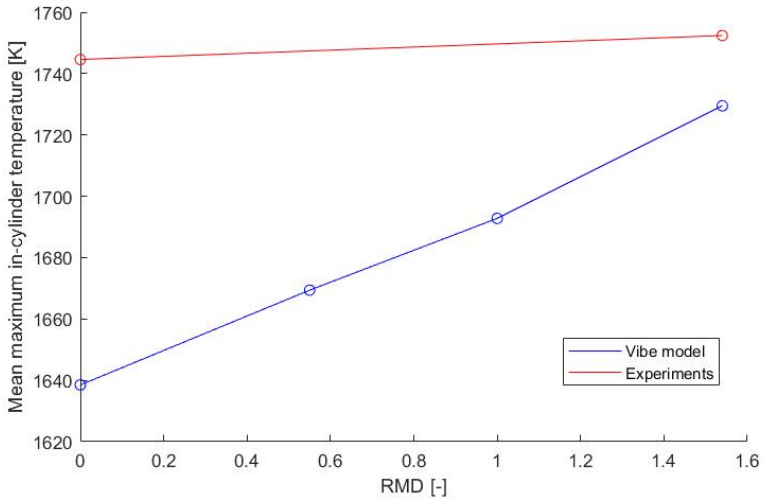

FIGURE 5.12: Maximum mean in-cylinder temperature at -5.5^{o}CA

In Figure 5.12 the maximum mean in-cylinder temperature is shown. When the amount of methanol increases, the mean in-cylinder temperature raises according to the Vibe based model at an igition timing of -5.5^{o}CA. This increase in mean temperature is also suggested by the values of the post processing based on the pressure trace from the paper [1]. The increase of the maximum mean temperature of the experiments are not increasing as rapidly as the Vibe based model. This can be explained due to lack of influence of the ID when using more methanol there is more premixed combustion which results in lower temperatures compared to less premixed combustion. This explains the faster decrease when using less methanol.

The ID was calculated with Formula 4.87 where SOI is subtracted from CA05. CA05 is the Crank Angle where 5% of the heat is released. Due to change in heat released, caused by the change in fuel composition, the ID is not constant.

The indicated work is calculated by integrating pressure over the in-cylinder volume. The pressure trace of different RMD cases were calculated with similar shape parameters in the Vibe based model, however the mass of fuel input is changed resulting in a change in CRR. This change in CRR creates a change in the pressure trace, resulting in a different indicated work.

The ITE depends on the indicated work and the input of fuel energy. When changing the RMD the total energy is maintained, only the contribution of methanol and diesel is different. The indicated work changes resulting in a change of ITE. Similar trends of ITE and indicated work, computed in the Vibe based model, are shown. The same applies for the IMEP which is also dependent on the indicated work.

A SOI sweep cannot be made, due to the fact that the Vibe based model does not have the option to change the SOI.

More information on the validation of the Vibe based model can be found in Chapter 5.4.

5.2.1 Conclusion Vibe based model

The pressure trace of the Vibe model contains two peaks, where one peak indicates polytropic compression and the other peak the combustion. Experiments [1] indicate three peaks in the pressure trace instead of two. The mismatch is caused by the choice of Vibe functions used. There are two Vibe functions, one for methanol (single Vibe function) and one for diesel (double Vibe function). When using multiple Vibe functions, more variations can be obtained resulting in a possible better match. This needs to be investigated in future research.

The shape of the HRR of the Vibe based model does not show a similar trend as the HRR of the experiments. The first peak in the HRR of the Vibe based model is missing. It results in a non accurate calculations for IMEP and efficiency while these are based on the p-v diagram.

The Vibe based model can be calibrated for specific cases when the pressure trace is known.

Buyongjoo Lee [44] mad the assumption that the combustion duration of methanol and diesel are equal, this assumption is done due to lack of experimental results. New experiments need to be done in order to create two Vibe functions can for methanol and diesel combustion separately, combining the two new Vibe functions probably gives a more accurate result.

The disadvantages of the model are the case specific tuning necessity and the assumed SOC instead of calculating the ID.

5.3 Two zone model

In this section, the results of the two zone model are shown. The two zone model uses tuning parameters. These tuning parameters are obtained by changing them one by one to obtain the best visual fitted pressure trace and HRR with the experimental results [1]. The model tuning parameters are fitted for the case where the RMD = 1.54 and the SOI = -5.5. The calibrated tuning parameters stated in Table 5.4.

TABLE 5.4: Tuning parameters used for the SOI = -5.5 RMD = 1.54 case

Tuning Parameter	Tuned Value
TweakSpray	0.023
aIgn	14.1e11
KIcinicine	0.67e-13
CtFlame	1

The outcome of the two zone model is a pressure trace versus the crank angle, which is shown in Figure 5.13 when using the tuning parameters shown in Table 5.4.

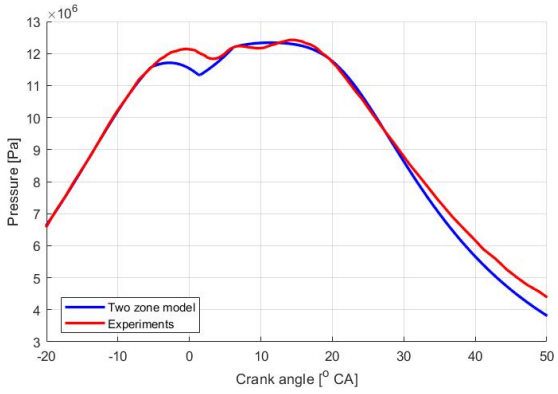

FIGURE 5.13: Pressure versus crank angle for experimental values and the two zone model outcome. RMD 1.54 and SOI -5.5

Figure 5.13 indicates that the pressure trace from the experiments and the two zone model have similar trends and are in the same range. A nearly perfect match is obtained before injection (between -20 ^{o}CA and -5.5 ^{o}CA). The peak pressure is close to 12 MPa which is comparable to the experimental results, namely 12.15 MPa [1]. The two zone model, calculates a bigger pressure drop after injection (at -5.5 ^{o}CA), when the diesel fuel starts evaporate. After the first pressure drop the two zone model rapidly rises, due to the combustion at the boundaries of the spray by flame propagation plus the diesel combustion. After a while the combustion will probably depend on only one combustion phenomena. The two zone model does only show two peaks on contradiction of the experimental data [1], whom shows three peaks. This mismatch between experiments and the two zone model can probably be solved with better tuning parameter tuning. This will be investigated later in this chapter.

The pressure trace (Figure 5.13) is inserted in the post processing model, resulting in the GAHRR, also called HRR, shown in Figure 5.14.

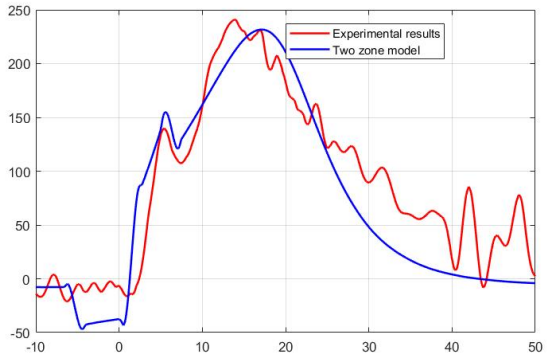

FIGURE 5.14: Heat release rate versus crank angle for experimental values and the two zone model outcome. RMD 1.54 and SOI -5.5

The pressure dip caused by fuel evaporation is also shown in the HRR trace, shown in Figure 5.14, where after injection a negative HRR is shown. A negative

HRR means that the diesel fuel absorbs heat from the cylinder in order to evaporate. The absorption of heat causes the in-cylinder temperature to decrease resulting in a lower pressure. The evaporation phenomena is also shown in the experimental HRR, however this is less compared to the two zone model.

In Table 5.5 the values for the IMEP, indicated work, Efficiency and T_{max} can be found.

TABLE 5.5: Results of two zone model versus experiments

Model	RMD/SOI	IMEP [bar]	Indicated work [kJ]	ITE [%]	Tmax [K]
Two zone	1.54/-5.5	14.12600	2.2898	38.63	1721.5
Experiments	1.54/-5.5	17.85	2.893	48.82	1752.4

The indicated work, ITE, IMEP and mean maximum in-cylinder temperature calculated with the two zone model are lower than the experiments [1]. This can be explained by the overestimated evaporation energy of the diesel in the two zone model.

5.3.1 Tuning parameter sweeps

In Table 5.4 the preliminary calibrated tuning parameters are indicated for RMD = 1.54 and SOI = -5.5. This calibration was done by hand and visual inspection on the pressure trace and the HRR. The parameters were tuned one by one to obtain a fit. The first step is to establish the influence of these parameters in the model. This can be done by sweeping the four tuning parameters.

TweakSpray tuning parameter

The first model tuning parameter is called 'tweakSpray' which influences the total mass conversion of unburnt zone into burnt zone. The pressure traces belonging to numerous tweakSpray values are shown in Figure 5.15. The other tuning parameters are kept constant when changing the tweakSpray.

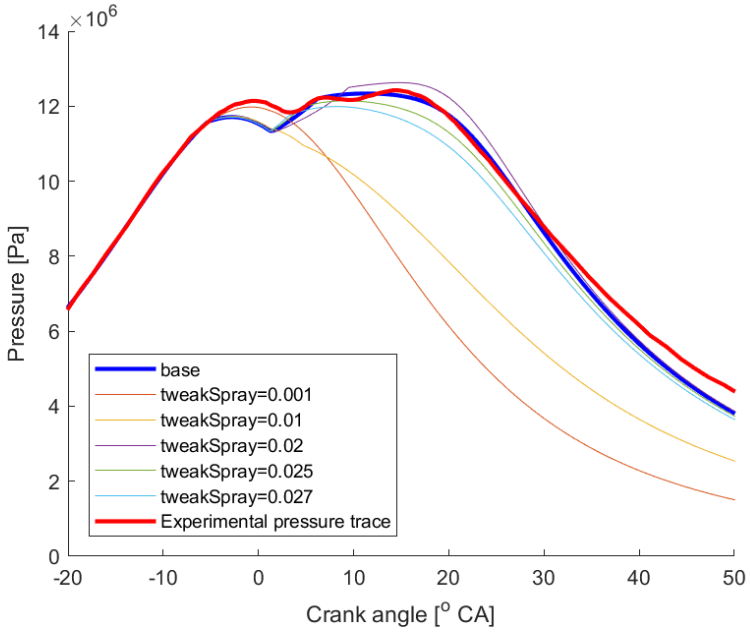

FIGURE 5.15: Pressure trace when sweeping the TweakSpray coefficient. In the base case tweakSpray=0.023

In Figure 5.15 is shown that if the value of TweakSpray is below 0.01 the second pressure peak is lower compared to the polytropic compression pressure peak. At the point where tweakSpray reaches a value of 0.001 there is only one peak left. This event occurs due to the limited conversion of unburnt zone into the burnt zone to obtain enough oxygen in the burnt zone for complete combustion of the fuel. In case of tweakSpray = 0.001 there is no combustion at all. When increasing the tweakSpray, the maximum pressure decreases due to the rapid conversion of unburnt zone into the burnt zone, resulting in lesser conversion by flame propagation calculated in the **methanol combustion model** (Figure 5.15).

In the pressure trace (Figure 5.15) is shown that when using a tweakSpray value of 0.001, there is no combustion. To investigate why this is possible the spray entrainment $\left(\left(\frac{dm_b}{dt}\right)_{spray}\right.$ is plotted in Figure 5.16. The spray entrainment should be positive in order for the spray to grow.

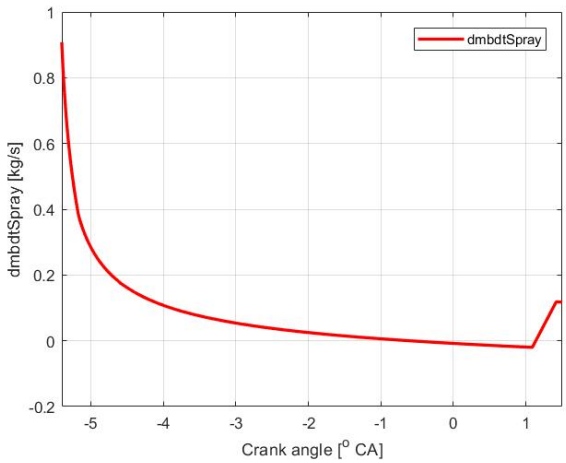

FIGURE 5.16: Mass change in the burnt zone by spray entrainment ($\frac{dm_{b,Spray}}{dt}$) when using a tweakSpray of 0.001

When the tweakSpray is decreased to 0.001, the influence of spray diffusion becomes negative as shown in Figure 5.16. The explanation of this phenomena is that the spray surface is decreasing during injection, which will not be the case in reality. Mathematical explained (derived from Equation 4.57) :

$$tweakSpray * \rho_u * \frac{dV_b}{dt} < \frac{dm_{b,fuel}}{dt} \tag{5.1}$$

When the tweakSpray is increased to 0.01 the mass change of the burnt zone by spray entrainment does not become negative during injection. The reason for the lack of combustion when using a tweakSpray of 0.001 is caused by the fact that the model calculates the spray to decrease during injection, which means that the burnt zone entrains the unburnt zone instead of the other way around.

Figure 5.17 gives the HRR when changing the tweakSpray.

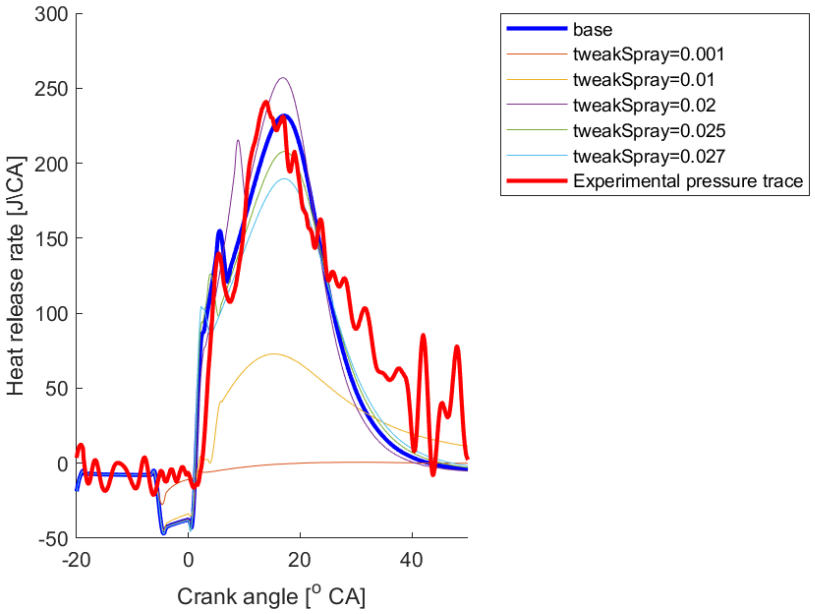

FIGURE 5.17: Pressure trace when sweeping the TweakSpray coefficient. In the base case tweakSpray=0.023

Figure 5.17 shows a higher evaporation energy for all values of tweakSpray, indicated by the negative HRR after injection (SOI = -5.5), for the two zone model compared to the experiments. As explained earlier, when the tweakSpray reaches 0.001 there is no combustion which is confirmed by zero heat release after evaporation in Figure 5.17. When increasing the tweakSpray from 0.001 to 0.01, more fuel is able to combust, however the low HHR indicates not a complete combustion. At tweakSpray = 0.02 the biggest heat release is shown, similar to the pressure trace. Increasing the value of tweakSpray even more results in an earlier premixed combustion (first peak shifts to the left) due to the fast entrainment of oxygen into the burnt zone, resulting in earlier combustion. In the afterburn phase the HHR will decrease when the tweakSpray has a value of above 0.02. This is due to an earlier explained phenomena, where the influence of the **methanol combustion model** is limited caused by the lack of present unburnt zone, while entrainment of the unburnt zone into the burnt zone was mainly done during injection. Chapter 4.2.2 explains this entrainment of unburnt zone into the burnt zone. More information on premixed combustion and diffusive combustion can be found in Appendix B.

The CHR, for different values of tweakSpray is shown in Figure 5.18.

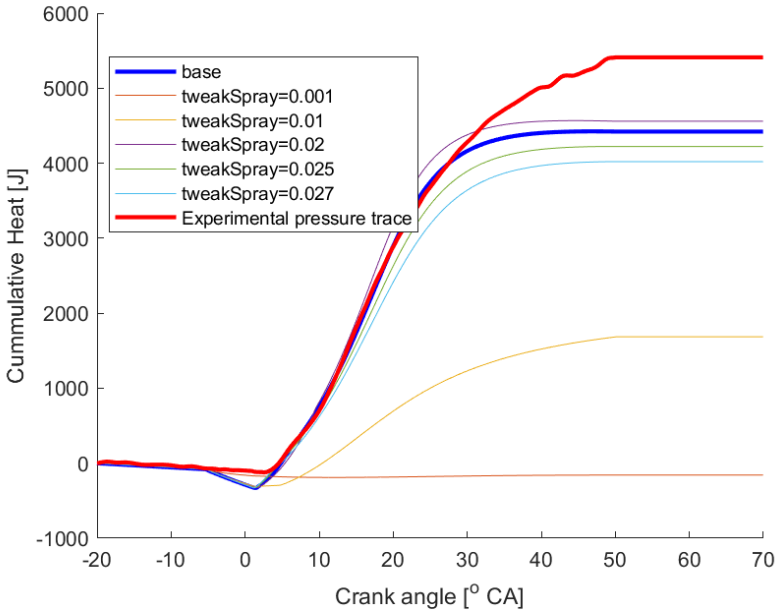

FIGURE 5.18: Pressure trace when sweeping the TweakSpray coefficient. In the base case tweakSpray=0.023

Figure 5.18 indicates that the CHR of the experiments is higher compared to the two zone model. Partially, the lower CHR is caused by the higher evaporation energy calculated with the two zone model, shown by the decrease in CHR after injection (SOI = -5.5). The perspective is that the biggest difference in CHR is caused by the amount of combusted fuel. This will be investigated by comparing the fuel masses inside the two zones when changing the tweakSpray. The results of the fuel mass investigation are shown in Figure 5.19.

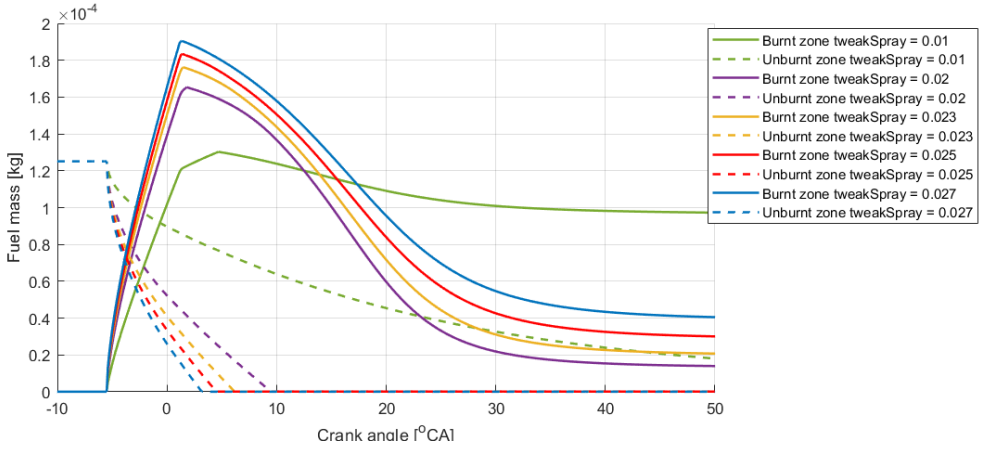

FIGURE 5.19: Fuel mass in unburnt and burnt zone when using different tweakSpray values

Figure 5.19 shows the total amount of fuel (mass of diesel and methanol) inside the burnt and unburnt zone when changing the tweakSpray. The same collared dashed and solid line belong to one value of tweakSpray. Diesel is injected into

the cylinder at -5.5 ^{o}CA, resulting in an increase of diesel inside the burnt zone as shown in Figure 5.19. During injection, the unburnt zone, which is substance containing methanol and air, entrains the burnt zone resulting in a decreases of the mass of fuel in the unburnt zone. This entrainment increases the mass of fuel inside the burnt zone as well. When increasing the tweakSpray the peak in the burnt zone mass increases due to faster entrainment and the unburnt zone disappears faster. End Of Injection (EOI) occurs for all cases at 1.4 ^{o}CA and SOC also occurs at around that same time except for the tweakSpray = 0.01 case. The SOC when tweakSpray = 0.01 starts at 4.7^{o}CA. The mass of fuel in the burnt zone decreases at the SOC caused by the combustion reaction converting diesel and methanol in CO_2 and H_2O. The higher the tweakSpray, the higher the mass of fuel in the burnt zone. This is due to the lack of influence of the **methanol combustion model**, and not all fuel can be combusted by the **diesel combustion model**.

Figure 5.19 shows that the unburnt zone is rapidly disappearing due to the big spray entrainment. The consequence of this is the lack of influence of the **methanol combustion model**, which should have influence on the combustion. This too fast entrainment indicates a too fast volume change of the burnt zone ($\frac{v_b}{dt}$) calculated in Equation 4.53. Further investigation needs to be done on this burnt zone volume change caused by the spray.

The fuel fractions in the cylinder never reach zero, which indicates that not all fuel is combusted in the end. The amount of fuel left is depending on the combustion efficiency which is not known for the experiments. The discrepancies in CHR in Figure 5.18 can be caused by possibly lower combustion efficiencies.

In addition, the spray entrainment model is used until all mass of the unburnt zone is entrained into the burnt zone. The assumption is that due to kinetic energy the change in burnt volume remains the same after the injection stops, while the basic driving force of this calculation is the injection pressure. Chapter 4.2.2 describes that influence of the injection pressure. After injection this total spray formation is still calculated based on the injection pressure of the fuel as in Equation 4.53, where 'S' is dependent on injection pressure. The spray entrainment should be less than calculated resulting in a longer time to convert unburnt zone into burnt zone, which is beneficial for the CHR as described above. Figure 5.20 shows how the spray entrainment (S) behaves in the model.

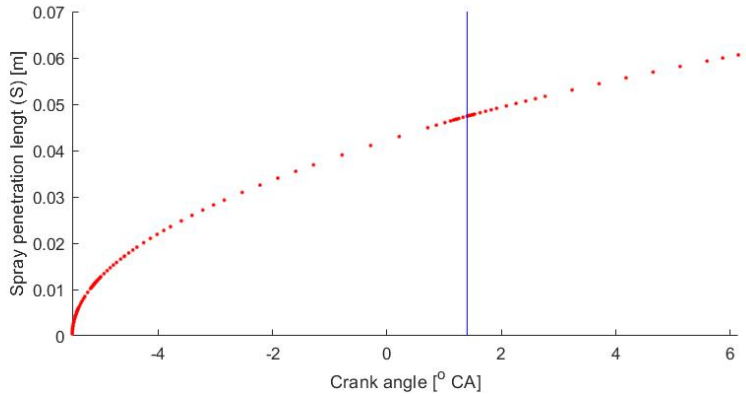

FIGURE 5.20: Penetration length of the spray. at SOI=-5.5, RMD=1.54 and the base case tuning parameters.

Figure 5.20 indicates the spray entrainment behaviour is seen even after injection. The penetration length (S) is growing in its similar curve (after the blue vertical line) as during injection (before blue vertical line). The vertical blue line indicates the EOI and the graph starts at SOI (-5.5^{o}CA). The bore diameter of the cylinder is 0.126m similar to a radius of 0.63 m. The results of the spray penetration length indicates that the spray reaches the walls of the cylinder.

In Figure 5.21 the calculated values for efficiency, maximum temperature, IMEP and indicated work are given. When the tweakSpray has a value below 0.02, not all unburnt zone was converted into burnt zone at EVO meaning not all fuel can be combusted. This is indicated by the extreme low efficiencies, maximum temperature, IMEP and the indicated work. The Tmax is perhaps a result of rapid heat release due to the fast combustion after ignition. At that point, the **Spray entrainment model**, **methanol combustion model** and the **diesel combustion model** influences the rate of combustion, shown by the peak in the HHR graph.

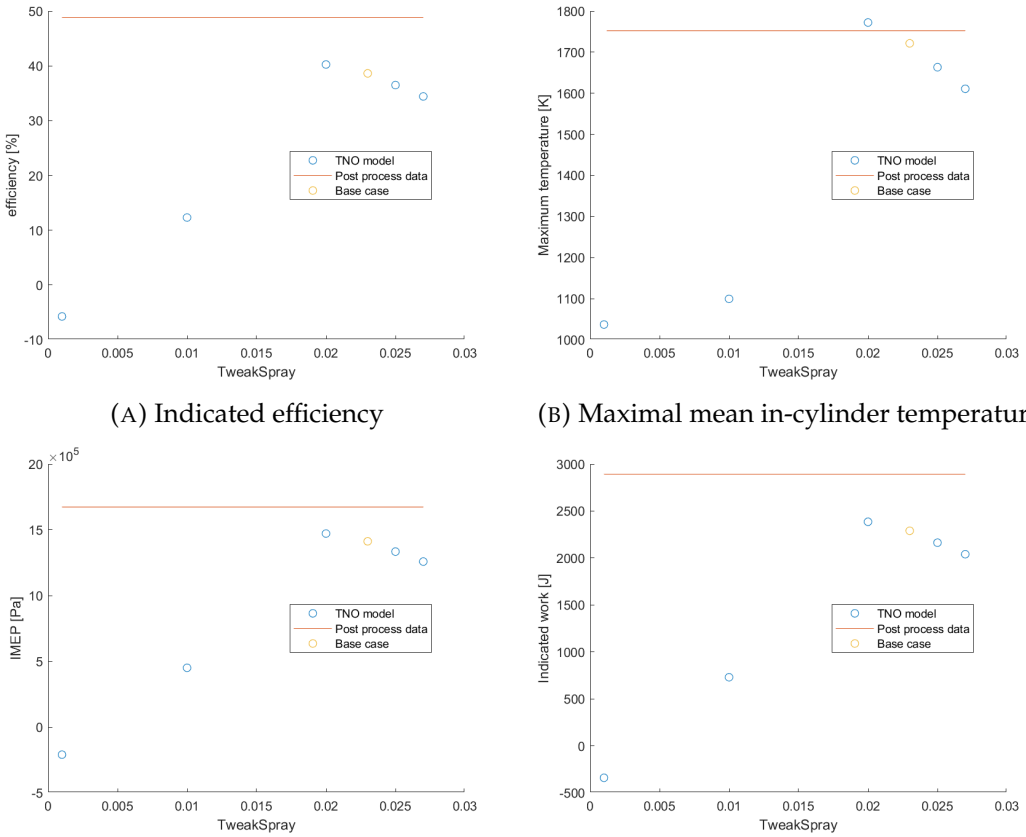

(A) Indicated efficiency

(B) Maximal mean in-cylinder temperature

(C) IMEP

(D) Indicated work

FIGURE 5.21: TweakSpray sweep. In the base case tweakSpray=0.023

aIgn tuning parameter

In the calculation for the SOC, aIgn is introduced. In this section the aIgn sweep is described to establish the influence of this tuning parameter.

Figure 5.22 gives the pressure trace result of an aIgn sweep in the two zone model.

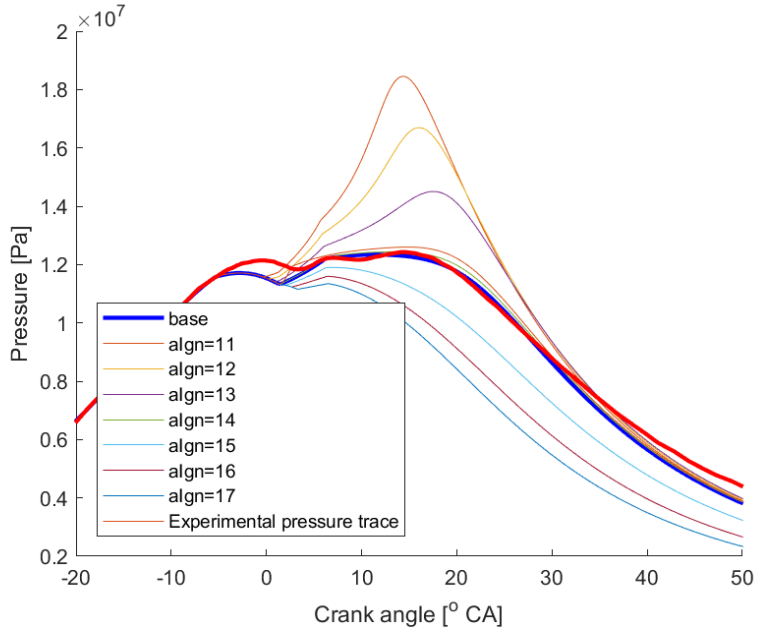

FIGURE 5.22: Pressure trace when sweeping the aIgn coefficient. In the base case aIgn=14.1e11

The SOC can be identified by the start of the pressure rise shown in Figure 5.22. The first peak in the pressure trace in Figure 5.22 is the polytropic compression. The second peak is caused by combustion and starts to arise when the combustion starts. According to Figure 5.22 the tuning parameter aIgn, influences the second peak rather than the first peak. The tuning parameter aIgn is used in the model to indicate when the **methanol combustion model** is used, namely after ignition. Therefore it influences the second peak. It shows that when the ID is less then the influence of the **methanol combustion model** is bigger due to more residual of unburnt zone after injection.

Figure 5.23 shows the HHR when sweeping aIgn.

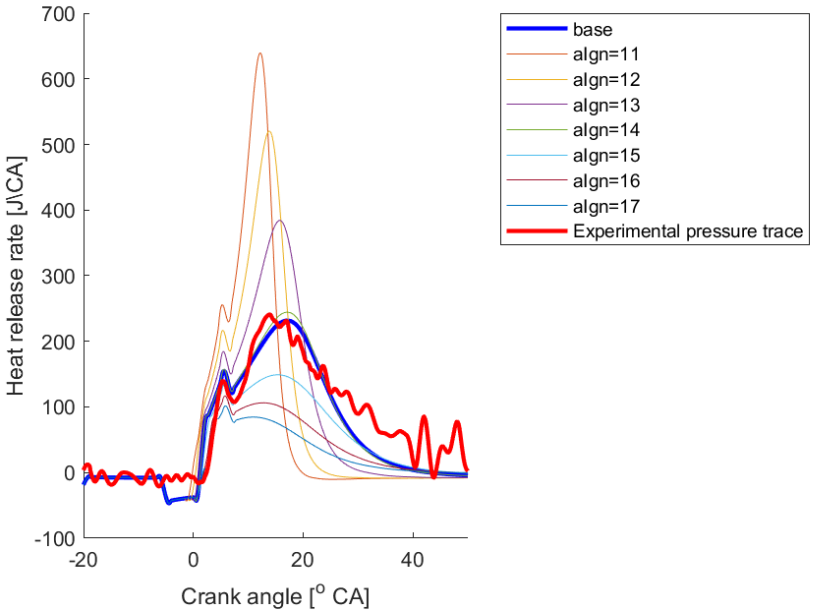

FIGURE 5.23: HRR when sweeping the aIgn coefficient. In the base case aIgn=14.1e11

In Figure 5.23 the peak in HHR is higher when having a lower aIgn. The SOC occurs earlier when decreasing aIgn. The combustion duration is also lower when using a lower aIgn value. The difference between the premixed combustion (first peak) and the non-premixed combustion is bigger when having a smaller ID and visa versa. What would be expected when increasing the ID, is that more fuel combusts in the premixed phase, while more fuel can enter the burnt zone. More combusted fuel in the premixed phase would result in a bigger HRR, only Figure 5.23 suggest differently.

Figure 5.24 shows the CHR when changing the tuning parameter aIgn.

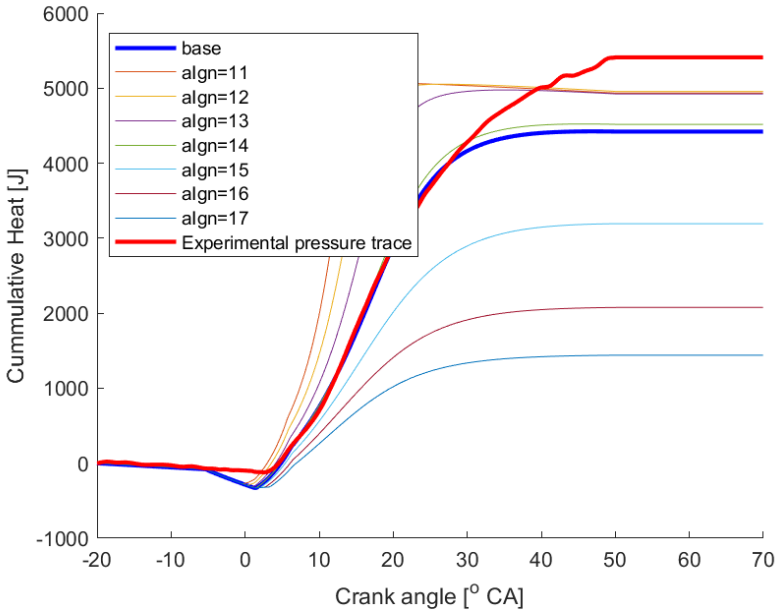

FIGURE 5.24: Mass of fuel in the two zones

The model generates more heat when having a smaller value for aIgn, indicating a shorter ID, as shown in Figure 5.24. This phenomena is probably caused by the amount of fuel combusted. To understand this phenomena the mass of fuel inside the two zones is plotted in Figure 5.25 .

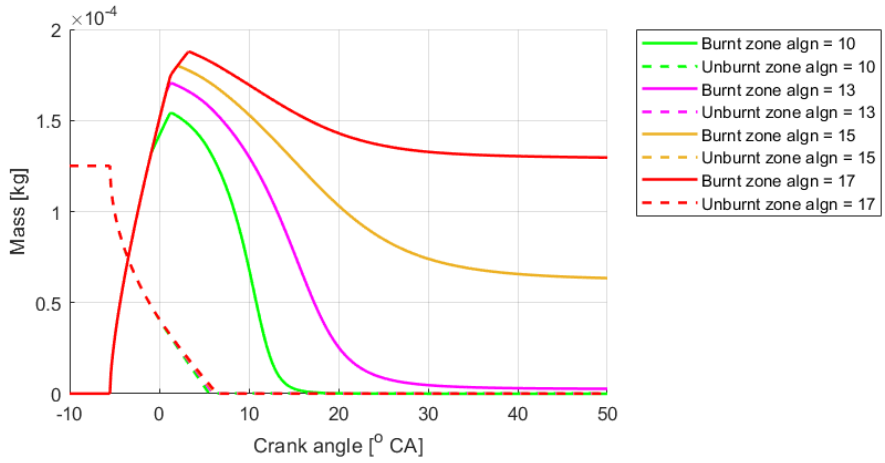

FIGURE 5.25: Burning rate

Figure 5.25 indicates that when increasing aIgn the fuel mass remaining in the cylinder after combustion is increased and visa versa. This explains the higher CHR (Figure 5.24) when decreasing aIgn and the lower CHR when increasing aIgn.

The incomplete combustion of the fuel is caused by the constraints put on the use of two sub models namely: **methanol burning model** and the **Spray entrainment model**. The constraint says that if 0.5% of the total mass in the unburnt zone before ignition, is left, there is no more influence of the spray entrainment and the

methanol burning velocity during the combustion reaction. This results in a combustion reaction only depending on the **diesel combustion model**. Decreasing aIgn results in a decrease of ID and a earlier SOC. Due to the earlier SOC the **methanol burning model** and the **Spray entrainment model** start influencing the combustion velocity earlier and longer resulting in the combustion of more fuel inside the burnt zone.

When increasing aIgn, the efficiency, mean maximum in-cylinder temperature, indicated work and IMEP are decreasing and visa versa (Figure 5.26). This decrease in efficiency, mean maximum in-cylinder temperature, indicated work and IMEP is caused by the incomplete combustion of the fuel inside the cylinder. In the ID calculation the global ϕ, and the pressure are used. The pressure is assumed constant in the cylinder ($p_b = p_u$) and is constant in the whole model. Better would be to use the local ϕ for the burnt zone (ϕ_b).

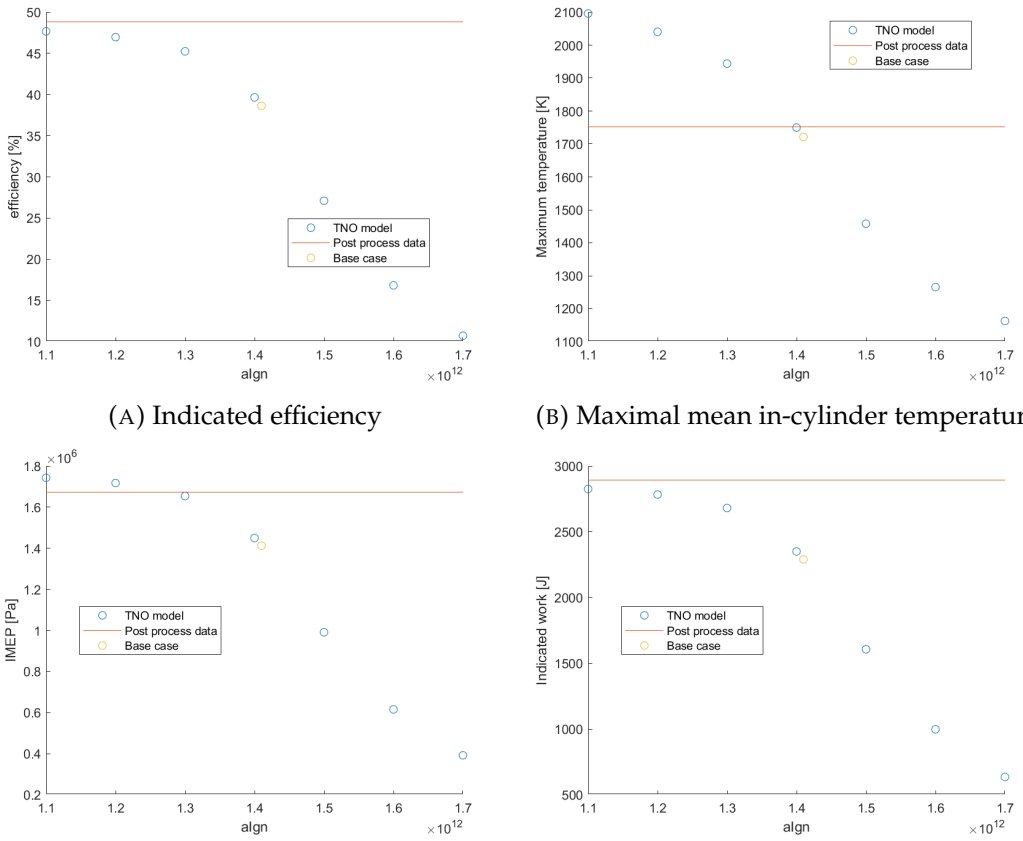

(A) Indicated efficiency

(B) Maximal mean in-cylinder temperature

(C) IMEP

(D) Indicated work

FIGURE 5.26: aIgn sweep. In the base case aIgn=14.1e11

CTFlame tuning parameter

In this section the sensitivity of the model on the CTFlame parameter is discussed. This parameter has influence on the difference between laminar burning velocity and the turbulent burning velocity in the methanol combustion model. When CTFlame = 1 it means that the laminar burning velocity is equal to the turbulent burning velocity in the cylinder. Meaning that there is no turbulence in the cylinder.

Figure 5.27 shows the pressure traces for multiple CTFlame tuning parameter values.

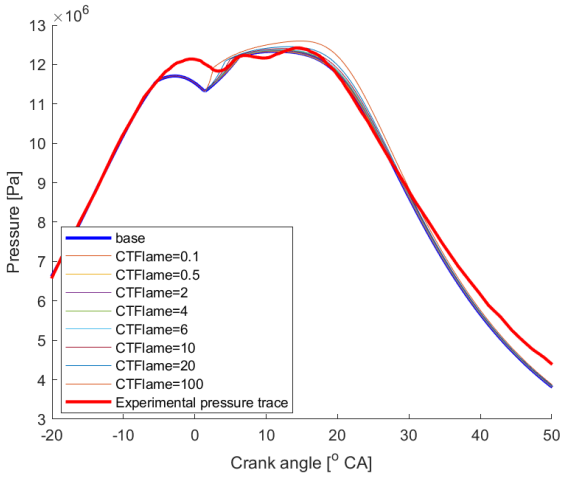

FIGURE 5.27: Pressure trace when sweeping the CTFlame coefficient. Base case CTFlame = 1

Figure 5.27 shows, when CTFlame = 100 the pressure peak is highest, similar to the rise in pressure trace when combustion starts. CTFlame = 0.1 indicates a lower flame velocity than the laminar flame velocity. The differences in the pressure trace are minimal, caused by insignificant influence of CTFlame.

The flame propagation is calculated after ignition and indicates the flame front, which is only present when the unburnt zone still contains mass. In Chapter 5.3.1 in Figure 5.19 is shown that there is a rapid entrainment of the unburnt zone into the burnt zone and that almost no mass is left in the unburnt zone when the ignition starts. This explains the insignificant influence of the **methanol combustion model**.

In Figure 5.28 the HRR is shown for multiple values for the tuning parameter CTFlame.

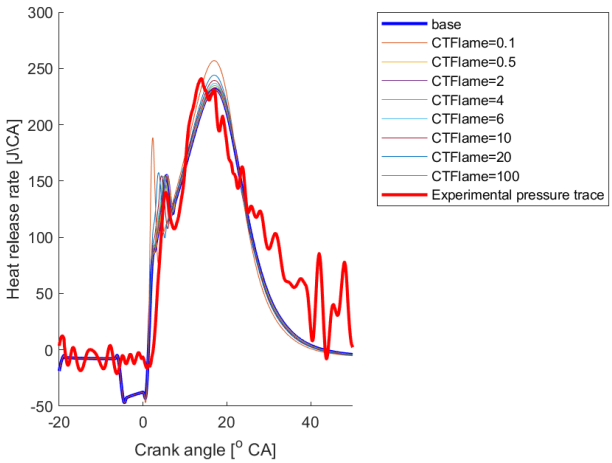

FIGURE 5.28: Heat release rate when sweeping the CTFlame coefficient

Figure 5.28 indicates that the first peak (premixed combustion) is higher when the CTFlame is higher. This is caused by the increased burning velocity in direction of the unburnt zone. A faster combustion results in higher HRR. The duration of the premixed burn phase is smaller when having a fast flame propagation velocity. The second peak in the HRR (Figure 5.28) is also slightly higher, when increasing CTFlame.

In Figure 5.29 the results for CHR when changing the CTFlame tuning parameter is shown.

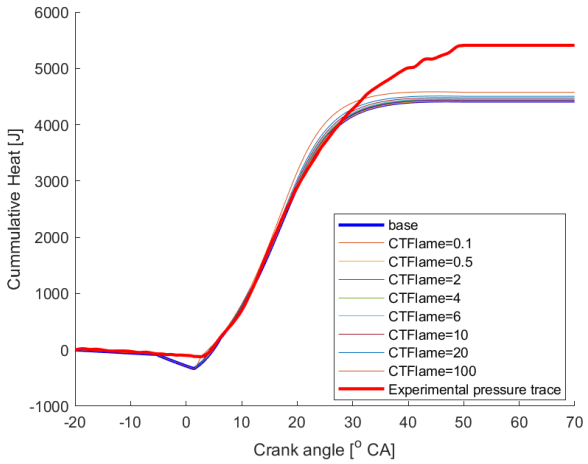

FIGURE 5.29: CHR when sweeping the CTFlame coefficient

From Figure 5.29 can be concluded that the CTFlame parameter in the current form of the model has no significant influence.

From Figure 5.30 one can note that the only significant difference, when changing the value for CTFlame, is the mean maximum in-cylinder temperature. When

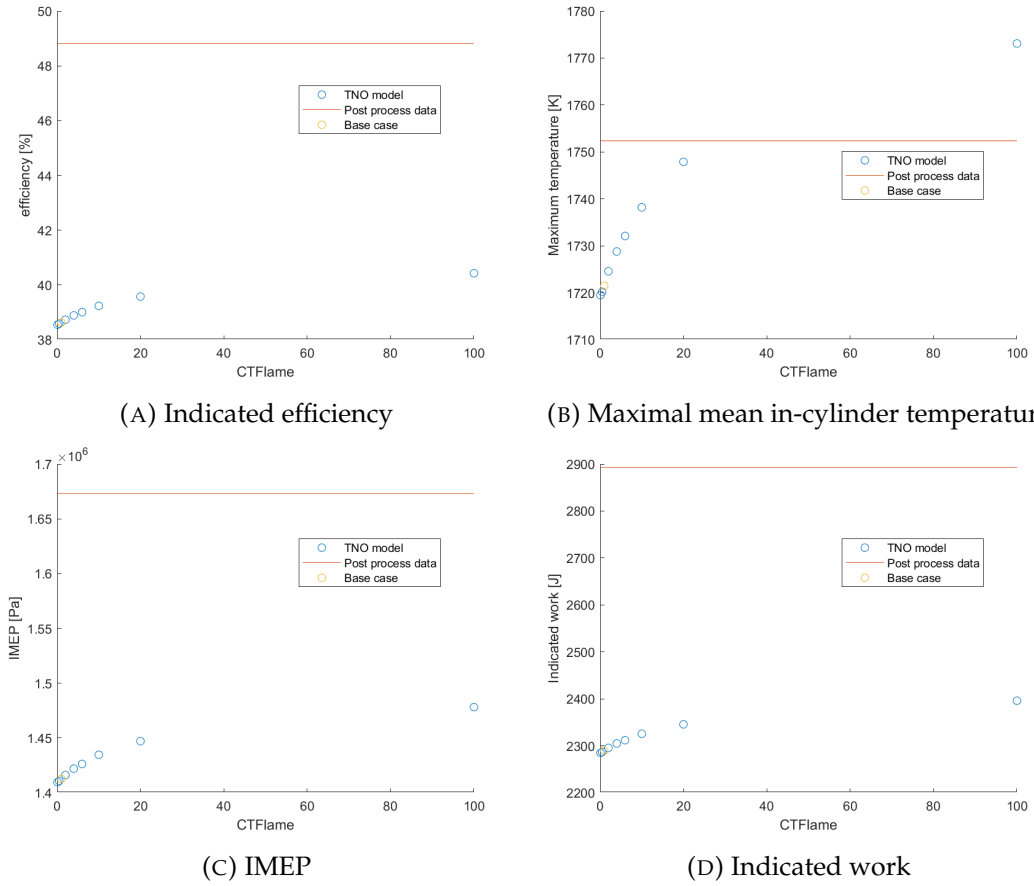

(A) Indicated efficiency

(B) Maximal mean in-cylinder temperature

(C) IMEP

(D) Indicated work

FIGURE 5.30: CTFlame sweep

using CTFlame = 100 the highest mean maximun in-cylinder temperature occurs, which is also visible in the higher HRR shown in Figure 5.28.

kIcinicine tuning parameter

kIcinicine is the last swept tuning parameter in this thesis. kIcinicine is the parameter that influences the diesel combustion velocity in the **diesel combustion model**. The Arrhenius equation is used for the calculation of the combustion velocity, similar to the **ignition model** with tuning parameter aIgn.

Figure 5.31 shows the pressure traces with different values for kIcinicine.

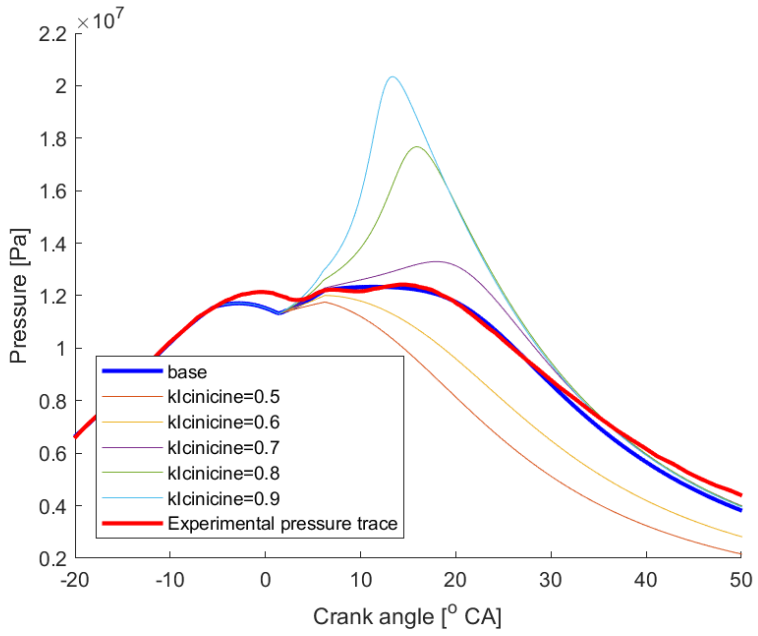

FIGURE 5.31: Pressure trace when sweeping the kIcinicine coefficient. Base case kIcinicine=0.67e-14.

As shown in Figure 5.31 the second peak in the pressure trace is heavily influenced by the tuning parameter kIcinicine. When increasing the value for kIcinicine the pressure increases due to the increase of the combustion velocity and vice versa. In contradiction with the tuning parameter aIgn, kIcinicine does not influence the ID, which is shown by the non changing first peak in Figure 5.31.

Figure 5.32 shows the HHR when changing the value of kIcinicine.

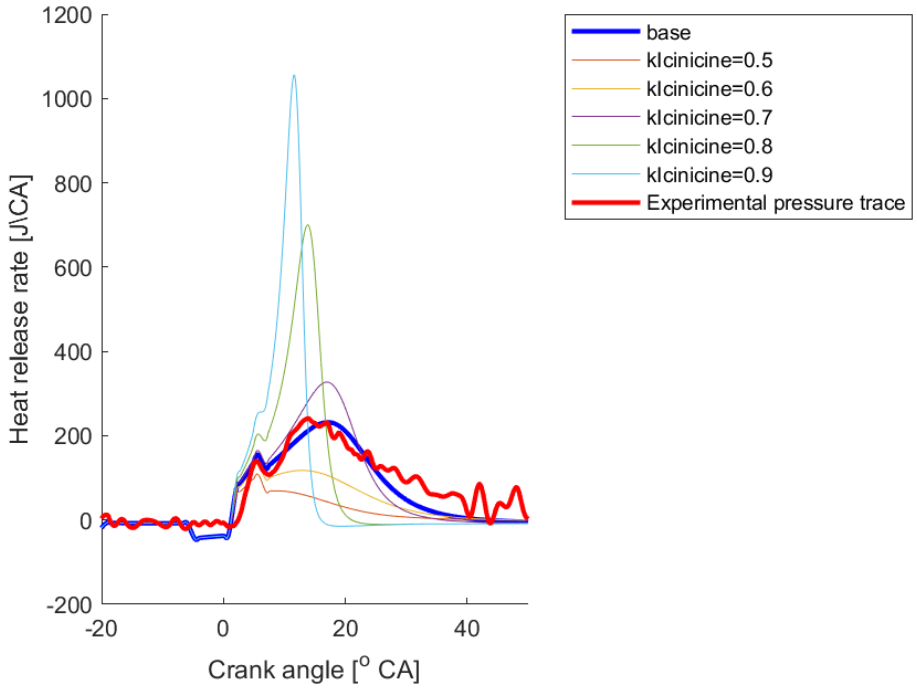

FIGURE 5.32: HRR when sweeping the kIcinicine coefficient. Base case kIcinicine=0.67e-14.

Figure 5.32 indicates a smaller combustion duration when the value for kIcinicine is increased. The EOC is indicated when the HRR is zero.

The global fuel-air equivalence ratio (ϕ) is a parameter in the calculation of the combustion velocity which should be adjusted to a local ϕ for the burnt zone (ϕ_{burnt}). This is due to the fact that the combustion reaction only takes place in the burnt zone.

Figure 5.33 shows the CHR of numerous values for kIcinicine.

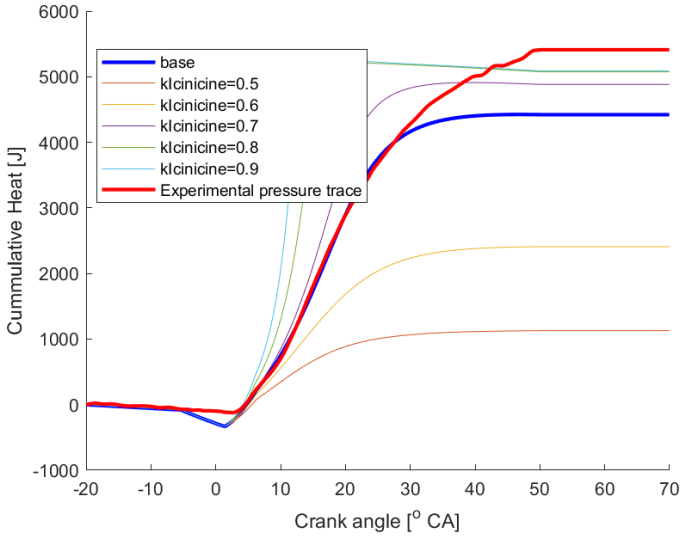

FIGURE 5.33: CHR when sweeping the kIcinicine coefficient. Base case kIcinicine=0.67e-14.

In the CHR versus crank angle figure (Figure 5.33) is shown that when decreasing kIcinicine the CHR after combustion is lower than when increasing the value for kIcinicine. A faster combustion results the possibility of combusting more fuel in the burnt zone, resulting in a a higher CHR (Figure 5.33). The change in CHR is more rapidly increasing at a higher value for kIcinicine.

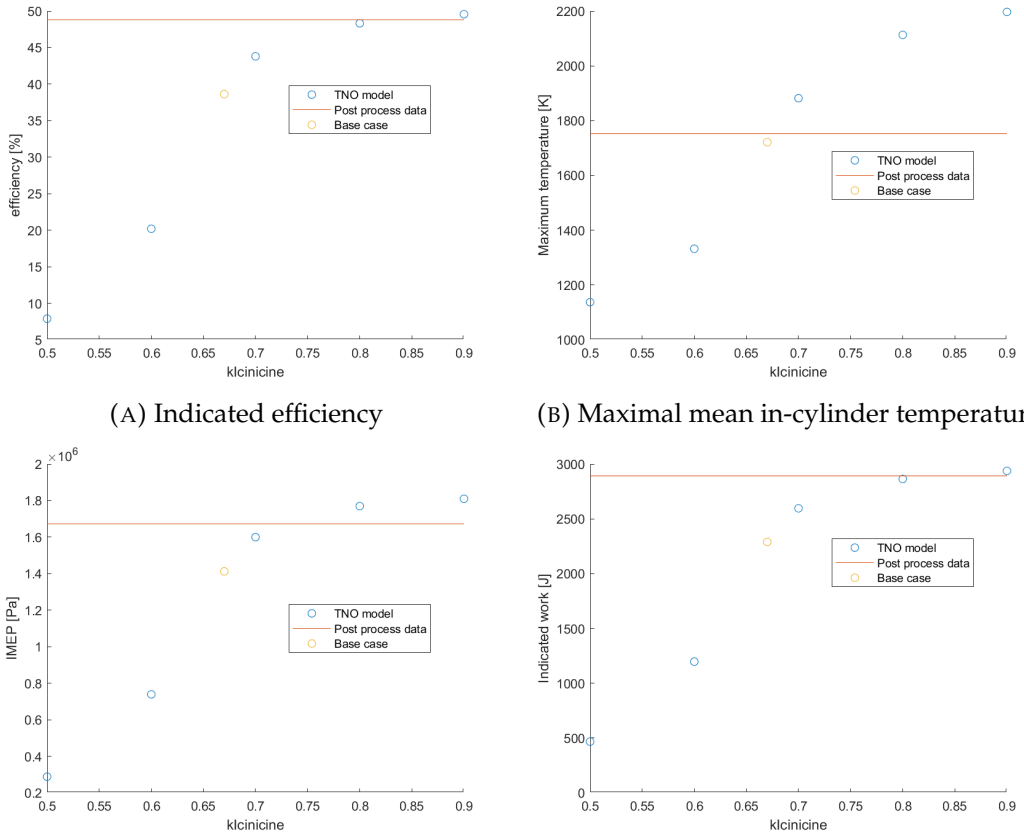

(A) Indicated efficiency

(B) Maximal mean in-cylinder temperature

(C) IMEP

(D) Indicated work

FIGURE 5.34: kIcinicine sweep. Base case kIcinicine=0.67e-14

As shown in Figure 5.34, the efficiency of the increased kIcinicine gives a better result than the base case due to the bigger amount of fuel combusted. The maximum in cylinder temperature is best suited for the base case. IMEP and the indicated work are also better when increasing the combustion velocity by a little, by increasing kIcinicine.

5.3.2 Operational parameter sweep

In this section operational parameters are swept. This is done to observe the sensitivity of the model and to check whether the used tuning parameters are also valid for cases when changing RMD and SOI.

Experiments were done when changing the blend ratio and the injection timing [1]. In Chapter 5.1 the post processing model was introduced with RMD = 0 and RMD = 1.54. These are also used in this chapter for validation. The sweep in blend ratio is done with RMD = 0, RMD = 0.55, RMD = 1 and the base case RMD = 1.54. The SOI timing is swept from -5.5 to 3, for the RMD = 1.54 case, because of the availability of data [1].

Blend ratio

This section describes the validation of the two zone model when changing the RMD of the fuel.

Figure 5.35 shows the pressure traces when using various RMD values in the model. The two zone model has an error when trying to run on only diesel as fuel or with a methanol content of 0.000001 kg.h^{-1}. It dictates a constraint for the RMD working range, therefore RMD = 0 is not present in the figure while the model was not able to run for this blend ratio. The pressure traces are compared to the experimental pressure traces stated in the paper [1]. The green and yellow line are the experimental and the two zone model pressure traces for RMD = 1.54, respectively. This is the calibrated case, and therefore an acceptable match.

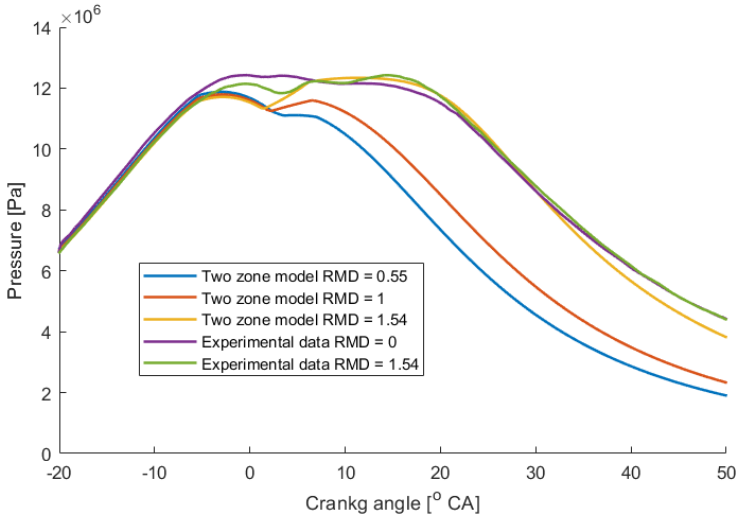

FIGURE 5.35: Pressure traces when changing RMD for the two zone model and the experimental data when using SOI = -5.5

The first pressure peak in the pressure trace (Figure 5.35) increases when using less methanol and more diesel according to the experiments. When injecting more diesel the temperature of the cylinder decreases due to the evaporation energy of diesel. The decreased temperature results in a decrease in the pressure as well, hence the lower pressure in the first peak when running on RMD = 1.54. This phenomena is also shown in the two zone model, only the impact is less compared to the experiments. The higher pressure in the first peak is also shown in the two zone model, however the change is less significant compared to the experiments. When decreasing the RMD in the two zone model the second peak of the pressure trace is decreasing earlier than when using RMD=1.54.

Figure 5.36 shows the HHR when changing the blend ratio for the two zone model and the experiments

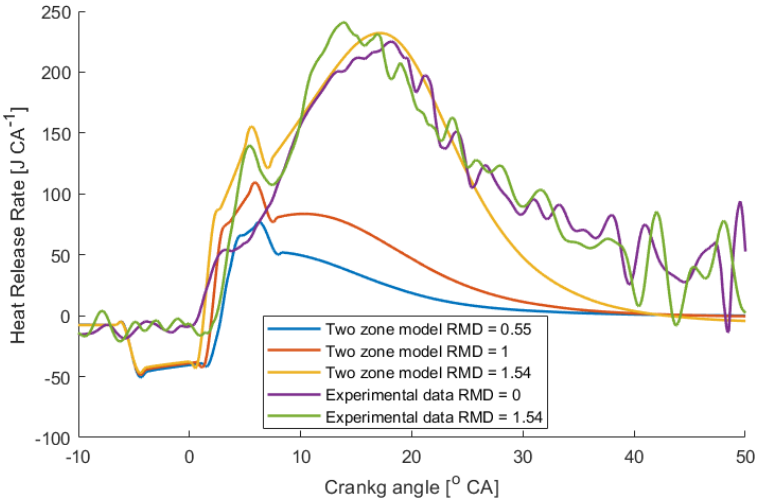

FIGURE 5.36: SOI = -5.5

When looking at the experimental results it is shown that the first peak in the HRR goes down when increasing the diesel content (Figure 5.36 by purple and green line, RMD=0 and RMD=1.54 respectively). The longer the ID the more time diesel has to evaporate resulting in more fuel combustion in the premixed phase shown by the bigger first peak in the HRR. The ID is higher when more methanol is used which can be explained by the lower temperature in the cylinder preventing the diesel atomize and to autoignite. Another expaination is that there is less oxygen in the cylinder due to the lower overall AFR. Combustion needs air in order to react, which is less present in the cylinder when more methanol is used. The explaination of [1] is that the ID is caused by the conversion of active OH into H_2O_2 which is inactive. This effects results in a less effective atomization of diesel, resulting in an increased ID. The result remains the same, the first peak of the HRR will increase when the ID is higher.

Figure 5.36 shows that the decrease in RMD causes the ID to increase in the two zone model. This is in contradiction with the experimental observations. The ID is dependent on the pressure, the aIgn tuning parameter and ϕ. Due to the dependency of ϕ the expectation was that the ID would be estimated properly, this is not true as discussed in chapter 5.3. ϕ used is the global ϕ and not specified for the burnt zone. aIgn indicates the frequency factor, which specifies the amount of collissions in a reaction. This is specific for each reaction. When changing the amount of fuels this value may change.

In Figure 5.37 the CHR for the various RMDs are shown.

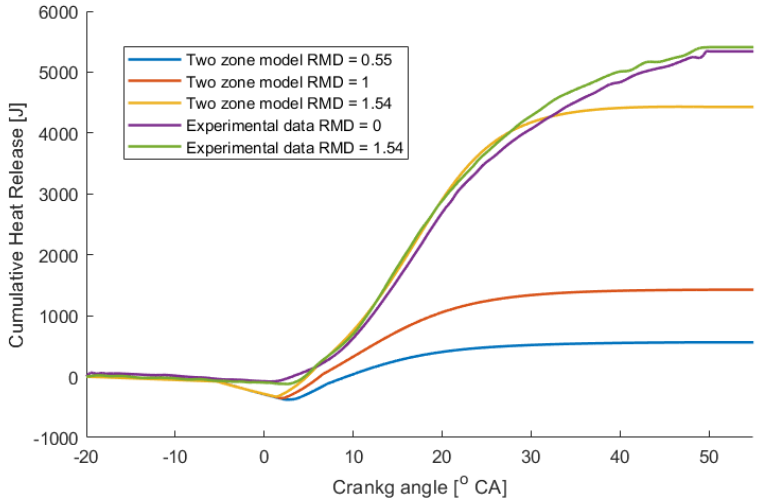

FIGURE 5.37: CHR when changing RMD, with SOI = -5.5

Figure 5.37 shows that when changing the RMD not all fuel is combusted hence the lower CHR.

Table 5.6 indicates the results of the IMEP, indicated work, efficiency and mean maximum in-cylinder temperature when changing the SOI and RMD. The conclusion that the model is not predictive which can be concluded from Table 5.6. When decreasing the RMD from RMD = 1.54 to RMD = 1 the efficiency drops almost 28% and the indicated work drops almost 1654 J. These drops are not present in the post processing model (see Table 5.3). When decreasing the RMD to RMD = 0.55 the efficiency drops to 2% and the energy in the form of indicated work decreases to 636 J. These values are only possible when having a incomplete combustion. The SOI sweep is discussed in the following chapter (chapter 5.3.2).

TABLE 5.6: Parameters when sweeping SOI and RMD

SOI	RMD	IMEP [Pa]	Indicated work [J]	Efficiency [%]	T_{max} [K]
-5.5	1.54	1412600	2289.8	38.63	1721.5
0	1.54	-85664	-138.8589	-2.3429	1043.5
3	1.54	No result			
-5.5	0	No result			
-5.5	0.55	73626	119.346	2.0512	1060.5
-5.5	1	392410	636.0901	10.9107	1178.4

SOI

Figure 5.38 gives results for the injection timing of 0 when keeping the base tuning parameters as described in table 5.4. The polytropic compression is comparable with the experimental pressure trace, however after injection the pressure of the two zone model drops down.

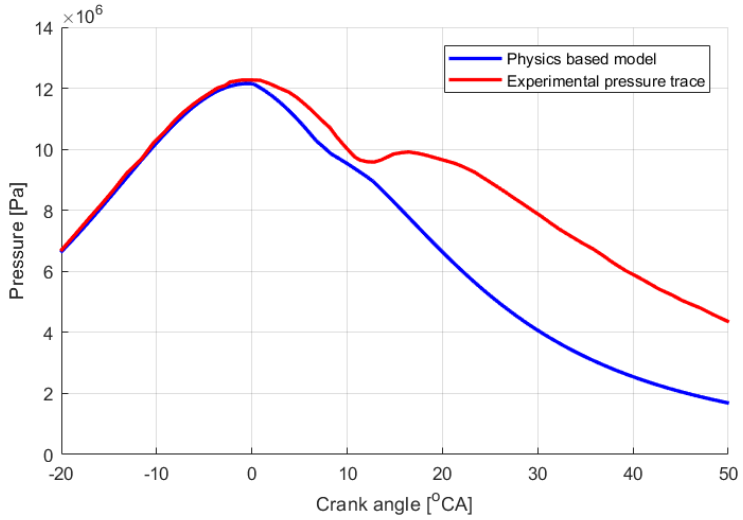

FIGURE 5.38: Pressure trace of SOI = 0

Figure 5.39 shows the results of the HRR of the two zone model and the experiments when SOI = 0. The HRR shows immediately that complete combustion does not take place due to lack of heat created inside the cylinder.

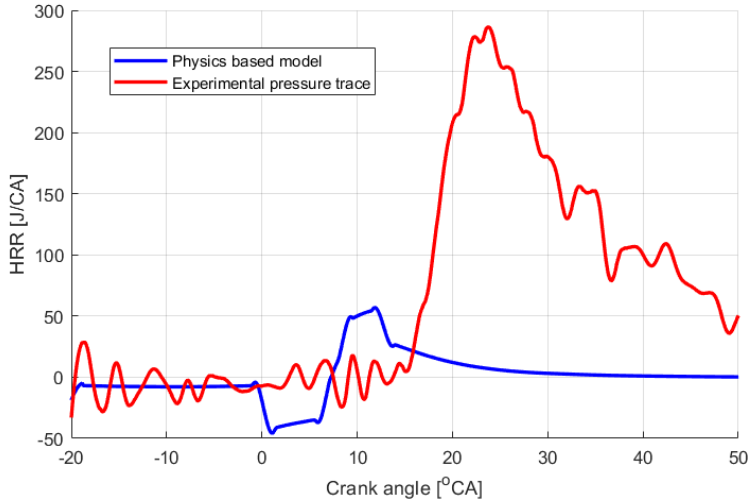

FIGURE 5.39: Heat release rate of SOI = 0

Figure 5.40 shows the CHR results of the experiments and the two zone model.

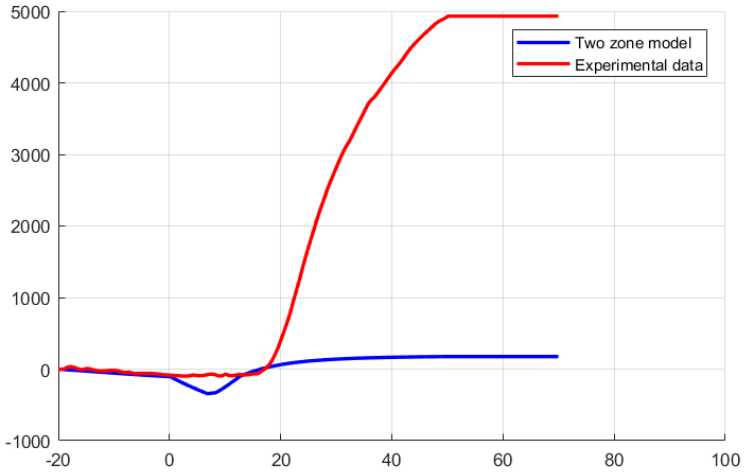

FIGURE 5.40: Cumulative heat release of SOI = 0

The limited combustion of fuel is confirmed by Figure 5.40 where the CHR is far below the experimental CHR. Later SOI (SOI = 3) resulted in a model error.

In Table 5.6 results for IMEP, indicated work, ITE and maximum mean in cylinder temperature are shown. When running the model for SOI = 0, results for IMEP, indicated work and efficiency are negative. This means that it costs energy to run the engine with these specifications instead of delivering energy.

5.3.3 Conclusion two zone model

The **Spray entrainment model** uses the tuning parameter TweakSpray to calculate the overall mass inside the burnt zone during injection. The **injection model** calculates the influence of the injection of diesel during that period. The influence of the injection of diesel is significant lower than the spray entrainment from the unburnt zone into the burnt zone. This indicates a mistake in the calculation of the total volume change of the burnt zone ($\frac{V_b}{dt}$) during injection. Equation 4.53 calculates this volume change of the burnt zone and when checking the units, it does not add up, with as a result can be concluded that the equation is wrong. This error in the calculation of the change in volume of the spray, results in a bigger spray entrainment.

The spray entrainment model is still used after injection, due to the assumption that the kinetic energy in the spray still results in a similar growth of the spray. However the spray entrainment is calculated by the overall change of volume of the burnt zone minus the injection. After injection the influence of the injection is zero, however the influence of the spray is now equal to the overall spray entrainment minus zero, which is not likely to happen in reality.

CTFlame is used in the **flame propagation model**, and it converts the calculated laminar flame velocity into turbulent flame velocity in the cylinder. The influence of CTFlame is insignificant. The insignificant influence of CTFlame is due to the fast spray entrainment resulting from the error in the calculation of $\frac{V_b}{dt}$ in the **Spray entrainment model**. The fast spray entrainment results in a fast conversion of unburnt zone into the burnt zone and the **flame propagation model** is only valid when there

is still mass in the unburnt zone left.

The Ignition model calculates the Ignition Delay (ID) with an Arrhenius equation, where the temprature in the burnt zone and the fuel-air equivalence ratio. In the model the global fuel-air equivalence ratio (ϕ) is calculated. However the local fuel-air equivalence ratio in the burnt zone is needed to establish the ignition timing. This local fuel-air equivalence ratio in the burnt zone changes when the methanol and air mixture entrain the spray resulting in different ignition timings.

In the diesel combustion model uses an Arrhenius equation for the velocity of the burning rate of diesel in the spray. This equation, similar to the ignition model, calculates this combustion rate with the use of ϕ and the global ϕ is used. In this case the local ϕ in the burnt zone should be used for a better match.

Tuning parameters aIgn and KIcinicine are indicating the collision frequency between molecules. It is known that, when changing the reaction these parameters are different. To what extend these parameters will change when changing the RMD is not known and can be investigated in another study. The tuning parameters are tuned by hand. In a future research an optimizer tool can be used in order to find better fitted parameters.

The two zone model cannot be used for predictive purposes in this state. Changing Start of Injection (SOI) and the Ratio Methanol Diesel (RMD) results in poor fits for the pressure trace, Heat Release Rate (HRR) and Cumulative Heat Release (CHR). Adjusting the model with the suggested changes might result in a model with a predictive behaviour and need to be research in a following research.

5.4 Differences and similarities of the two models

Both models lack the ability to change input settings such as SOI and RMD. The two zone model was expected to be able to run with different SOI and RMD, however this is not the case. When changing RMD and SOI the HRR and CHR did not match with the experiments. For the cases RMD = 0 SOI = -5.5 and RMD = 1.54 SOI = 3 the model was not able to generate results at all. The Vibe based model, is as expected not able to predict the trends when changing the input parameters. The Vibe based model uses shape parameters which need to be calibrated per case. This is currently the case for the model/tuning parameters of the two zone model also.

Table 5.7 gives an overview on CAXX values. These values describe the amount of heat released at a certain crank angle. CA05 indicates 5% of the total heat is released. CA50 indicates 50% of the total heat is released and CA90 90% of the total heat release is released.

TABLE 5.7: CA05, CA50 and CA90 parameters for both the two zone and Vibe based model.

		Two zone model			**Vibe based model**		
SOI	*RMD*	*CA05*	*CA50*	*CA90*	*CA05*	*CA50*	*CA90*
-5.5	1.54	6.22	17.05	27.31	6.448	18.874	34.036
-5.5	1	7.018	14.656	26.74	6.448	18.988	34.72
-5.5	0.55	9.75	15.454	28.11	6.334	19.102	35.29
0	1.54	16.708	21.952	35.746	-	-	-

As shown in Table 5.7, the Vibe based model results in similar values for each of the CAXX values when changing the RMD. The small changes in CAXX values is caused by the definition used for CAXX where a percentage of the total energy is combusted. The total combusted energy changes slightly when changing RMD, resulting in a change in the CAXX values. In reality, there is a smaller ID when having less methanol (lower RMD). In case of the two zone model the CA05 values decrease indicating in an ID decrease as expected.

The Vibe based model has a hard coded SOC, meaning it will not change when adjusting RMD. As discussed in chapter 4.2.2 the ID (indicated with τ in this equation) can be calculated with Equation 4.58. It can be investigated whether it is possible to implement this equation in the Vibe based model. The disadvantage of the ID equation is that it uses the temperature of the burnt zone in the two zone model. The Vibe based model makes no distinction between zones, leading to the assumption of an even divided temperature in the cylinder. SOC than can be calculated by SOI+τ. The two zone model includes this calculation, however it is not influencing the ID significantly. This can be caused by the use of ϕ_{global} instead of ϕ_{burnt}. The variables B, m, n and A in Equation 4.58 should be checked for dual fuel with methanol combustion.

The Vibe based model was already modeled meaning the parameters were already calibrated for the engine described in the paper [1]. The same engine is used in the two zone model. An injection pressure of 100MPa is used in the Vibe based model. With this injection pressure the shape parameters were calibrated for the RMD = 1.54 SOI = -5.5 case. For the same reason an injection pressure of 100MPa is used in the two zone model. The paper [1] however describes a maximum injection pressure of 160MPa for the diesel injectors used. The difference in injection pressure results in a different spray pattern resulting in different results. Further investigation can be done on tweaking the injection pressure to the best possible match.

To obtain the initial pressure at IVC the two models introduce a formula for the polytropic compression (Equation4.27). This equation contains r_c, p_2 and n_{comp}. The two zone model uses an effective compression ratio (r_c) of 12 instead of 13.2427, which was calculated by $\frac{V_1}{V_2}$ and used in the Vibe based model. The choice of changing r_c in the two zone model is due to a better match in the polytropic compression phase in the pressure trace. The p_2 value is changed for the same reason. The Vibe model takes the pressure (p_2) at SOC, which was an assumed value. The two zone model takes a value for p_2 which is consistent with the height of the first pressure peak in paper[1]. The polytropic compression index is used to calculate the initial pressure (p_1) with Equation 4.27. n_{comp} is the polytropic compression index, which is different for each fluid. According to [54] an increase in methanol should decrease

the polytropic compression index (n_{comp}) resulting in a different pressure at the first peak. n_{comp} currently has a value of 1.365.

Chapter 6

Conclusions and recommendations

6.1 Conclusions

Waterborne transport currently runs on Internal Combustion Engines (ICE) using diesel as fuel. Governmental intention is to reduce Green House Gas (GHG) emissions where the diesel fuel Compression Ignition (CI) engines are not advantageous. The possibilities for using methanol in ICEs is investigated due to its renewable character. However the process of producing methanol by hydrogenation of CO_2, considered renewable, is currently economical insufficient. This production process is in its development stage and therefore in the future, when more research is done, it is expected that these production costs will decrease.

Combustion of methanol in ICE

The Lower Heating Value (LHV) is lower for methanol compared to diesel, resulting in the need of bigger fuel storage tanks to travel the same distance. Methanol already contains oxygen and therefore needs less air for combustion, resulting in the possibility to use similar cylinder volumes as diesel CI engines to produce the same amount of energy. Methanol has a significant lower cetane number compared to diesel, meaning deficient self ignition. To establish combustion an ignition source is needed when using methanol. An ignition source can be caused by a spark, similar to a gasoline engine, a high cetane number fuel is the combustion initiator, or the fuel is altered to a higher cetane number fuel. The disadvantages of using methanol concern poor lubrication, which can be solved by adding a lubricant. Its corrosive character, where material choice becomes more important and methanol is harmful to human beings, however it is easily decomposed by the environment, therefore suitable for marine applications. Considering all properties of methanol it can be concluded that methanol is usable as fuel in ICEs. The most redundant known method to use methanol as fuel in an ICE is the conventional dual fuel combustion engine, where a high cetane number fuel is the combustion initiator.

Post processing model

For validation of the two models, the Vibe based model and the two zone model, a post processing model is used and validated. The HRR results shown in Figure 5.1 and 5.2 have similar trends, resulting in a visually approved model. The spiky behaviour of the HRR of the post processing model is caused by the use of a different filter compared to the paper [1]. The differences in MEP and efficiencies between

the experimental results [1] and the post processing model is due to mechanical efficiencies. The mechanical efficiencies are calculated to be between 80% and 90%. According to literature the mechanical efficiencies should be between 70% and 92%. Therefore the post processing model is approved as such for usage in this thesis.

Vibe based model

The Vibe based model is a model where for the Combustion Reaction Rate (CRR) the Vibe functions are introduced. There are two Vibe functions used, one for methanol (single Vibe function) and one for Diesel (double Vibe function). These two Vibe functions and the combustion duration are needed to calculate the CRR. The combustion duration is dependent on the input parameters SOC and EOC and considered equal for methanol and diesel. The model is only able to model the combustion period (between SOC and EOC). The polytropic compression (Figure 5.9) of the Vibe based model lays lower compared to the experiments. This is caused by the choice of the pressure at the start of the iso-volumetric combustion (p_2). Which is considered the the pressure at SOC which is an input parameter. The compression ratio (r_c) is calculated with $\frac{V_1}{V_2}$. The pressure trace contains 2 peaks instead of the 3 peaks present in the experiments. The surface of the HRR results of the Vibe based model (Figure 5.10) are in line with the experimental results. This is confirmed by the ITE of the RMD = 1.54 and SOI = -5.5 case. Where the ITE is 50.15% and 48.82% for the Vibe based model and the experiments, respectively. The IMEP of the same case for the Vibe based model is 18.34 bar and for the experiments is 17.82 bar. The premixed combustion (first peak around 5^oCA) is not visual in the Vibe based results, probably caused by the choice of Vibe functions. When changing the RMD, the trends of the HRR do not change as the experimental HRR does. The Vibe based model does change however. This change can be seen when decreasing the methanol content, the first peak (around 15^oCA) decreases from 230J/CA to 200J/CA and the bump occurring around 35^o CA increases from 70 J/CA to 90 J/CA.

Two zone model

The two zone model is a model where the CRR is calculated with several sub models, namely: **injection model**, **spray entrainment model**, **Ignition delay model**, **methanol combustion model** and the **diesel combustion model**.

The **injection model** is used to calculate the mass flow of diesel injection. This injection causes the burnt zone (the zone where the combustion reaction can occur) to grow.

The sub-model, **spray entrainment model**, calculates the burnt zone mass flow, where entrainment of the unburnt zone into the burnt zone and fuel injection are combined. This model is used until the unburnt zone has 0.05% mass left of its size before ignition. This calculation is based on the injection pressure so after EOI its driving force has disappeared, however the model assumes this driving force is kept by kinetic energy. This results in a rapid increase of the burnt zone. The rapid increase of the burnt zone is also caused by the error in the calculation for the volume change in the burnt zone($\frac{dV_b}{dt}$) (Equation 4.53). This $\frac{dV_b}{dt}$ is used in Equation 4.52 to establish the total mass flow of the burnt zone. An alternative calculation for $\frac{dV_b}{dt}$

is shown in Appendix C.

Due to the fast entrainment of unburnt zone into the burnt zone before ignition, the **methanol burning model**, where the flame propagation is calculated, has insignificant influence on the model. The tuning parameter, CTFlame converts a laminar flame speed into turbulent flame speed. Due to the insignificant influence of the methanol combustion model, the CTFlame sweep is also not of significant influence.

The **ignition model** is the model where calculations are made with an Arrhenius equation. The tuning parameter involved is aIgn which indicates the frequency of collisions between molecules in a reaction. When changing the blend ratio another value for aIgn could be valid. The biggest remark is the use of the fuel-air equivalence ratio (ϕ), where now the overall value is used. Better would be to calculate the value of ϕ in the burnt zone. The same is valid for the Diesel burning model, where kIcinicine is the tuning parameter.

In its current stage, the two zone model is not predictive. When changing the SOI and RMD it leads to poor results.

6.2 Recommendations

In the two models, the injection pressure is estimated to be 100MPa, however the paper indicates a maximum injection pressure ability of 160MPa. By doing your own experiments these uncertainties can be excluded. The compression index n_{comp} is used to establish the initial pressure p_1 which was not given in the paper [1]. The value of n_{comp} = 1.365, which is commonly used for diesel. However according to [54] an increase in methanol should decrease the polytropic compression index (n_{comp}). The influence of this can be investigated to improve the two models.

Vibe based model

The Vibe model is non predictive due to the assumption of SOC and EOC. The SOC can be calculated with the ID calculation as discribed in the two zone model. When adding the ID value up to SOI, this might give a predictive behaviour concerning the SOC. Additional assumptions need to be made, namely the temperature in the cylinder is constant, while there is no distinction in two zones as the two zone model has. The does not show the premixed peak in the model, this might be resolved by using multiple Vibe functions. This needs to be further investigated.

Future research can be done on the combustion duration, where methanol and diesel do not have similar combustion durations.

The Vibe based model now uses a double Vibe function for diesel and a single Vibe function for methanol. This results in a pressure trace with two peaks. According to the literature, dual fuel methanol and diesel combustion has 3 peaks. Investigation can be done on whether a using multiple Vibe function can be beneficial. This can create the premixed combustion.

Two zone model

The sub model, 'spray entrainment model', contains an error when calculating the change in burnt zone volume ($\frac{dV_b}{dt}$). In Appendix C the corrected equation is described. This equation should be implemented and the tuning parameters need to be retuned. An optimizing tool might give more accurate tuning parameter values. The 'spray entrainment model' is also used after the injection stopped, caused by the assumption that kinetic energy will result in a similar spray propagation. An investigation can be done whether this is the most optimal way of modeling.

Investigate whether the use of aIgn and kIcinicine (used in the **ignition model**, describing the frequency of collisions between molecules during a reaction in the ignition model, is changed when changing RMD. When aIgn and kIcinicine change it can be investigate whether there is a correlation between the methanol content versus the value.

The calculation for ID in the **ignition model** and the diesel burning rate in the **diesel combustion model** are influenced by the global ϕ, which can be optimized by using the burnt zone ϕ where combustion takes place.

Appendix A

Input parameters of the two models with the corresponding used values

The input parameters of the two models are described in the table.

TABLE A.1: Model input parameters

Variable	**TNO**	**Delft**	**Value**
Number of revolutions per cycle	k_cycle	k_cycle	2
Engine speed [rpm]	Neng	N_eng_nom	1900
Number of cylinders	Ncyl	I-cyl	6
Stroke length [m]	S	L_s	0.13
Bore [m]	B	D_b	0.126
Inlet valve open [deg CA]	IVO	IO	324 and 55
Inlet valve close [deg CA]	IVC	IC	-114 and 65
Exhaust valve open [deg CA]	EVO	-	102
Exhaust valve closed [deg CA]	EVC	EC	390 and 65
Degrees from Exhaust valve open	-	delta_EO	5
Nominal engine power [kW]	-	P_eng_nom	247
Maximum cylinder pressure at nominal load [bar]	-	p_max_nom	125
Geometric compression ratio [-]	eta	epsilon	17
Effective compression ratio [-]	r_c	r_c=V1/V2	12 and 13.2427
Connecting rod length [m]	L	L_CR	0.219
Crank radius [m]	R	R_CR	0.065
Temperature injected fuel [C]	Tf	T_fuel_inj	25
Injection pressure [Pa]	dpInj	P-fuel-inj	100 EE6
Diesel fuel density [kg/m3]	rhof	-	830

Air to fuel ratio [-]	afr	afr	19.3
Mass flow diesel [kg/h]	m_dot_diesel _kgh	m_diesel-h	27.98
Mass flow methanol [kg/h]	m_dot_methanol_kgh	m_alcohol_h	43.01
Pressure intake manifold [Pa] (methanol inlet pressure)	p_int	p_gfuel_inj	0.4MPa
Pressure exhaust manifold [Pa]	p_exh	-	1.06 EE5
Temperature intake manifold [K]	T_int	T_IR	315
Temperature exhaust manifold [K]	T_exh	-	250+273
Mass-based stoichiometric coefficient for heptane	sFuel	-	3.52
Start of injection	soi	-	-5.5
Nozzle diameter (diesel nozzle) [m]	dNoz	-	150 EE-6
Number of nozzle holes	nNoz	-	7
Nozzle dischargecoefficient	Cd	-	0.9
Number of cycles (1cycle=720CA)	Ncyc	-	1
Start of heat release (SOH	-	SOH	160
End of combustion	-	EOC	230
Combustion duration	wiebecoef. comb_dur	-	49.5
Combustion efficiency	wiebecoef. comb_eff	a_1_v, a_2_v, a_3_v, a_4_v = 6.908 due to combustion effiency of 99%	0.99
Residual diesel combustion gas		x_1_sg	0.001
Residual alcohol combustion gas [%]		x_1_ssg	0.001
Universal gas constant	Runiv	R_u	8.3145
Polytropic exponential	n_comp	n_comp	1.365
Ambient temperature	-	p_amb_0	1.00E+05
Wall temperature	Twall	T_cyl_wall	400
Crown piston temperature [K]	-	T_piston_crown	600
Cylinder head temperature	-	T_cyl_head	580
Swirl factor	-	swirl	10

Heat loss coefficient	-	C_hl	120
a	0.016	-	
IVD	0.04	-	
EVD	0.038	-	
wiebecoef_alpha1	5	-	
wiebecoef_alpha2	3	-	
Sparktiming	wiebecoef_ST	-	-5.5
	dmbdtComb	-	0
Value for flame propagation	Bm	-	0.3692
Value for flame propagation	T0	-	298
Value for flame propagation	po	-	1.00E+05
Value for flame propagation	phi_m	-	1.11
Value for flame propagation	B_phi	-	-1.4051
Value for flame propagation dilluted gas fraction	xb	-	0
	-	phi_3	160
	-	phi_4	175
Begin interval calculation max. temperature rise	-	phi_9	210
End interval calculation max. temperature rise	-	phi_10	220
Length interval for determination T_EO	-	d_phi	32
Vibe parameters	-	b_1_v	0.8605
Vibe parameters	-	b_3_v	0
Vibe parameters	-	b_4_v	0
Vibe parameters	-	m_1_v	1.341
Vibe parameters	-	m_2_v	6.057
Vibe parameters	-	m_3_v	0
Vibe parameters	-	m_4_v	0

Appendix B

Combustion

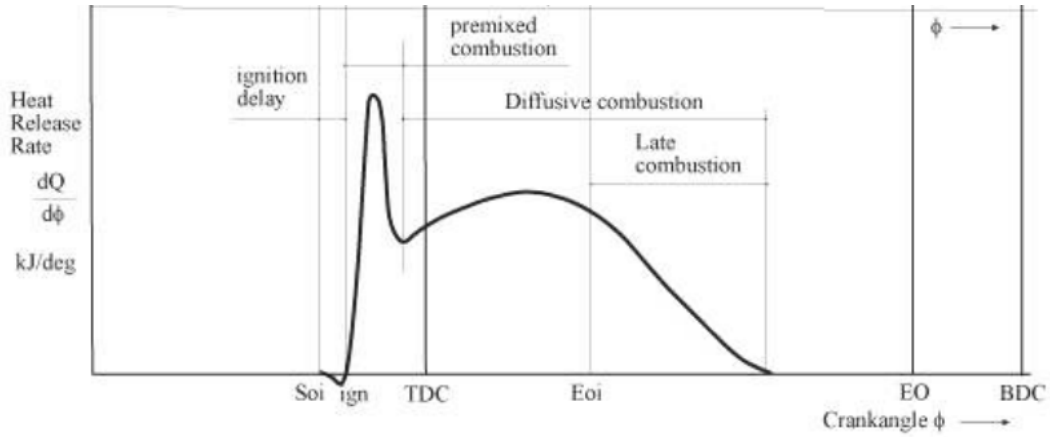

FIGURE B.1: HHR combustion [55]

The premixed combustion is a fast combustion reaction. The combustion is a result of mixing of fuel and air during the ID period. The bigger ID the higher the premixed combustion HHR. After the premixed combustion the diffusive combustion starts which is combustion at the flame front due to diffusion of oxygen into the burnt zone.

Appendix C

Volume change of burnt zone

The dimensions of Equation 4.53 are not consistent. The spray is assumed to be a perfect cone spray, and is therefore eligible to use Equation C.1, where r is the biggest radius of the cone, and h the cone height. The height change ($\frac{dS}{dt}$) is used for h. The radius can be calculated by taking $r = tan(\frac{\theta}{2}) * S(t)$. The equation for $\frac{V_b}{dt}$ becomes Equation C.2. The recommendation is to use the new equation for burnt zone volume change in a next research.

$$V = \frac{\pi}{3} * r^2 * h = \frac{\pi}{3} * tan\left(\frac{\theta}{2}\right)^2 * S^2(t) * S(t) = \frac{\pi}{3} * tan\left(\frac{\theta}{2}\right)^2 * S^3(t) \tag{C.1}$$

When assuming θ is constant the derivative of V becomes as follows:

$$\frac{dV_b}{dt} = \frac{\pi}{3} * tan\left(\frac{\theta}{2}\right)^2 * 3 * S(t)^2 * \frac{dS}{dt} = \pi * tan\left(\frac{\theta}{2}\right)^2 * S(t)^2 * \frac{dS}{dt} \tag{C.2}$$

Bibliography

[1] Lijiang Wei et al. "Effects of methanol to diesel ratio and diesel injection timing on combustion, performance and emissions of a methanol port premixed diesel engine". In: *Energy* 95 (2016), pp. 223 –232. ISSN: 0360-5442. DOI: https://doi.org/10.1016/j.energy.2015.12.020. URL: http://www.sciencedirect.com/science/article/pii/S036054421501662X.

[2] New Energy and Industrial Technology Development Organization. *VII International Symposium On Alcohol Fuels*. Tokyo, Japan: Sanbi Insatsu Co, 1988.

[3] *Methanol in Racing*. URL: http://emsh-ngtech.com/methanol/methanol-in-racing/.

[4] Xudong Zhen and Yang Wang. "An overview of methanol as an internal combustion engine fuel". In: *Renewable and Sustainable Energy Reviews* 52.Supplement C (2015), pp. 477 –493. ISSN: 1364-0321. DOI: https://doi.org/10.1016/j.rser.2015.07.083. URL: http://www.sciencedirect.com/science/article/pii/S1364032115007303.

[5] Alliance Consulting International. *Methanol Safe Handling Manual*. Virginia, USA: Methanol Institute Arlington, 2008.

[6] Magin Lapuerta et al. "Modeling viscosity of butanol and ethanol blends with diesel and biodiesel fuels". In: *Fuel* 199.Supplement C (2017), pp. 332 –338. ISSN: 0016-2361. DOI: https://doi.org/10.1016/j.fuel.2017.02.101. URL: http://www.sciencedirect.com/science/article/pii/S0016236117302521.

[7] Shenghua Liu et al. "Study of spark ignition engine fueled with methanol/gasoline fuel blends". In: *Applied Thermal Engineering* 27.11 (2007), pp. 1904 –1910. ISSN: 1359-4311. DOI: https://doi.org/10.1016/j.applthermaleng.2006.12.024. URL: http://www.sciencedirect.com/science/article/pii/S1359431107000257.

[8] Michael P. Walsh. *alternative fuels: fuel table*. URL: http://walshcarlines.com/pdf/fueltable.pdf.

[9] *LNG Information Paper NO.1. About LNG*. URL: http://www.giignl.org/sites/default/files/PUBLIC_AREA/About_LNG/4_LNG_Basics/090801publique_lngbasics_lng_1_-_basic_properties_7.2.09_aacomments.pdf.

[10] Yaopeng Li et al. "Numerical study on the combustion and emission characteristics of a methanol/diesel reactivity controlled compression ignition (RCCI) engine". In: *Applied Energy* 106.Supplement C (2013), pp. 184 –197. ISSN: 0306-2619. DOI: https://doi.org/10.1016/j.apenergy.2013.01.058. URL: http://www.sciencedirect.com/science/article/pii/S0306261913000676.

[11] J. van Ommen W. de Jong. "Biomass as sustainable energy source for the future". In: (2015).

[12] Sayan Kar et al. "Advances in catalytic homogeneous hydrogenation of carbon dioxide to methanol". In: *Journal of {CO2} Utilization* 23 (2018), pp. 212 –218. ISSN: 2212-9820. DOI: https://doi.org/10.1016/j.jcou.2017.10.023. URL: https://www.sciencedirect.com/science/article/pii/S2212982017306650.

[13] Suhas G. Jadhav et al. "Catalytic carbon dioxide hydrogenation to methanol: A review of recent studies". In: *Chemical Engineering Research and Design* 92.11 (2014), pp. 2557 –2567. ISSN: 0263-8762. DOI: https://doi.org/10.1016/j.cherd.2014.03.005. URL: http://www.sciencedirect.com/science/article/pii/S0263876214001282.

[14] D. Bellotti et al. "Feasibility study of methanol production plant from hydrogen and captured carbon dioxide". In: *Journal of CO2 Utilization* 21.Supplement C (2017), pp. 132 –138. ISSN: 2212-9820. DOI: https://doi.org/10.1016/j.jcou.2017.07.001. URL: http://www.sciencedirect.com/science/article/pii/S2212982017302007.

[15] "METHANOL AS A MARINE FUEL, A SAFE, COST EFFECTIVE, CLEAN-BURNING, WIDELY AVAILABLE MARINE FUEL FOR TODAY AND THE FUTURE". In: *Methanex* (). URL: https://www.methanex.com/sites/default/files/about-methanol/MMF-web-2017.pdf.

[16] Carlo N Hamelinck and André P.C Faaij. "Future prospects for production of methanol and hydrogen from biomass". In: *Journal of Power Sources* 111.1 (2002), pp. 1 –22. ISSN: 0378-7753. DOI: https://doi.org/10.1016/S0378-7753(02)00220-3. URL: http://www.sciencedirect.com/science/article/pii/S0378775302002203.

[17] MAN Diesel and Turbo. *ME-LGI Engines, Liquid gas injection, methanol and LPG*. 2014. URL: http://www.marine.man.eu/docs/librariesprovider6/methanol-campaign/brochures/3010-0318-00ppr_the-me-lgi-concept_web.pdf?sfvrsn=8.

[18] "Costs and Beneæts of Alternative Fuels for an LR1 Product Tanker". In: *DieselFacts* (). URL: http://www.marine.man.eu/docs/librariesprovider6/dieselfacts/dieselfacts-2016-01.pdf?sfvrsn=4.

[19] *Fuel flexible power plants from Wartsila*. URL: https://www.wartsila.com/twentyfour7/in-detail/fuel-flexible-power-plants-from-wartsila.

[20] Toni Stojcevski. *METHANOL AS ENGINE FUEL: CHALLENGES AND OPPORTUNITIES*. 2016. URL: www.sjofart.ax/files/attachments/page/converting_stena_germanica_into_methanol_toni_stojcevski.pdf.

[21] Christopher Browne. *Horizons*. 2015. URL: http://www.lr.org/en/_images/229-79180_LR_Horizons_January_2015_spreads.pdf.

[22] Insyde Webdesign. *Schonere schepen met Lean Ships*. URL: http://www.maritiemnederland.com/nieuws/damen-shipyards-coordineert-lean-ships/item1651.

[23] *Stena Germanica - Brandstof*. URL: https://www.stenaline.nl/schepen/stena-germanica/methanol-ferry/methanol.

[24] Edwin Lampert. *Methanol-fuelled tankers one year on*. 2017. URL: http://www.tankershipping.com/news/view,methanolfuelled-tankers-one-year-on_47529.htm.

[25] EffShip. *Welcome to the final EffShip Seminar*. 2013. URL: http://www.effship.com/PublicPresentations/Final_Seminar_2013-03-21/09_EffShip-Handout.pdf.

[26] EffShip. *EffShip- Project Description 091021*. 2009. URL: http://www.effship.com/ProjectDescriptionShort.pdf.

[27] URL: http://www.summeth.marinemethanol.com/?page=home.

[28] URL: https://www.greenpilot.se/project.

[29] *SPIRETH - Methanol as marine fuel*. URL: https://www.sspa.se/alternative-fuels/spireth-methanol-marine-fuel.

[30] Martin Tuner. "Combustion of Alternative Vehicle Fuels in Internal Combustion Engines". In: *Report within project. A pre-study to prepare for interdisciplinary research on future alternative transportation fuels , financed by The Swedish Energy Agency* 3.2 (2016).

[31] X.L.J. Seykens. "Development and validation of a phenomenological diesel engine combustion model". In: *Technische universiteit Eindhoven* (2010).

[32] Maarten Van De Ginste Louis Sileghem. "Methanol as a Fuel for Modern Spark-Ignition Engines: Efficiency Study". In: *Researchgate* (). URL: http://users.ugent.be/~lsileghe/documents/extended_abstract.pdf.

[33] Martin Tuner. "Review and Benchmarking of Alternative Fuels in Conventional and Advanced Engine Concets with Emphasis on Efficiency, CO2, and Regulated Emissions". In: *SAE International* (2016). ISSN: 1359-4311. DOI: https://doi.org/10.4271/2016-01-0882. URL: https://doi.org/10.4271/2016-01-0882.

[34] Maarten Verbeek et al. "Onderscheidende kenmerken van brandstoftypen als alternatief voor diesel". In: (2017).

[35] California Freight Advisory Committee. "CLEAN DIESEL FUEL: THE CASE FOR IGNITION-IMPROVED METHANOL". In: *California Sustainable Freight Action Plan* (). URL: http://www.casustainablefreight.org/documents/Comments/133_CleanDieselFuel.pdf.

[36] James Robert Jennings and Glyn David Short. *ENHANCED FUEL AND METHOD OF PRODUCING ENHANCED FUEL FOR OPERATING INTERNAL COMBUSTION ENGINE*. 2016.

[37] G. Najafia and T. F Yusafb. "Experimental investigation of using methanol-diesel blended fuels in diesel engine". In: (2009). URL: https://eprints.usq.edu.au/5058/2/Najafi_Yusaf_2009_VoR.pdf.

[38] Sundarraj Chockalingam and Saravanan Ganapathy. "Performance and Emission Analysis of a Single Cylinder Constant Speed Diesel Engine Fuelled with Diesel-Methanol-Isopropyl Alcohol Blends". In: *SAE Technical Paper*. SAE International, Sept. 2012. DOI: 10.4271/2012-01-1683. URL: https://doi.org/10.4271/2012-01-1683.

[39] Tino Tuominen. "Potential of methanol in dual fuel combustion; Metanolin potentiaali dual fuel -palamisessa". en. G2 Pro gradu, diplomityö. 2016-01-25, p. 75. URL: http://urn.fi/URN:NBN:fi:aalto-201602161368.

[40] Shui Yu et al. "Ignition control for liquid dual-fuel combustion in compression ignition engines". In: *Fuel* 197.Supplement C (2017), pp. 583 –595. ISSN: 0016-2361. DOI: https://doi.org/10.1016/j.fuel.2017.02.047. URL: http://www.sciencedirect.com/science/article/pii/S0016236117301928.

[41] M Venkatesan et al. “Hydrous Methanol Fuelled HCCI Engine Using Ignition Improver CAI Method-ANN Approach”. In: *Mechanics and Mechanical Engineering* 19.1 (2015), pp. 31–49.

[42] SR Munshi et al. “Development of a partially-premixed combustion strategy for a low-emission, direct injection high efficiency natural gas engine”. In: *Proceedings of the AMSE 2011 Internal Combustion Engine Division Fall Technical Conference, Morgantown, West Virginia, USA*. 2011.

[43] Rolf D Reitz and Ganesh Duraisamy. “Review of high efficiency and clean reactivity controlled compression ignition (RCCI) combustion in internal combustion engines”. In: *Progress in Energy and Combustion Science* 46 (2015), pp. 12–71.

[44] Byungjoo Lee. “The effects of methanol fuel on combustion in premixed dual fuel engine”. In: *TU Delft Repository* (2016). URL: https://www.google.nl/url?sa=t&rct=j&q=&esrc=s&source=web&cd=7&cad=rja&uact=8&ved=0ahUKEwiQqtmPl6XZAhWPZFAKHY6CCDcQFgg9MAY&url=https%3A%2F%2Frepository.tudelft.nl%2Fislandora%2Fobject%2Fuuid%3A60b7233f-d7f9-4439-829a-1166429d4233%2Fdatastream%2FOBJ%2Fdownload&usg=AOvVaw0pK9tkUoYiM_q9CN1Ha1JF.

[45] D. Stapersma. “Diesel Engines, Volmume 3 Combustion”. In: *TU Delft* 3 (2010).

[46] Yu Ding. “Characterising Combustion in Diesel Engines”. In: *TU Delft Repository* (2011). URL: https://www.google.nl/url?sa=t&rct=j&q=&esrc=s&source=web&cd=1&ved=0ahUKEwjtrqCVm6XZAhXHLFAKHQDYADYQFggtMAA&url=https%3A%2F%2Frepository.tudelft.nl%2Fislandora%2Fobject%2Fuuid%3A10e25404-4b8e-443b-9f16-5e6e5c2a7444%2Fdatastream%2FOBJ%2Fdownload&usg=AOvVaw0LsWr20K-o0BJas7ERCmJN.

[47] D. Hountalas and R. Papagiannakis. “A Simulation Model for the Combustion Process of Natural Gas Engines with Pilot Diesel Fuel as an Ignition Source”. In: *SAE Technical Paper* 2001-01-1245 (2001). DOI: https://doi.org/10.4271/2001-01-1245.

[48] Dennis L. Siebers. “Scaling Liquid-Phase Fuel Penetration in Diesel Sprays Based on Mixing-Limited Vaporization”. In: *SAE Technical Paper* 1999-01-0528 (1999). DOI: https://doi.org/10.4271/1999-01-0528.

[49] J J Hernández et al. “Ignition delay time correlations for a diesel fuel with application to engine combustion modelling”. In: *International Journal of Engine Research* 11.3 (2010), pp. 199–206. DOI: 10.1243/14680874JER06209. eprint: https://doi.org/10.1243/14680874JER06209. URL: https://doi.org/10.1243/14680874JER06209.

[50] Toshikazu KADOTA, Hiroyuki HIROYASU, and Hideo OYA. “Spontaneous Ignition Delay of a Fuel Droplet in High Pressure and High Temperature Gaseous Environments”. In: *Bulletin of JSME* 19.130 (1976), pp. 437–445. DOI: 10.1299/jsme1958.19.437.

[51] Ali M. Pourkhesalian, Amir H. Shamekhi, and Farhad Salimi. “Alternative fuel and gasoline in an SI engine: A comparative study of performance and emissions characteristics”. In: *Fuel* 89.5 (2010), pp. 1056 –1063. ISSN: 0016-2361. DOI: https://doi.org/10.1016/j.fuel.2009.11.025. URL: http://www.sciencedirect.com/science/article/pii/S0016236109005341.

[52] Atul Aravindakshan Nair. "Sensitivity Analysis and validation of TNO's Two-Zone Combustion Model For Operation In Ultra-Low Injection Regime". In: (2018).

[53] D. Stapersma. "Diesel Engines, Volmume 1 Performance analysis". In: *TU Delft* 1 (2010).

[54] Hongbo Zou et al. "Ignition delay of dual fuel engine operating with methanol ignited by pilot diesel". In: *Frontiers of Energy and Power Engineering in China* 2.3 (2008), pp. 285–290. ISSN: 1673-7504. DOI: 10.1007/s11708-008-0060-z. URL: https://doi.org/10.1007/s11708-008-0060-z.

[55] S.N. Soid and Z.A. Zainal. "Spray and combustion characterization for internal combustion engines using optical measuring techniques – A review". In: *Energy* 36.2 (2011), pp. 724 –741. ISSN: 0360-5442. DOI: https://doi.org/10.1016/j.energy.2010.11.022. URL: http://www.sciencedirect.com/science/article/pii/S0360544210006675.